STUDY OF STRENGTH AND DUCTILITY OF GALVANIZED IRON WIRE REINFORCED CONCRETE

by

Md. Abul Bashar Emon

A thesis submitted to the Department of Civil Engineering, Bangladesh University of Engineering and Technology, Dhaka, in partial fulfilment of the degree of Master of Science in Civil & Structural Engineering**.**

DEPARTMENT OF CIVIL ENGINEERING

BANGLADESH UNIVERSITY OF ENGINEERING AND TECHNOLOGY

September, 2014

The thesis titled “STUDY OF STRENGTH AND DUCTILITY OF GALVANIZED IRON WIRE REINFORCED CONCRETE”, submitted by Md. Abul Bashar Emon, Student number- 0412042366P and session April/2012 has been accepted as satisfactory in partial fulfilment of the requirement for the degree of Master of Science (Civil & Structural Engineering) on 21 September, 2014.

Board of Examiners

(1)	Dr. Tanvir Manzur Assistant Professor Department of Civil Engineering BUET, Dhaka-1000	Chairman (Supervisor)
(2)	Dr. A.M.M. Taufiqul Anwar Professor and Head Department of Civil Engineering BUET, Dhaka-1000	Member (Ex-officio)
(3)	Dr. Syed Ishtiaq Ahmad Professor Department of Civil Engineering BUET, Dhaka-1000	Member
(4)	Dr. Sharmin Reza Chowdhury Associate Professor Department of Civil Engineering Ahsanullah University of Science & Technology	Member (External)

DECLARATION

I certify that, although I have conferred with others in preparing this thesis and drawn upon a range of sources cited in this work, the content and concept of this thesis is my original work. Neither the thesis nor any part has been submitted to or is being submitted elsewhere for any other purposes.

(Signature of the Student)

Md. Abul Bashar Emon

ACKNOWLEDGEMENT

The author wish to express his deepest gratitude and sincere appreciation to Dr. Tanvir Manzur, Assistant Professor, Department of Civil Engineering, BUET for his constant guidance, invaluable suggestions, motivation in difficult times and affectionate encouragement, which were extremely helpful in accomplishing this study.

The author also takes the opportunity to pay his heartfelt thanks to Salehin Sharif and Fahim Tanvir for their essential and painstaking contributions to the research and experimental work.

ABSTRACT

Fiber Reinforced Concrete is one of the most promising construction techniques of modern times and steel fiber is, by far, the front runner in the field of reinforcing fibers. A very recent investigation on the properties of locally available Galvanized Iron wire (GI wire) which is basically mild steel wire with a thin coating of Zinc has discovered that it has the potential to be a viable low-cost alternative of commercially available steel fibers. Therefore, a research has been conducted to study the performance of locally available GI wire fiber reinforced concrete (GWRC). This paper presents the findings of the research that made an effort to explore several basic characteristics of GWRC primarily related to strength, ductility and durability. The prime focus of the study was on the effect of fiber content on the foregoing properties of GWRC. Consequently, within the scope of the work, fiber dosage was varied within low volume content (1 to 3.5% by weight) while the concrete mix-design and fiber properties were kept unchanged. A wide variety of tests including compressive and splitting tensile strength, modulus of elasticity, and beam flexure test; Rapid Chloride Permeability Test (RCPT) and water absorption test (Sorptivity) were performed on suitable test specimens. Encouraging results were observed for compressive and tensile strengths and modulus of elasticity with significant increase in capacity. Durability test i.e. Sorptivity revealed that GI wire fiber inclusion has helped GWRC to reduce water absorption and thereby rendered GWRC more durable than normal concrete. RCPT proved indecisive in assessing durability of GWRC but the results can be considered for an indication to dispersion of fibers in the matrix. The major finding of the research was related to flexural capacity and ductility of GWRC. The beam flexure tests have shown a maximum of 30% increment of toughness; first-crack load increment up to 22%; and a maximum of 27% increase in the ultimate load with respect to the capacities of control beams (beams without GI wire fibers). Furthermore, cost analysis and comparison with steel fibers clearly depict that use of GI wire fiber instead of steel fiber comes with a substantial financial advantage from the perspectives of Bangladesh; a fact that makes the study even more worthwhile.

TABLE OF CONTENTS

CHAPTER 3: MATERIALS

CHAPTER 4: EXPERIMENTAL PROGRAM

CHAPTER 5: RESULT AND ANALYSIS

CHAPTER 6: CONCLUSION

LIST OF FIGURES

LIST OF TABLES

NOTATIONS

BC- Brick Chips

FRC- Fiber Reinforced Concrete

GI wire- Galvanized Iron Wire

GWRC- Galvanized iron Wire Reinforced Concrete

IA- Initial Absorption

MoE- Modulus of Elasticity

RCPT- Rapid Chloride Permeability Test

SA- Secondary Absorption

SC- Stone Chips

SFRC- Steel Fiber Reinforced Concrete

S_i –Initial absorption rate, mm/sec$^{1/2}$

S_s–Secondary absorption rate, mm/sec$^{1/2}$

V_f – Volume fraction of fiber

w/c ratio- Water to Cement ratio

ρ_b- Balanced reinforcement ratio

This page is intentionally left blank.

CHAPTER 1

Introduction

1.1 General

Concrete has been the most widely used construction material throughout the world. Therefore, concrete has always been very important from the civil engineering perspective and there has been a constant urge for improving the performance of concrete. The greatest limitation of concrete being lack of ductility, improving this aspect of concrete is a prime concern for civil engineers. In this pursuit for better ductility in concrete, considerable amount of studies are being carried out by incorporating various types of fibers (steel fiber, glass fiber, fiber polymer, natural fiber, nano-fiber etc.) within concrete. Concrete with these fibers, generally known as FRC (Fiber Reinforced Concrete), is one of the most promising new construction materials due to its improved ductility and better performance against flexure.

In the field of FRC, steel fiber is, by far, the front runner as a suitable reinforcing material; since performance of steel fiber in concrete to improve mechanical properties such as tensile strength, ductility, toughness, fatigue life, impact resistance etc. has been established in a number of researches. But additional cost for steel fibers has always been an issue to ponder. In this concern, fibers from GI (Galvanized Iron) wire can provide a viable low cost substitute for steel fibers, especially for Bangladesh since steel fiber for use in FRC is not available in local market and importing from the cheapest of sources proves quite expensive. Moreover, GI wire is locally produced and is available at a relatively low price. Consequently, the circumstances paved the way for GI wire fiber to usher into the scenario. As a very recent development, research with GI wire as a suitable fiber reinforcing material in concrete is just in the budding phase. Hence, from the perspectives of fiber reinforced concrete technologies, a field of prospective research has just emerged on the horizon.

1.2 Background and Present State of the Problem

As a matter of recent development, very little background knowledge about GI wire fiber reinforced concrete is available at present. A research has lately been carried out by Karim et al. [1] to investigate the properties of GI wire so that a proper comparison can be established between the properties of steel fiber and GI wire fiber. It was also studied if GI wire fiber conforms to the ACI and ASTM standards for steel fibers to be used in SFRC (Steel Fiber Reinforced Concrete). In addition, compressive strength of GWRC (Galvanized Wire Reinforced Concrete) was determined and was compared to compressive strength of SFRC to assess the performance of GI wire fiber as fiber in concrete. The study is regarded as one of the pristine attempts to incorporate GI wire fiber as a substitute for steel fiber in FRC. Therefore, the research followed the guidelines and specifications available in the literature concerning steel fiber reinforced concrete. Considering this study as a stepping stone, the present research attempts to move the current state of affairs forward and to lay the groundwork for future research in this field by exploring the prospects of GI wire fiber reinforced concrete.

1.3 Objectives

The objectives of this research are:

a) To use GI wire bits to produce Galvanized Wire Reinforced Concrete (GWRC) with varying fiber contents.
b) To investigate various mechanical properties i.e. compressive strength, tensile strength, modulus of elasticity and ductility of GWRC.
c) To investigate the durability of GWRC.
d) To investigate strength and ductility of GWRC beams.

1.4 Scope of the Study

The main focus of the study is on strength, ductility and durability of GWRC. Three basic strength properties, namely compressive strength, split-cylinder tensile strength and modulus of elasticity have been determined for GWRC. Ductility has been assessed by flexural test of beams. Durability of concrete has been verified

through Rapid Chloride Permeability Test and water absorption capacity (Sorptivity) tests. Three types of coarse aggregate were used- crushed stone chips, gravel/ stone chips mixture and crushed clay bricks. The focus of the study is on concrete with brick chips as coarse aggregate, stone chips was used for comparing with previous works in relevant field. Due to a wide range of tests, mix-design of the concrete was kept the same with only variation being fiber content. Low volume fraction of fiber was deployed for the GWRC i.e. 1% to 2.5% on weight basis. Fiber content up to 6% by weight is not uncommon for SFRC; but for initial study, low fractions were preferred to judge the suitability of GI wire fiber as a substitute of steel fiber in FRC.

1.5 Thesis Organization

The thesis commences with presentation of knowledge acquired through perusal of literature regarding the topic of interest, Fiber Reinforced Concrete. Since little or no literature was available concerning GI wire fiber in concrete, most of the study was limited to steel fiber reinforced concrete and the information is offered in Chapter 2. Various types of materials such as cement, coarse aggregate, fine aggregate, GI wire etc. were used for the preparation of test specimens. Properties and relevant information about the materials are provided in Chapter 3. Mix-design principles, schedule of experimentation, methodology of experiments and their significance etc. are indispensible elements of a thesis if experiment is the basis of the thesis. Chapter 4 contains all these information with appropriate illustrations and also explanations for the choice of experiments. Chapter 5 covers the most significant part of the thesis- results of the experiments and their analysis. This chapter presents the findings from the experimental results and provides explanation for the behavior observed. Chapter 6 summarizes the overall research work and presents the conclusions and recommendations. Appendix A displays the stress strain curves from Modulus of Elasticity tests and Appendix B contains the raw data from Rapid Chloride Permeability Tests.

CHAPTER 2

Literature Review

2.1 Introduction

Fiber reinforcement of building materials has been used for hundreds of years for the purpose of construction. In early period, straw was used as additives in clay which made bricks stronger against failure. The method of adding these ingredients to bricks were unknown earlier, but the benefits of including them were clearly obvious for the improvement of bricks' strength. With the passage of time, numerous better performing materials were established and used for construction. Cement is one of the revolutionary materials in construction sector. But there has always been an incessant urge for further improvement and addition of fiber in cement matrix to change and enhance material characteristics is establishing itself over the past few decades.

Fiber material is being used with the intention to reinforce brittle matrices to enhance their mechanical properties. Concrete is a well-known brittle material which is strong in compression and weak in tension. Fibers increase the flexural strength by diminishing and arresting development of cracks in concrete and improve toughness by furnishing energy dissipating mechanisms. Fibers influence many other properties including shear and compressive strength. The strength and toughness of fiber reinforced concrete is affected by many parameters e.g. properties of the fiber, the matrix, the fiber-matrix interface, size, geometry and volume/weight fraction of fibers.

A good number of researches are found in the recent concrete history on Fiber Reinforced Concrete (FRC). However, no literature is available on use of GI wire as fiber in concrete. Therefore, researches on steel fiber reinforced concrete would provide the necessary guideline for the present research on GI wire fiber reinforced concrete. This chapter focuses on the previous works on Fiber Reinforced Concrete.

2.2 Fiber Reinforced Concrete

2.2.1 General

Fiber reinforced concrete (FRC) is a concrete mix containing water, cement, aggregate and discontinuous fibers of various shapes and sizes. According to Bentur & Mindess [2], fibers have been used as reinforcement for a long time. Asbestos was the first material widely used in the beginning of the 20th century. Man-made fibers produced from steel, glass, synthetics, asbestos and natural fibers such as cellulose, sisal and jute are examples of materials that are being used in contemporary FRC. Unreinforced concrete is, as known, a brittle material with high compressive strength but low tensile strength. Therefore, concrete requires reinforcement. The most known method is to use ordinary continuous reinforcing bars in order to increase the load carrying capacity in the tensile and shear zones. Fibers that are short materials randomly spread in the concrete mix, are however discontinuous. They do not enhance the (tensile) strength remarkably, but due to their random distribution in the mix, they are very effective and useful when it comes to controlling cracks. As a result, the ductility of fiber reinforced members is increased. Fibers can also be used in thin and complex members where ordinary reinforcement cannot fit well.

2.2.2 History

The use of fibers to reinforce and enhance the properties of construction materials can be traced back at least 3500 years ago, when straw was used to reinforce sun-baked bricks in Mesopotamia,. Cement-bound products have been reinforced by various types of fibers since the beginning of the last century at least. Furthermore, steel and synthetic fibers have increasingly been used to improve the properties of concrete for the past 30 or 40 years. Steel fibers reinforced concrete (SFRC) was introduced commercially into the European market in the second half of the 1970's, as mentioned by ccanz [3]. At that time any standards or recommendations were unavailable and this was the foremost restriction for the wide recognition of this new technology. Initially, steel fibers were mostly used as a substitute for secondary reinforcement or for controlling cracks in less critical parts of a construction. At present, steel fibers are extensively used as an integral and unique reinforcing for industrial floor slabs, shotcrete and prefabricated concrete products. They are also

being used and considered for structural purposes in reinforcement of slabs on piles, full replacement of the standard reinforcing cage for tunnel segments, concrete cellars, foundation slabs and shear reinforcement in prestressed elements.

2.2.3 Fiber Types and Classifications

According to Naaman[4], fibers used in cementitious composites can be classified as follows:

a. Origin of fibers:

According to origin, the fibers can be classified as natural organic (cellulose, sisal, bamboo, jute etc.), natural inorganic (asbestos, wollastonite, rock wool etc.) and man-made (steel, glass, synthetic etc.)

b. Physical/Chemical properties:

Fibers are classified based on their physical/chemical properties such as density, surface roughness, flammability, reactivity or non-reactivity with cementitious matrix etc.

c. Mechanical properties:

Fibers are also characterized based on their mechanical properties e.g. specific gravity, tensile strength, elastic modulus, ductility, elongation to failure, stiffness, surface adhesion etc.

d. Shape and size:

Classification of fibers is also based on geometric properties, such as cross sectional shape, length, diameter, surface deformation etc. Fibers can be of any cross sectional shape such as circular, rectangular, diamond, square, triangular, flat, polygonal, or any substantially polygonal shape. Figure 2.1 shows different cross sectional geometries of fibers.

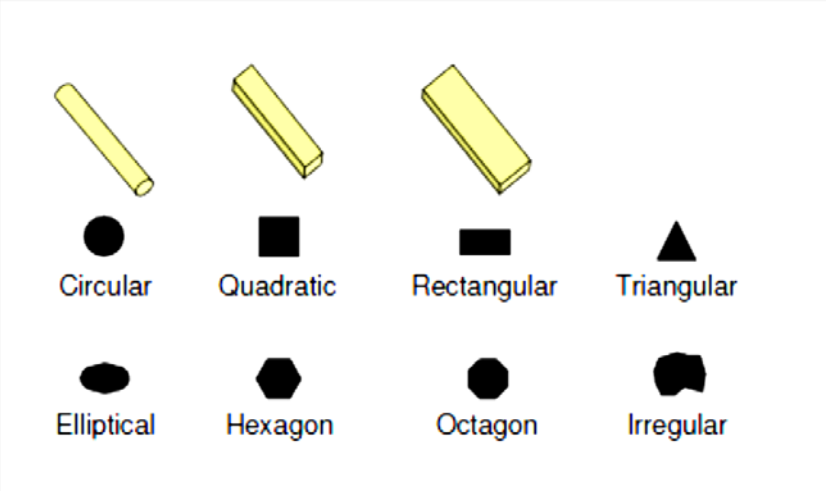

Figure 2.1: Various Cross sections of steel fibers used in FRC

2.3 Steel Fiber Reinforced Concrete

2.3.1 Introduction

Over the past years, the results of several research projects demonstrated that adding discrete, randomly distributed steel fibers could improve mechanical properties of concrete such as tensile strength, toughness, durability, fatigue life, and impact resistance [5-11]. The resulting composite material, typically referred to as steel fiber-reinforced concrete (SFRC), has several applications in the fields of shotcrete, rock slope stabilization, and tunneling. Because of its enhanced tensile strength and toughness in compression, SFRC has great potential for use in structural members. Previous investigations [12,13] suggested that SFRC can be used, for example, in columns to increase their toughness and delay spalling of the concrete cover.

2.3.2 Types of Steel Fiber

Steel Fiber Reinforced concrete (SFRC) utilizes steel fibers meeting one of the following four general types listed in ASTM A820. Based on shape, various types of steel fiber are shown in Figure 2.2.

a. Type I: Cold-drawn wire.

b. Type II: Cut sheet.

c. Type III: Melt-extracted.

d. Type IV: Other fibers

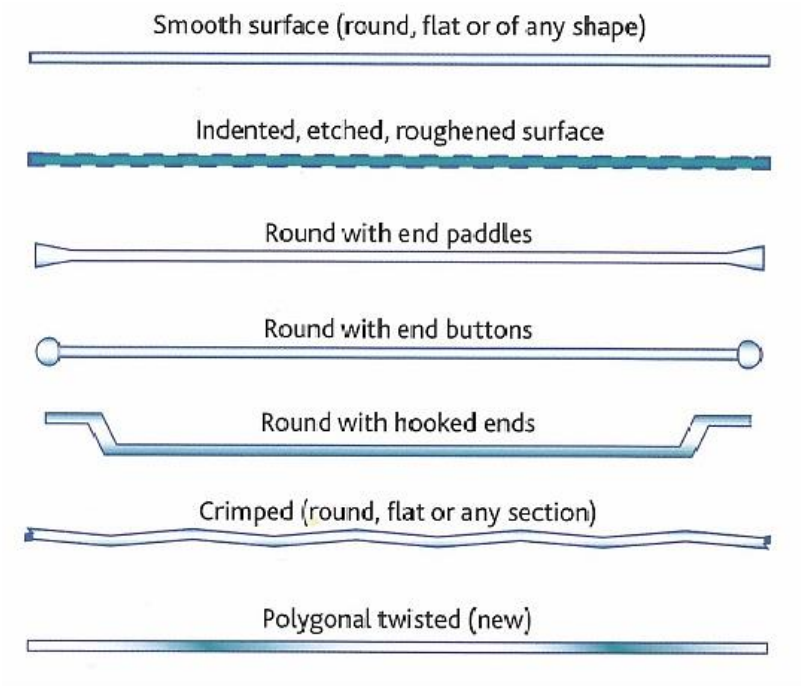

Figure 2.2: Various types of steel fibers used in FRC [2]

2.3.3 Specifications for Steel Fiber used in FRC

According to ACI 544.3R[14], the length of the steel fiber to be used in FRC generally varies between 0.5 in. (12.7 mm) to 2.5 in. (63.5 mm) and the most common fiber diameters are in the range of 0.017 in. (0.45 mm) to 0.04 in. (1.0 mm).In addition, the code stipulates that the aspect ratio should be between 30-100 with aspect ratio(λ) being the ratio of length(l) to diameter(d) or equivalent diameter(d_e). The specifications for aforementioned parameters of steel fibers in ASTM-A 820/A 820M[15] and BS EN 14889-1:2006[16] conforms fully to the specifications ofACI 544.3R. Moreover, the standard steel fiber must have a minimum ultimate tensile strength of 50,000 psi (345 MPa) but fibers are available with strengths up to 300,000 psi (2068 MPa) [14]. Furthermore, standard fiber must satisfy bending requirements which provide a general indication of fiber ductility, as may be important in resisting breakage during handling and mixing operations, in accordance with ASTM-A 820/A 820M.

2.3.4 Specifications for SFRC

Steel fiber reinforced concrete is usually specified by strength and fiber content. In certain applications, toughness parameters may be specified. These are defined in ASTM C 1018[17], ACI 544.2R[18], ACI 544.3R [14].

Whilst the flexural strength is normally specified for paving applications, compressive strength is generally specified for structural applications. A flexural strength of 700 to 1000 psi (4.8 to 6.9 MPa) at 28 days and a compressive strength of 5000 to 7000 psi (34.5 to 48.3 MPa) are considered as typical values. Although the addition of fibers does not significantly increase compressive strength, it enhances the compressive strain at ultimate load. As a result, general guidelines for concrete proportioning may be provided by specifying compressive strength, but it should not be allowed for the assessment of improvement in properties, such as flexural strength and toughness, that are directly attributable to fibers and other improvements such as increased tensile strain capacity and resistance to cracking [14].

For normal weight concrete, fiber contents vary from as low as 50 lb/yd³ (30 kg/m³) to as high as 265 lb/yd³ (157 kg/m³), although the high range limit is usually about 160 to 200 lb/yd³ (95 to 118 kg/m³). The amount of fibers that can be used without unacceptable loss of workability of SFRC depends upon the placement conditions, the degree of congestion of conventional reinforcement, the fiber shape and aspect ratio (l/d) and the type and amount of water-reducing admixtures used. Fiber manufacturers and technical literature should be consulted for more specific information. Similar consideration applies for lightweight concrete.

Toughness, which is the concrete property represented by the area under a load-deflection curve, or a toughness index, which is a function of that area and the area up to first crack (the point at which the load-deflection curve becomes nonlinear) may be specified to define the performance requirements of SFRC intended for use where post-cracking energy absorption or resistance to failure after cracking are important. The properties are essential in situations such as structures subjected to earthquakes or explosive blasts, impact loads, cavitation loads, thermal shock, and other dynamic loads. ASTM C 1018 [17] is the standard test for determining flexural toughness parameters and first crack strength. Flexural strength (modulus of rupture) can be determined by either ASTM C 78[19] or C 1018. The manufacture and placing

of SRFC is almost identical to conventional concrete. ASTM C 1116[20], Standard Specification for Fiber Reinforced Concrete and Shotcrete, covers the manufacture of SFRC. Most existing concrete specifications can be used for the placement of SFRC with some added requirements to account for the differences in material and application techniques.

2.3.5 Mixture Proportioning

As with conventional concrete, SFRC mixtures deploy a variety of mixture proportions depending upon the end use. Especially, they must be proportioned for a project or selected to be the same as a mixture previously used. In either case, they must be adjusted for yield, workability, cement content, maximum allowable water content, the type and amount of fibers to be used, and the type, name, and dosage of admixtures, if admixtures are being used.

In general, SFRC mixes contain higher cement contents and higher ratios of fine to coarse aggregate than do ordinary concretes, and thus the mix design procedures that apply to conventional concrete may not be applicable to SFRC entirely. Usually, to reduce the quantity of cement, up to 35% of the cement may be replaced with fly ash. In addition, to improve the workability of higher fibers volume mixes, water reducing admixtures and, in particular, super plasticizers are often used, along with air entrainment.

In many projects, steel fibers have been added without any changes to the conventional mixture proportions used by ready-mix suppliers for the required concrete compressive strength. However, when large amount of fibers per unit volume are used, some adjustments may be required. For getting better workability of the concrete, more paste is required in the mixture. Therefore, the ratio of fine to coarse aggregate is adjusted upward accordingly. To prevent wet fiber balls, avoid over-mixing and using a mixture with excessive coarse aggregate (more than about 55 percent of the total combined aggregate by absolute volume). In early applications, coarse aggregate larger than ¾ in. (19 mm) was not recommended for SFRC. However, based on the experiment conducted by Tatro[21], recent placements have successfully used aggregate as large as 1½ in. (38 mm) [22].

Procedures for proportioning of SFRC mixtures, with emphasis on good workability, are available in a number of literatures [2,23,24,25]. Some typical proportions that have been used are shown in Table 2.1 as provided in ACI 544.3R [14].

Table 2.1: Range of proportions for normal weight fiber reinforce Concrete

Material	9.5 mm maximum-sized	19 mm maximum-sized	38 mm maximum-sized
Cement (kg/m^3)	350-600	300-530	280-420
w/c ratio (kg/kg)	0.35-0.45	0.35-0.50	0.35-0.55
Fine/coarse aggregate ratio	0.45-0.60	0.45-0.55	0.40-0.55
Entrained air content percent	4-8	4-6	4-5
Fiber content, volume percent			
Smooth steel fiber	0.8-2.0	0.6-1.6	0.4-1.4
Deformed steel fiber	0.4-1.0	0.3-0.8	0.2-0.7

$1kg/m^3$= 1.6855 lb/yd^3; 1 in. = 25.4 mm; 1 steel fiber volume percent = 78.5 kg/m^3 (132.3 lb/yd^3).

For steel fibers reinforced shotcrete, different considerations apply, with most mix designs being arrived at empirically. Since fiber rebound is generally greater than aggregate rebound, usually a smaller percentage of fiber is used in shotcrete mixes. Typical mix designs for steel fibers shotcrete are given in table 2.2 as provided by Karim et al.[1]

Table 2.2: Typical steel fiber reinforce shotcrete mixes

Material	Fine aggregate mixture (kg/m^3)	9.5 mm Aggregate mixture (kg/m^3)
Cement	446-559	445
Blended sand (<6.35mm)	1438-1679	697-880
9.5 mm aggregate	-	700-875
Steel fiber, volume percent	35-157	39-150
Accelerator	Varies	Varies
w/c ratio	0.40-0.45	0.40-0.45

2.3.6 Behavior of SFRC

2.3.6.1 General

Steel fibers do not remarkably affect the compressive strength of the concrete that they are reinforcing, and the compressive strength is determined by standard cylinder tests in exactly the same way as for plain concrete. It is also generally accepted that steel fibers at normaldoses do not significantly enhance the tensile strength of concrete. In other words, steel fiber reinforced concrete will crack at approximately the same values of flexural or direct tensile stress as it would if it was unreinforced. However, when steel fibers are present, a number of them intercept micro-cracks as they form and continue to provide tensile capacity across the cracks. The level of tensile capacity provided across these cracks is usually evaluated in the laboratory using standard beam or panel tests and is expressed in terms of residual post-crack strength or energy absorption. This compares to conventional reinforcing that becomes effective only when macro-cracks have developed, as seen in Figure 2.3.

In most structural applications, traditional reinforcing is provided to ensure that the load bearing capacity of the cracked section exceeds the capacity of the plain concrete. At dosages of up to approximately 40 kg/m3 dependent on the aspect ratio of the fibers used, the post crack flexural capacity provided by the steel fibers is typically less than the capacity of the uncracked concrete [3], this type of behavior as shown in Figure 2.4 is described as strain softening.

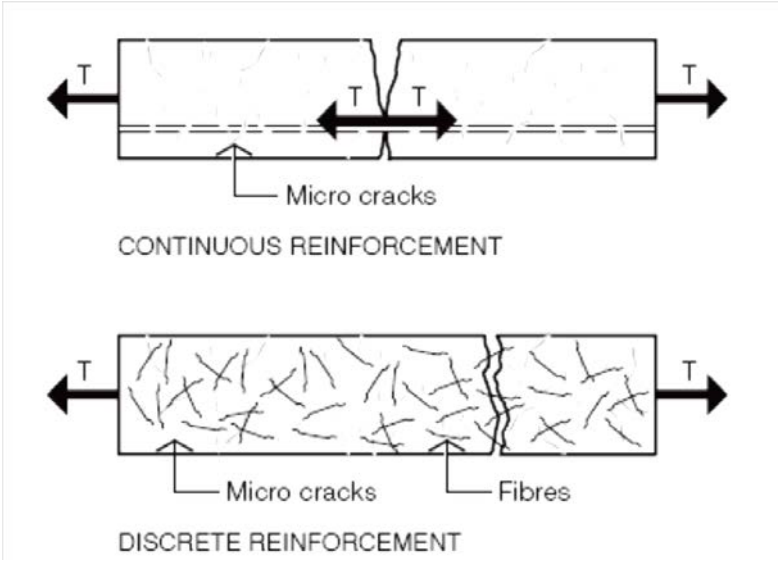

Figure 2.3: Reinforcement in a concrete mix [2]

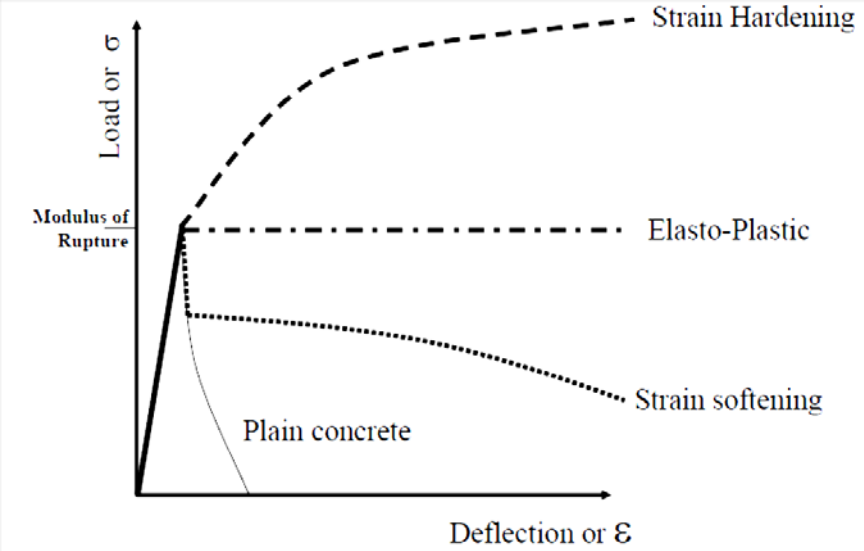

Figure 2.4: Typical load/ deflection (stress/ strain) plots of fiber reinforced concrete[3]

This strain softening characteristic means that at a crack the moment carrying capacity is less than in the adjacent uncracked concrete and the crack is effectively a plastic hinge. In elements where a single crack forming is enough to turn the element into a mechanism i.e. a simply supported or statically determinate beam, the post cracked load carrying capacity will be less than for the uncracked element. However, in statically indeterminate elements, where more than one crack is required to create a mechanism i.e. a built-in or continuous beam, in which moment redistribution can take place, the load carrying capacity will increase even as cracking occurs, right up until the last crack forms and the element becomes a mechanism. Once the mechanism is completed the load carrying capacity will then fall away.

Consequently, steel fibers are generally used as sub-critical reinforcing in statically determinate structures such as beams, columns, suspended slabs etc. However, in applications that are statically indeterminate where load redistribution is possible, e.g. ground supported slabs, shotcrete etc., and steel fibers have the ability to increase the load carrying capacity of the concrete element.

The tension provided by steel fibers across cracks as they continue to open allows load versus deflection curves to be plotted for fiber reinforced test samples. The area under such curves has the units Nm or Joules and measures the energy that can be absorbed by the element. When fiber reinforced sections are able to absorb significant levels of energy they are said to possess ductility or toughness, and

load/deflection tests are commonly referred to as ‘Toughness Tests’. Research results on various properties of SFRC are presented in the following section.

2.3.6.2 Compressive Strength

Fibers do little to enhance the static compressive strength of concrete, with increases in strength ranging from essentially nil to perhaps 25%. Even in members that contain conventional reinforcement in addition to the steel fibers, the fibers have little effect on compressive strength. However, the fibers do substantially increase the post-cracking ductility, or energy absorption of the material. This is shown graphically in the compressive stress-strain curves of SFRC in Figure 2.5 .

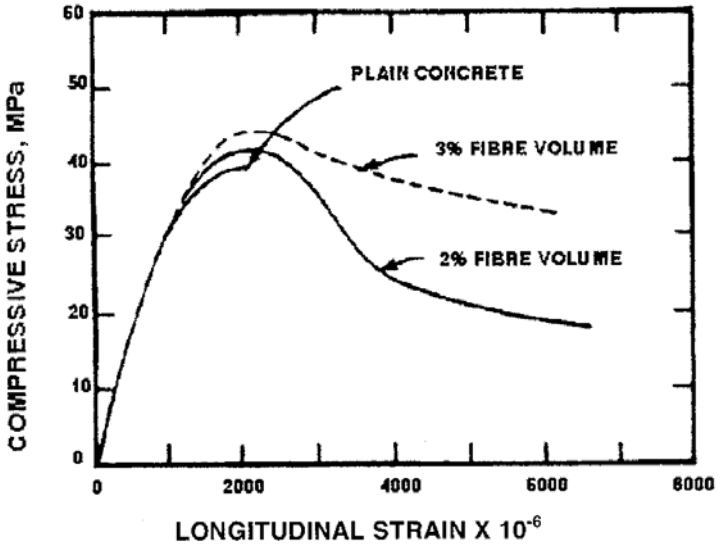

Figure 2.5: Stress-strain curves in compression for SFRC [26]

2.3.6.3 Tensile Strength

Fibers aligned in the direction of the tensile stress may bring about very large increases in direct tensile strength, as high as 133% for 5% of smooth, straight steel fibers [4]. However, for more or less randomly distributed fibers, the increase in strength is much smaller, ranging from as little as no increase in some instances to perhaps 60%, with many investigations indicating intermediate values, as shown in figure 2.6. Splitting-tension test of SFRC show similar result. Thus, adding fibers merely to increase the direct tensile strength is probably not worthwhile. However, as in compression, steel fibers do lead to major increases in the post-cracking behavior or toughness of the composites.

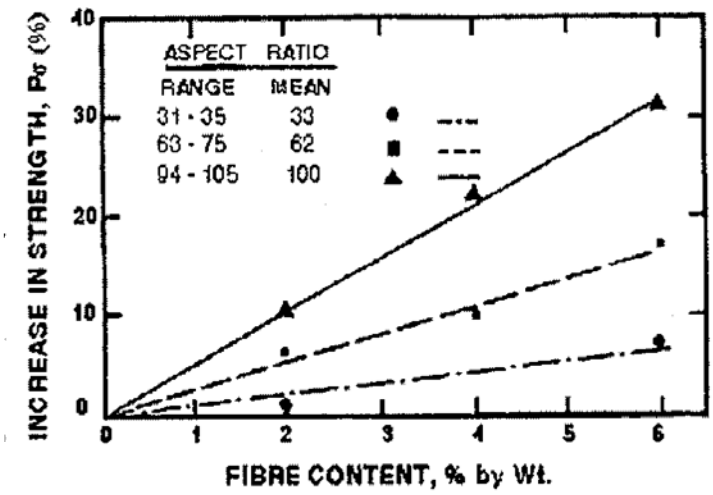

Figure 2.6: Influence of fiber content and aspect ratio on tensile strength. [26]

2.3.6.4 Flexural Strength

Steel fibers are generally found to have aggregate much greater effect on the flexural strength of SFRC than on either the compressive or tensile strength, with increases of more than 100% having been reported. The increases in flexural strength are particularly sensitive, not only to the fibers volume, but also to the aspect ratio of the fibers, with higher aspect ratio leading to larger strength increases. Figure 2.7(a) describes the fibers effect in terms of the combined parameter W*l/d*, where *l/d* is the aspect ratio and W is the weight percent of fibers. It should be noted that for W*l/d* > 600, the mix characteristics tended to be quite unsatisfactory. Deformed fibers show the same types of increases at lower volumes, because of their improved bond characteristics.

Fibers are added to concrete not to improve the strength, but primarily to improve the toughness, or energy absorption capacity. Commonly, the flexural toughness is defined as the area under the complete load-deflection curve in flexure; this is sometimes referred to as the total energy to fracture. Alternatively, the toughness may be defined as the area under the load-deflection curve out to some particular deflection, or out to the point at which the load has fallen

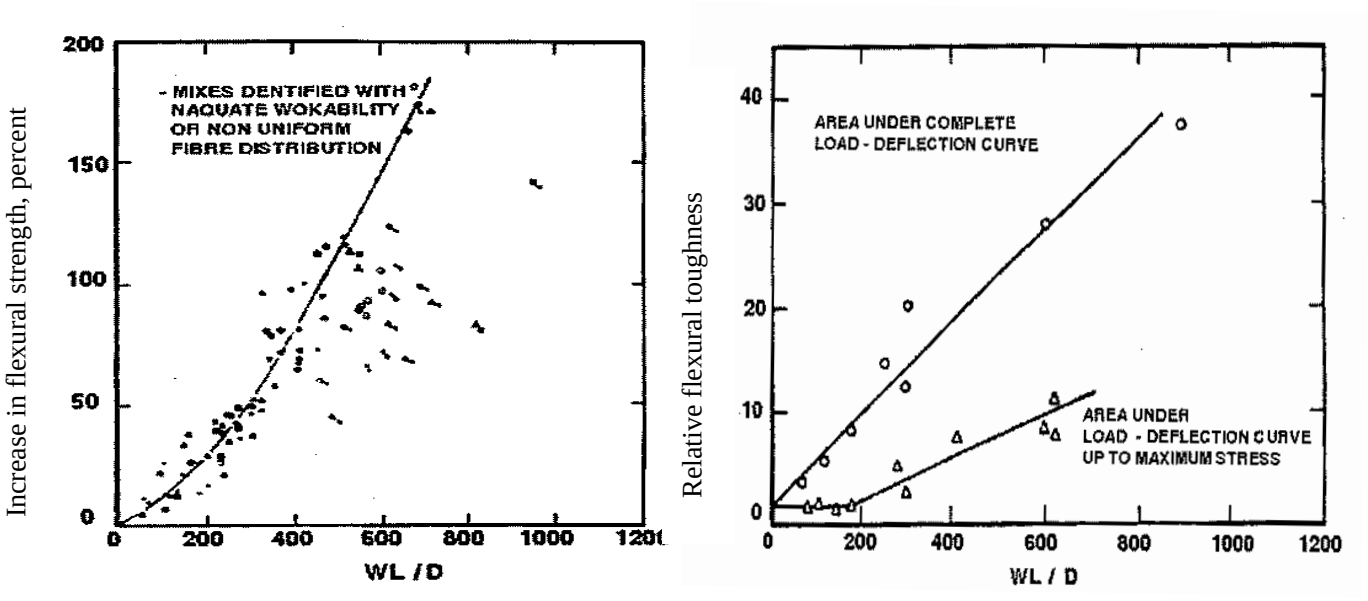

Figure 2.7: (a) Effect of Wl/d on the flexural strength of mortar and concrete [26]

(b) The effect of Wl/d on the flexural deflection curves toughness of SFRC[26]

back to some fixed percentage of the peak load. Probably the most commonly used measure of toughness is the toughness index proposed by Johnston and incorporated into ASTM C1018. As is the case with flexural strength, flexural toughness also increases at the parameter W*l/d* increases, as shown in figure 2.7(b).

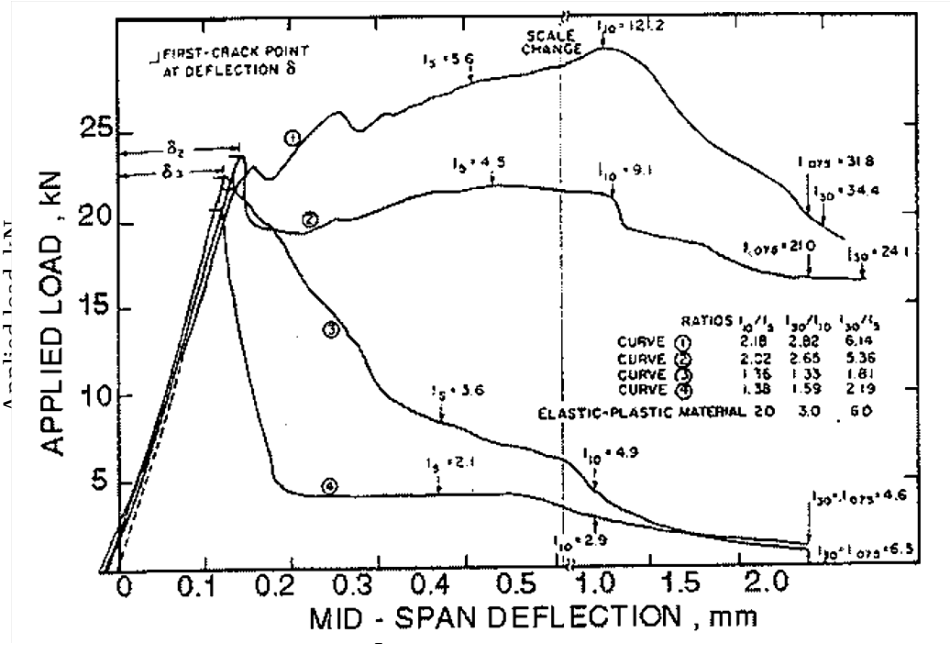

Figure 2.8: A range of load-deflection curves obtained in the testing of steel fiber reinforced concrete [27]

The load-deflection curves for different types and volumes of steel fibers can vary enormously, as was shown previously in figure 2.8. For all of the empirical measures of toughness, fibers with better bond characteristics (i.e. deformed fibers, or fibers with greater aspect ratio) give higher toughness values than do smooth, straight fibers at the same volume concentrations.

2.3.7 Behavior of SFRC with conventional reinforcement

After the inception of the idea of steel fiber reinforced concrete, most studies, for many years, were confined to the investigation of plain fiber-reinforced concrete beams without main steel reinforcements. Since the application of fibers to reinforced concrete structural members is one of the major areas of fiber use in structural engineering, investigation on the effects of fiber reinforcement on conventional reinforced concrete members followed eventually [28-30].

A research was carried out by Byung Hwan Oh [9] to explore the mechanical behavior of reinforced concrete beams containing steel fibers. The fiber contents of reinforced concrete beams for each series were varied from 0% to 2% by volume and various properties were measured during the tests in order to explore the mechanical characteristics of fiber-reinforced concrete beams. Notable findings of the research are discussed in the following sections.

2.3.7.1 Flexural Strength

The tests indicated that the flexural strength of fiber-reinforced concrete was greatly enhanced due to the addition of steel fibers. The rate of increase of flexural strength was about 60% when the fiber content was increased to 2% (see Figure 2.9). One more important feature in flexural behavior is that the fiber-reinforced concrete showed a remarkable ductility and energy absorption capacity.

2.3.7.2 Load-Deflection Behavior

The load-deflection curves were plotted for both singly and doubly reinforced concrete beams. Figure 2.10 shows the load-deflection curves for singly reinforced concrete beams with reinforcement ratio $\rho = 0.40\rho_b$. The figure indicates that the ultimate resistance of fiber-reinforced concrete beams is remarkably increased with an increase of fiber contents. The rate of increase of maximum load capacity reaches up

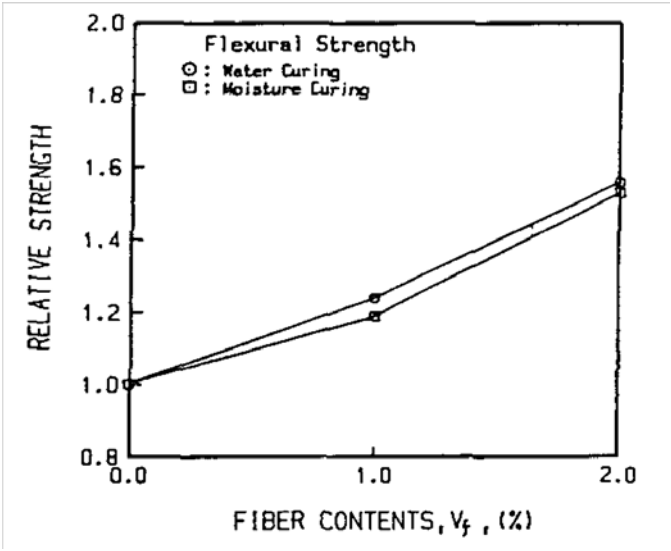

Figure 2.9: Relative increase of flexural strength due to fiber addition [9]

to 50% for the fiber content of 2%. The ductility and energy absorption capacity are also considerably increased with the addition of steel fibers. This salient feature is the foremost advantage of fiber-reinforced concrete and can be applied to earthquake-resistant structures.

Figure 2.11 represents the load-deflection behavior for the singly reinforced concrete beams that have slightly higher reinforcement ratios, i.e., $\rho = 0.65\rho_b$. Figure 2.12 depicts the load-deflection curves obtained from the doubly reinforced concrete beams. It is evident from these figures that the effect of steel fibers is more pronounced for the case of lightly reinforced concrete beams. The increase of load-carrying capacity due to fiber addition for the moderately reinforced fiber concrete beams (Figure 2.11) is less than that of lightly reinforced concrete beams. This may occur due to the fact that the steel fibers play a crucial role to curb the crack occurrence and exhibit considerable resistance to tensile cracking of concrete.

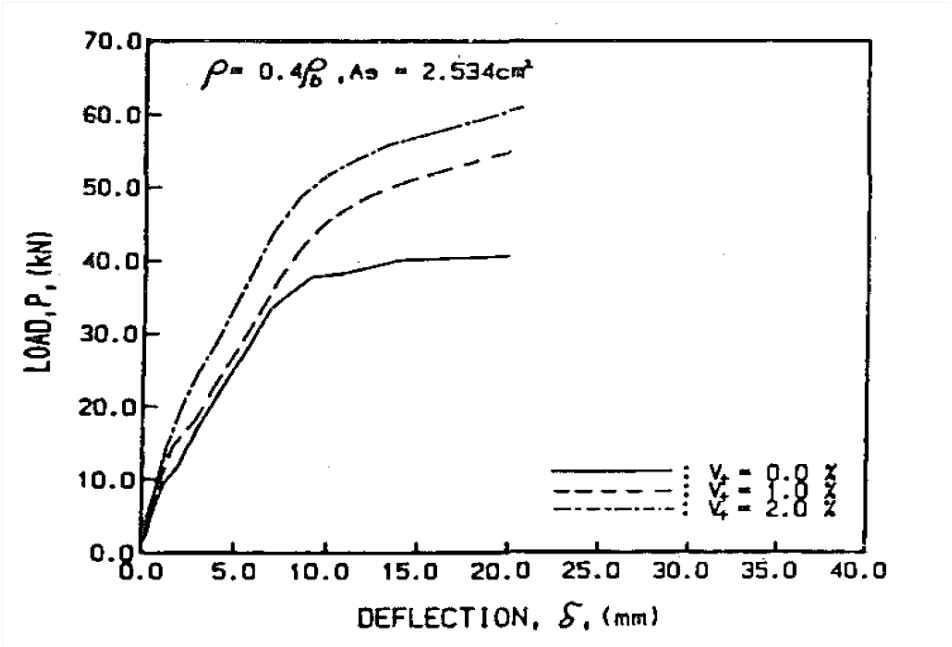

Figure 2.10: Load-deflection curves for singly reinforced concrete beams ($\rho = 0.40\rho_b$) [9]

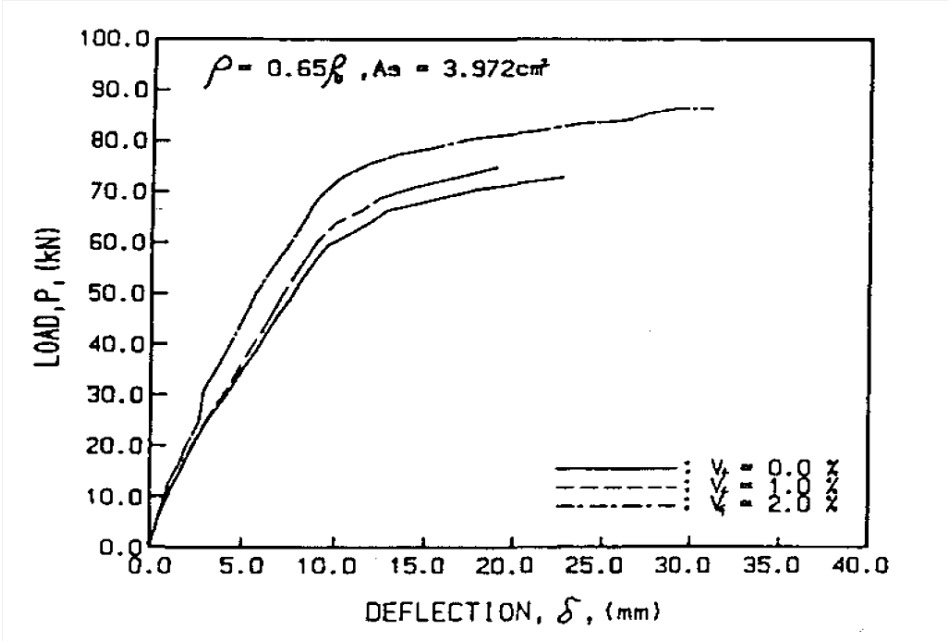

Figure 2.11: Load-deflection curves for singly reinforced concrete beams ($\rho = 0.65\rho_b$) [9]

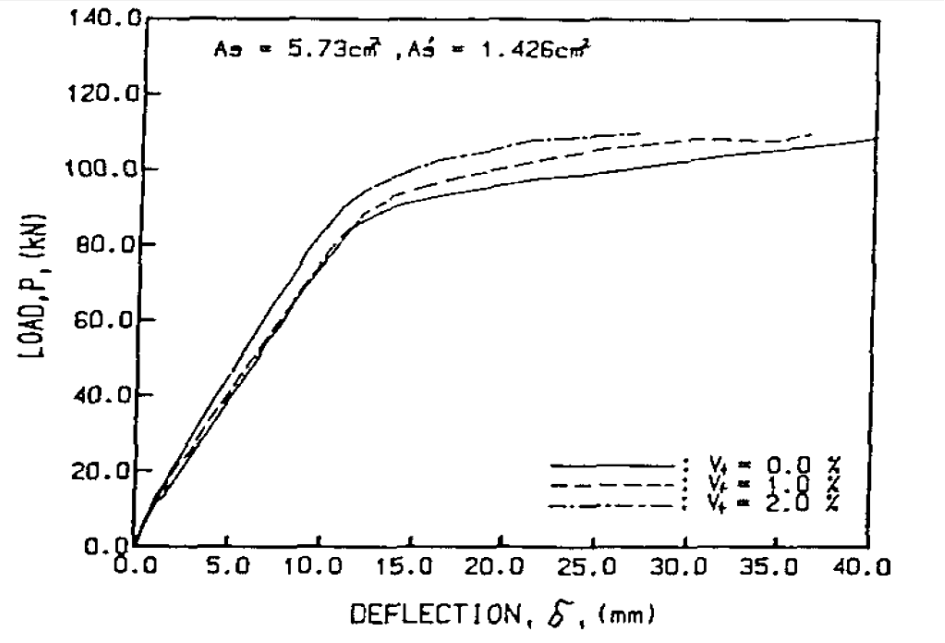

Figure 2.12: Load-deflection curves for doubly reinforced concrete beams [9]

2.4 Galvanized Iron Fiber Reinforced Concrete

2.2.1 General

Performance of steel fiber in FRC to improve mechanical properties of concrete such as tensile strength, ductility, toughness, fatigue life, impact resistance etc. has already been established in a number of researches. But additional cost for steel fibers has always been an issue to address. In this concern, fibers from GI (Galvanized Iron) wire can provide a viable low cost substitute for steel fibers, especially for Bangladesh since steel fiber for use in FRC is not available in local market and importing from the cheapest of sources proves quite expensive. Moreover, GI wire is locally produced and is available at a relatively low price. Hence, a research has recently been carried out by Karim et al. [1] to investigate the properties of GI wire so that a proper comparison can be established between the properties of steel fiber and GI wire fiber. It was also studied if GI wire fiber conforms to the ACI and ASTM standards for steel fibers to be used in SFRC (Steel Fiber Reinforced Concrete). In addition, compressive strength of GWRC (Galvanized Wire Reinforced Concrete) with variable GI fiber percentage was tested so that an initial comparison can be made between GI wire in GWRC and steel fiber in SFRC.

2.2.2 Performance of GI wire as Fiber

Tests were performed on GI wire with three different diameters: 0.50mm, 0.70mm and 1.00mm as per ASTM A 370. 3 specimens of each diameter were tested for both tensile and bending requirements.

All the G.I wires showed similar behavior during each test under tensile stress. From the various test results, it was found that all the GI wire samples have produced stress-strain curves which are similar to those typically produced by steel in tension as found by Holt [31].

2.2.3 Performance of GI wire fiber reinforced concrete (GWRC)

ACI standard mix design used for determining concrete mix ratio. To achieve a characteristic strength of 35 MPa at 28 days, water cement ratio was taken as 0.47. GI wire fiber content was 0.5%, 1.0%, 1.5%, 2.0% and 2.5% by weight. Suitable length for the GI wire fibers was taken to be 1.5 in. (37.5 mm). The resulting aspect ratio of 53.57 falls within the limit of 30 to 100 as specified in ACI 544.3R or ASTM-A820/A820M. Therefore, 0.70 mm diameter GI wire was cut into 1.5 in. pieces to produce GI wire fiber which was used to prepare GWRC with an aim at comparing with SFRC.

All the specimens were prepared, cured and tested according to ASTM C192/C192M [32]. Result from the compression tests is tabulated in Table 2.3. The GWRC samples showed increased compressive strength as compared to normal concrete samples. GWRC samples also showed increased ductility and toughness as fibers within the matrix bridge across the cracks and provide a confining effect which adds to the strength and also helps carry a significant stress over a large strain capacity even during the post-cracking phase.

Table 2.3: Results from Compressive strength test

Serial	Sample type	Compressive Strength(Mpa)			Strength increase (28 days)
		7 Days	14 Days	28 Days	
1	Standard	18.81	24.67	30.08	-
2	0.50% G.I Wire	21.62	22.66	31.05	3.22%
3	1.00% G.I Wire	21.86	22.78	31.13	3.49%
4	1.50% G.I Wire	24.17	25.73	31.9	6.05%
5	2.00% G.I Wire	26.11	28.72	36.98	22.94%
6	2.50% G.I Wire	28.11	36.14	39.23	30.42%

ASTM C 1609 was followed for determination of flexural strength. Beams having cross sectional dimension of 150mm X 150mm and a length of 500 mm were tested with mid-point loading. Load-deflection curves from the tests are presented in Figure 2.13. Comparison between the performances of the samples can be made from the flexural strength chart in Figure 2.14.

The results show significant improvement in flexural strength and ductility for GWRC. The peak load deflection is smaller in GWRC samples compared to normal concrete samples. The ultimate failure load and ductility were higher than the standard sample. The experimental results show that increase in flexural strength was 4.5% and 19%.for 1.5% and 2% GI fiber content respectively.

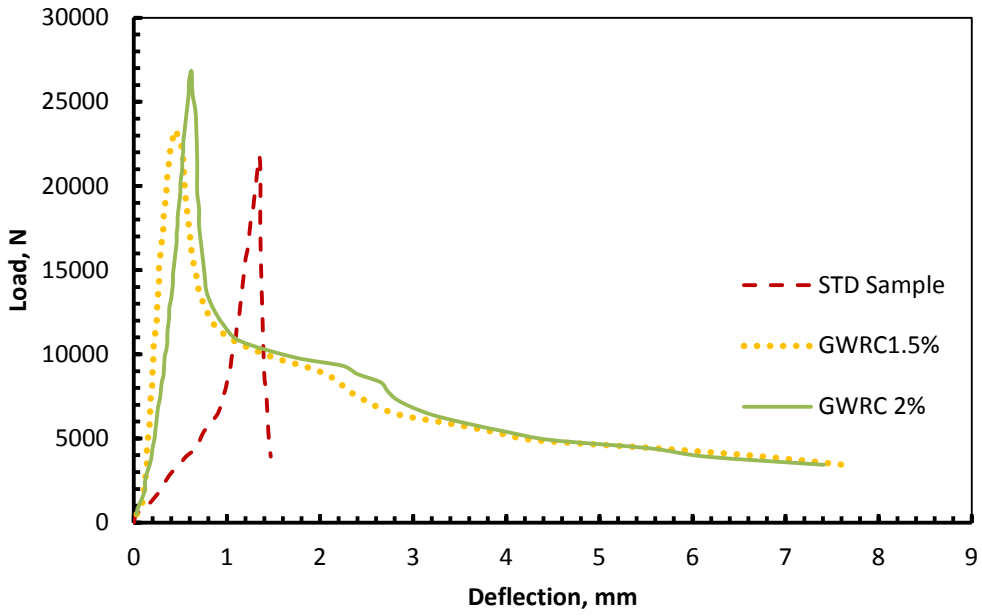

Figure 2.13: Load-deflection curves of normal concrete and GWRC

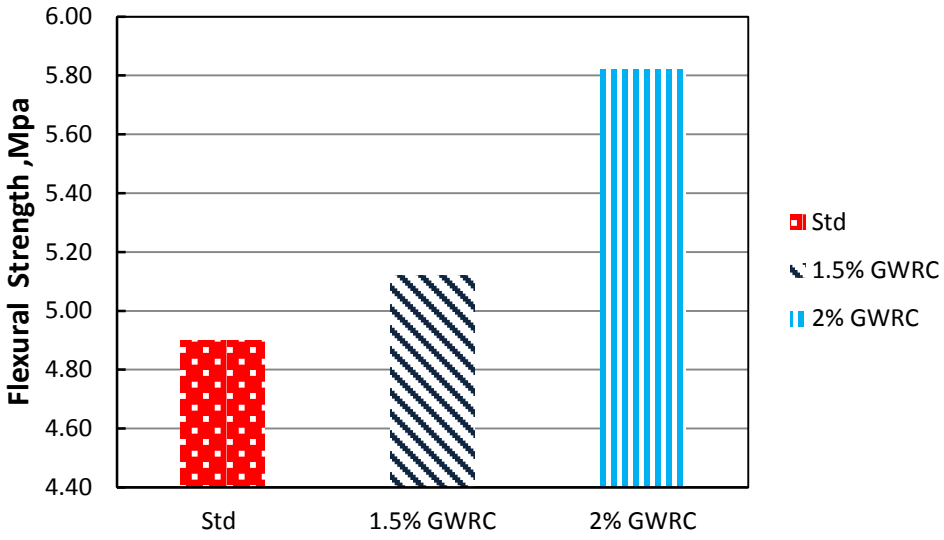

Figure 2.14: Flexural strength of normal concrete and GWRC

CHAPTER 3

Materials

3.1 Introduction

Concrete is a stone like material obtained by permitting a carefully proportioned mixture of cement, sand and gravel or other aggregate, and water to harden in the forms of the shape and dimensions of the desired structure [33]. The bulk of the material consists of fine and coarse aggregate. Cement and water interact chemically to bind the aggregate particles into solid mass. Even though aggregate typically accounts for 70% to 80% of the concrete volume, it is commonly thought of as inert filler having little effect on the finished concrete properties since cement is the material that has the adhesive and cohesive properties necessary to bond these inert aggregates into a solid mass of adequate strength and ductility. Yet, aggregate plays a substantial role in determining workability, strength, dimensional stability, and durability of the concrete and also have a significant effect on the cost of the concrete mixture. Therefore, properties of both cement and aggregates are of utmost importance in ensuring the desired performance of conventional concrete. But for fiber reinforced concrete, fiber is one of the most important elements and has a vital role to enhance the mechanical properties of the concrete. Efficiency of fiber reinforcement is dependent on the achievement of uniform distribution of fiber within the concrete, their interaction with the cement matrix and the ability of the concrete to be successfully cast or spread. Though, addition of fiber affects the workability of the concrete and also impedes the placement, the problem can be overcome with careful mixing and good workmanship. Hence, selecting materials with the proper attributes is one of the prerequisites of achieving desired performance from concrete.

3.2 Cement

3.2.1 General

Cement is the binding material in concrete and thereby, the most important component of concrete. The main ingredient of cement is clinker which is manufactured by blending and grinding limestone, sand, clay and iron and heating to a temperature of 1450˚C (2640˚F) in a rotary kiln. The cement obtained from pulverizing clinker and gypsum is called Portland cement which is the most widely used cement all over the world. Portland cement is categorized as hydraulic cement since hydration of key ingredients of cement is the primary mechanism of strength development. About 90-95% of Portland cement is comprised of the four main cement minerals, which are Tricalcium Silicate (C_3S), Dicalcium Silicate (C_2S), Tricalcium Aluminate (C_3A), and Tetracalcium Aluminoferrite **(**C_4AF), with the remainder consisting of calcium sulfate, alkali sulfates, unreacted (free) CaO, MgO, and other minor constituents left over from the clinkering and grinding steps. The four cement minerals play different roles in the hydration process that converts the dry cement into hardened cement paste. The C_3S and the C_2S contribute virtually all of the beneficial properties by generating the main hydration product, C-S-H gel. However, the C_3S hydrates much more quickly than the C_2S and thus is responsible for the early strength development. The C_3A and C_4AF minerals also hydrate, but the products that are formed contribute little to the properties of the cement paste.

3.2.2 Classifications

Portland cement can be classified in various ways. In Bangladesh, based on the percentage of clinker, Portland cement is classified into two main categories: Ordinary Portland Cement (OPC) and Portland Composite Cement (PCC). Ordinary Portland Cement and Portland Composite Cement are designated as CEM-I and CEM-II respectively. OPC consists 95-100% of clinker and 0-5% of gypsum. On the other hand, PCC contains about 65-80% clinker, 0-5% gypsum and 15-35% pozzolanic materials such as slag, fly ash, silica fume etc.

The ASTM has designated five types of Ordinary Portland Cement, designated Types I-V. Physically and chemically, these cement types differ primarily in their

content of C_3A and in their fineness. In terms of performance, they differ primarily in the rate of early hydration and in their ability to resist sulfate attack. The general characteristics of these types are listed in Table 3.1.

Table 3.1: Classification of OPC according to ASTM

	Classification	**Characteristics**	**Applications**
Type I	General purpose	Fairly high C_3S content for good early strength development	General construction (most buildings, bridges, pavements, precast units, etc)
Type II	Moderate sulfate resistance	Low C_3A content (<8%)	Structures exposed to soil or water containing sulfate ions
Type III	High early strength	Ground more finely, may have slightly more C_3S	Rapid construction, cold weather concreting
Type IV	Low heat of hydration (slow reacting)	Low content of C_3S (<50%) and C_3A	Massive structures such as dams. Now rare.
Type V	High sulfate resistance	Very low C_3A content (<5%)	Structures exposed to high levels of sulfate ions
White	White color	No C_4AF, low MgO	Decorative (otherwise has properties similar to Type I)

3.2.3 Selection

The objective of the present study is to investigate strength and ductility of GI wire fiber reinforced concrete and comparing the results with the performance of

ordinary concrete without fiber. Therefore, cement properties are not of prime importance for the current research and any locally available cement would meet the requirements as long as all the specimens were prepared using the same cement. Consequently, the research was conducted using *Holcim Portland Composite Cement* due to its availability.

3.3 Aggregates

3.3.1 General

Aggregates are inert granular materials such as sand, gravel, or crushed stone that is thought to serve as the filler within the concrete mix. But aggregates have a significant influence and play a key role in the properties of both fresh and hardened concrete. Changes in gradation, maximum size, unit weight, and moisture content in the aggregates can all cause alteration in the character and performance of the concrete mix. Hence, the importance of using the right type and quality of aggregates cannot be exaggerated. Generally, aggregates constitute 60% to 75% of the concrete volume (70% to 85% by mass) and are divided into two distinct categories- coarse and fine. Fine aggregates generally consist of natural sand or crushed stone with most particles smaller than 5mm (0.2 in.) and thereby pass through a 3/8-inch sieve. Coarse aggregates are any particles greater than 5mm (0.2 in.), but generally range between 9.5 mm and 37.5 mm ($^{3}/_{8}$ in. and $1^{1}/_{2}$ in.) in diameter [34]. Gravels constitute the majority of coarse aggregate used in concrete with crushed stone making up most of the remainder.

3.3.2 Properties

Aggregates strongly influence both fresh and hardened properties of concrete, mixture proportions, and economy. Consequently, selection of aggregates is an important process. Although some variation in aggregate properties is expected, characteristics that are considered include:

- Grading
- Durability

- Particle shape and surface texture
- Strength and shrinkage
- Abrasion and skid resistance
- Unit weights and voids
- Absorption and surface moisture
- Presence of undesirable components and coatings
- Resistance to acid and other corrosive substances
- Fire resistance and thermal properties etc.

Grading refers to the determination of the particle-size distribution for aggregate. Grading limits and maximum aggregate size are specified because these properties affect the amount of aggregate used as well as cement and water requirements, workability, pumpability, and durability of concrete. In general, if the water-cement ratio is chosen correctly, a wide range in grading can be used without a major effect on strength. When gap-graded aggregate are specified, certain particle sizes of aggregate are omitted from the size continuum. Gap-graded aggregate are used to obtain uniform textures in exposed aggregate concrete. Close control of mix proportions is necessary to avoid segregation [34].

Particle shape and surface texture influence the properties of freshly mixed concrete more than the properties of hardened concrete. Rough-textured, angular, and elongated particles require more water to produce workable concrete than smooth, rounded compact aggregate. Consequently, the cement content must also be increased to maintain the water-cement ratio. Generally, flat and elongated particles are avoided or are limited to about 15 percent by weight of the total aggregate. Unit-weight measures the volume that graded aggregate and the voids between them will occupy in concrete.

The void content between particles affects the amount of cement paste required for the mix. Angular aggregates increase the void content. Larger sizes of well-graded aggregate and improved grading decrease the void content. Absorption and surface

moisture of aggregate are measured when selecting aggregate because the internal structure of aggregate is made up of solid material and voids that may or may not contain water. The amount of water in the concrete mixture must be adjusted to include the moisture conditions of the aggregate.

Abrasion and skid resistance of an aggregate are essential when the aggregate is to be used in concrete constantly subject to abrasion as in heavy-duty floors or pavements. Different minerals in the aggregate wear and polish at different rates. Harder aggregate can be selected in highly abrasive conditions to minimize wear.

3.3.3 Coarse Aggregate

Coarse aggregate consists of particles that are more than 9.5 mm ($^3/_8$in.) and generally less than 37.5 mm ($1\ ^1/_2$in.) in size. Coarse aggregate can be extracted from various sources. The usual sources of coarse aggregate are quarry rock, boulders, cobbles, gravels etc. There are some other sources that are not common everywhere but provides materials to be used as coarse aggregate in concrete such as crushed air-cooled blast furnace slag, burnt clay bricks, synthetic aggregates, recycled concrete etc. In North America, close to half of the coarse aggregates used in Portland cement concrete are gravels; most of the remainder are crushed stones [34]. In Bangladesh, however, crushed clay bricks provide a valuable source of lightweight aggregate and are used massively in concrete along with crushed stone and gravels. For the present research, three kind of coarse aggregate is used-

- Crushed stone (Stone chips)
- Crushed clay bricks (Brick chips)
- Mixture of gravel/shingle and crushed stone

3.3.3.1 Crushed stone (Stone chips)

The source of the boulders that were crushed to produce the aggregate is the riverbed of Surma River in Sylhet. The aggregate is strong, durable and free of any contaminating chemicals. Figure 3.1 shows the gradation curve of the stone chips used. Major properties of the aggregate were tested in the laboratory prior to casting and the properties are presented in Table 3.2.

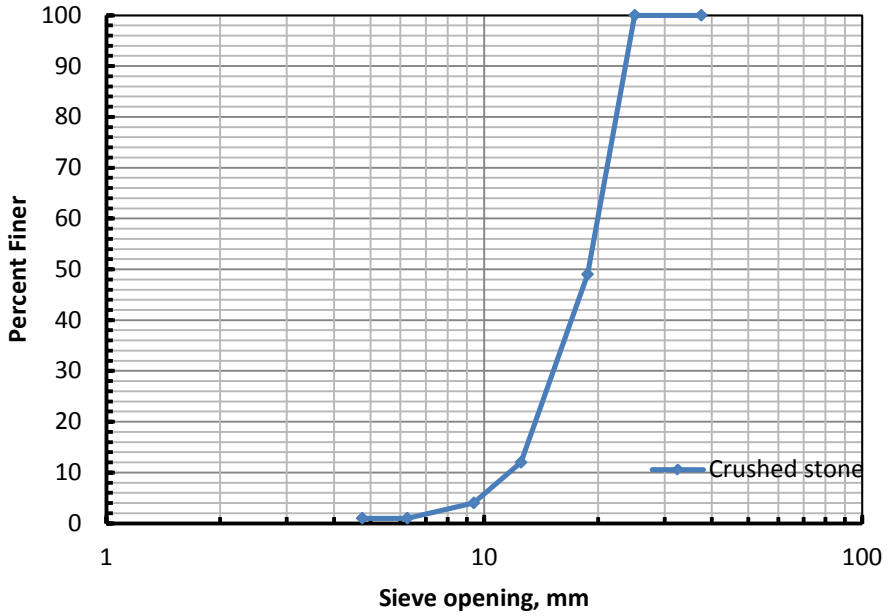

Figure 3.1: Gradation curve of Stone Chips

Table 3.2: Coarse Aggregate (Stone chips) properties according to ASTM C 29/C 29M-97[35] and ASTM C 127-88 [36]

Basic Property	Condition	Crushed Stone Chips
Density	Loose Unit weight	1440 kg/m^3
	Oven-Dry rodded Unit weight	1510 kg/m^3
	SSD rodded Unit weight	1530 kg/m^3
Specific Gravity	Oven-Dry bulk Sp. Gr.	2.53
	SSD bulk Sp. Gr.	2.56
	Apparent Sp. Gr.	2.61
Voids	Loose	43%
	Compacted by rodding	40%
Absorption capacity	-	1.3%

3.3.3.2 Crushed clay bricks (Brick chips)

Brick chips are produced by crushing burnt clay bricks and are regarded as lightweight aggregate. Burnt clay bricks are made by burning in a kiln the raw bricks that are made with a mixture of soft clay and a suitable quantity of sand. The temperature in the kiln is maintained at around 900-1000˚C. The duration of burning is very important in controlling the quality of bricks. Generally, the shorter the duration of burning, the weaker the brick and the longer the duration, the stronger becomes the brick. Excessive burning, though, deforms the shape and size of the brick and also diminishes the strength. The basic ingredients that bricks contain are as follows-

i. Silica (sand) – 50% to 60% by weight

ii. Alumina (clay) – 20% to 30% by weight

iii. Lime – 2 to 5% by weight

iv. Iron oxide – ≤ 7% by weight

v. Magnesia – less than 1% by weight

Brick chips used for the purpose of the current research work are manufactured by crushing moderate-highly burnt clay bricks which are locally called ‘Picket bricks’. Relevant tests were conducted for the aggregate. Gradation curve is presented in Figure 3.2 and the properties are tabulated in Table 3.3.

Table 3.3: Coarse Aggregate (Brick chips) properties according to ASTM C 29/C 29M-97 and ASTM C 127-88

Basic Property	Condition	Crushed Clay Bricks
Density	Loose Unit weight	960 kg/m^3
	Oven-Dry rodded Unit weight	1040 kg/m^3
	SSD rodded Unit weight	1190 kg/m^3

Specific Gravity	Oven-Dry bulk Sp. Gr.	1.80
	SSD bulk Sp. Gr.	2.06
	Apparent Sp. Gr.	2.43
Voids	Loose	47%
	Compacted by rodding	42%
Absorption capacity	-	14.3%

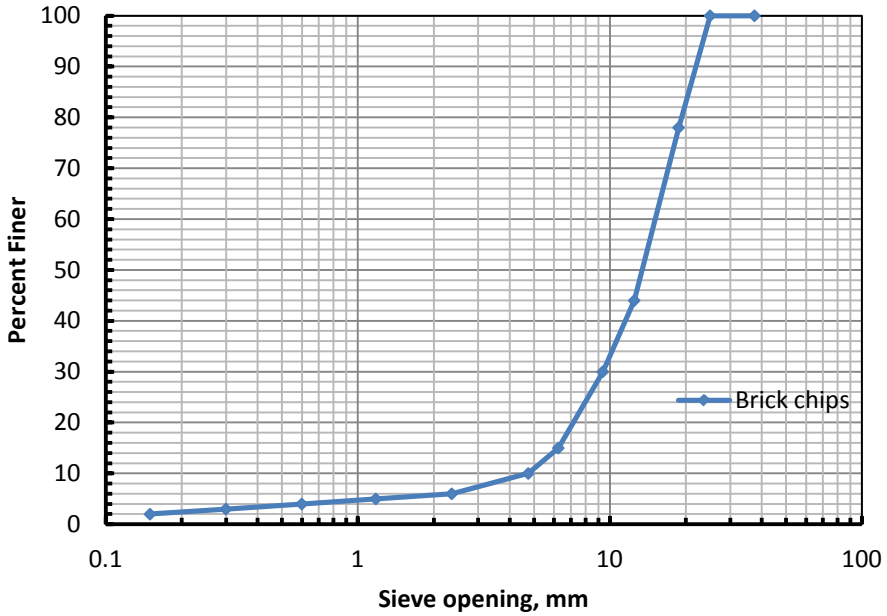

Figure 3.2: Gradation curve of Brick Chips

3.3.3.3 Mixture of gravel/shingle and crushed stone

Gravels are different to crushed stones chiefly with respect to shape and surface roughness/texture. Gravels generally have a polished smooth surface and more or less round shape unlike crushed stone chips which have relatively rough surface texture and angular shape. Therefore, these two types of aggregate perform in a different fashion in a concrete mix even if all other salient properties are kept identical. Gradation curve for this type of coarse aggregate is shown in Figure 3.3. Relevant properties were assessed and are charted in Table 3.4.

Table 3.4: Coarse Aggregate (Gravel/crushed stone mixed) properties according to ASTM C 29/C 29M-97 and ASTM C 127-88

Basic Property	Condition	Gravel/crushed stone mixed
Density	Loose Unit weight	1480 kg/m^3
	Oven-Dry rodded Unit weight	1580 kg/m^3
	SSD rodded Unit weight	1600 kg/m^3
Specific Gravity	Oven-Dry bulk Sp. Gr.	2.55
	SSD bulk Sp. Gr.	2.58
	Apparent Sp. Gr.	2.64
Voids	Loose	42%
	Compacted by rodding	38%
Absorption capacity	-	1.2%

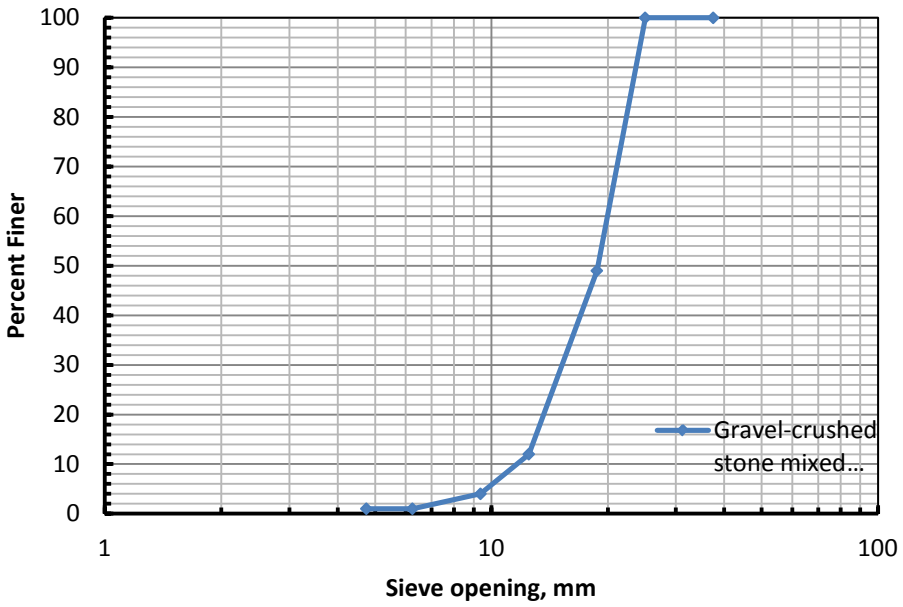

Figure 3.3: Gradation curve of Gravel/stone chips mixture

3.3.4 Fine Aggregate

In general, aggregate comprising of particles finer than 5 mm (0.2 in.) e.g. sand, crushed stone or crushed slag screenings etc. can be classified as fine aggregate. Fine aggregate is an essential constituent of aggregate since its primary function is to fill up the large voids between the particles of coarse aggregate and prevent honeycomb in the concrete matrix. For adequate consolidation of concrete, the desirable amount of air, water, cement, and fine aggregate (that is, the mortar fraction) should be about 50% to 65% by absolute volume (45% to 60% by mass) [34]. Rounded aggregate, such as gravel, requires slightly lower values, while crushed aggregate requires slightly higher values. Fine aggregate content is usually 35% to 45% by mass or volume of the total aggregate content [34]. It is imperative for the aggregate to be clean, inert, free of organic matter and deleterious substances, and relatively free of silt and clay.

Sylhet sand extracted from Surma river bed is utilized as fine aggregate in the concrete prepared for the study. Figure 3.4 shows the gradation curve. Table 3.5 presents property test results.

Table 3.5: Fine Aggregate (Sylhet sand) properties according to ASTM C 29/C 29M-97 and ASTM C 136-01 [37]

Basic Property	Condition	Sylhet sand
Density	Loose Unit weight	1430 kg/m^3
	Oven-Dry rodded Unit weight	1550 kg/m^3
	SSD rodded Unit weight	1600 kg/m^3
Specific Gravity	Oven-Dry bulk Sp. Gr.	2.45
	SSD bulk Sp. Gr.	2.52
	Apparent Sp. Gr.	2.64

Voids	Loose	38%
	Compacted by rodding	33%
Absorption capacity	-	3.0%
Fineness modulus	-	2.42

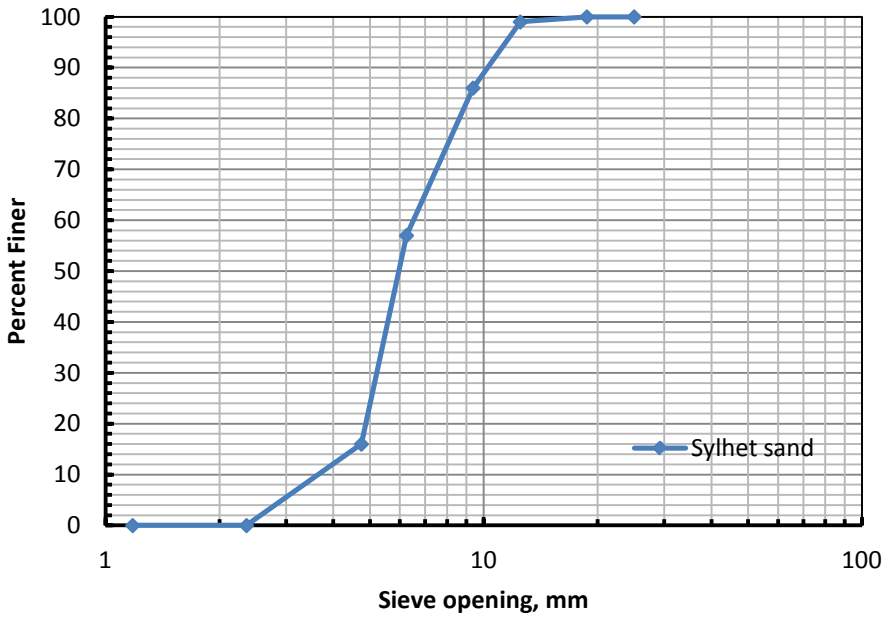

Figure 3.4: Gradation curveof Sylhet sand

3.3.5 Galvanized Iron Wire Fiber

3.3.5.1 General

Galvanized Iron (GI) wire is a slender strain like piece of filament of relatively rigid or flexible metal coated with Zinc to protect corrosion. It usually has a circular section and the diameter varies from 0.37 mm to 5 mm. The commonly available GI wires are either mild carbon or high carbon steel wires, which are coated with Zinc which impart the base wire with superior properties i.e. high resistance to moisture and mechanical damage and have a very bright and smooth surface finish. The primary application of GI wire does not include being used as fiber in concrete, but it has the potential for a very effective fiber to be used in FRC, especially in conditions

conducive to corrosion of steel in concrete. Where concrete is exposed to chloride, sulfate attack or carbonation, main reinforcement and fibers are expected to corrode and but Zinc coating in fiber can prove to be very convenient in inhibiting swift deterioration. Moreover, GI wire shows such filamentary nature that may allow the concrete to theoretically deform in a pseudo-ductile nature.

3.3.5.2 Classification

GI wire can be classified against two main features- wire material and coating technique. Materials used in GI wire do not vary a lot. The customary materials used in manufacturing are-

- Mild-carbon iron
- High-carbon iron
- Annealed carbon steel wire

Based on Zinc coating application technique i.e. galvanizing method, GI wire is divided into two categories-

i. Hot Dip G.I. wire
ii. Electro-galvanized wire

3.3.5.3 Characteristics

Hot-dip galvanized wire offers excellent flexibility and softness. The zinc coating can vary from 100g/m^2 to 300g/m^2 [38]. Common sizes available for this kind of wire range from 0.19 mm to 3.8 mm.

Electro-galvanized wire has the characteristics of uniform, good corrosion resistant and firm zinc coating.Wire diameter ranging from 0.19 mm to 5.0 mm of this kind of GI wire is mostly used by general consumers. Zinc coating in electro-galvanization is much more controlled than hot-dipping and thereby, a thin unbroken layer of 10 g/m^2 to 25 g/m^2 is usually applied on the wire. Tensile strength of electro-galvanized wire depends on the material used in the wire and normally varies from 40 to 85 kg/mm^2 (55to 120 ksi) [38].

3.3.5.4 Manufacturing information

There are a lot of manufacturers of GI wire around the country and world. In Bangladesh, leading companies are Gazi Wire, Moon Steel Limited, Razor Barbed Wire, Mushna Group of Industries etc. Along with locally produced wire, imported GI wires are also available in the market. Most of the imported GI wires are from China and India.

Low carbon steel wires are normally used in producing hot dip GI wire. The manufacturing process includes wire drawing, acid washing, rust removing, annealing and coiling. Electro-galvanized iron wire is usually made with mild steel and the metal is hard drawn into wire before galvanizing and packaging processes i.e. winding, coiling, cutting and packing. GI wires are commercially available in the form of baling wire, big coil, small coil and spool wire or even pre-processed straight-cut and U wire.

3.3.5.5 General use and application

GI wire is rust-resistant and very versatile in applications. It is mainly used in-

a. Construction as binding wire for reinforcements

b. Gardening for binding flowers, tying fences etc.

c. Wire mesh making as weaving wire

d. Agricultural settings and orchards as baling wire

e. Packaging of products and other daily uses

3.3.5.6 Selection and processing

Fibers used in fiber reinforced concrete are required to conform to specifications stipulated in various codes and standards e.g. ASTM C 1018 [17], ACI 544.2R [18], ACI 544.3R [14]. Five general types of steel fibers are identified in ASTM-A 820/A 820M based upon the product or process used as a source of the steel fiber material: Type I, cold-drawn wire; Type II, cut sheet; Type III, melt-extracted; Type IV, mill cut; Type V, modified cold-drawn wire. Fiber from GI (Galvanized Iron) wire falls in the category of Type V, modified cold-drawn wire. Therefore, for GI wire fiber, ASTM specifications for Type V are followed hereafter.

Performance of GI wire as concrete fiber was investigated by Karim et al.[1]and was found suitable in all possible aspects. All the samples satisfied the required mechanical properties, namely tensile and bending requirements, of steel fibers in FRC. Summary of the tests is presented in Table 2.3 of Chapter 2. According to the findings of the research, 0.70 mm diameter GI wire was chosen and suitable length for the GI wire fibers was taken to be 37.5 mm (1.5 in). The resulting aspect ratio of 53.57 falls within the limit of 30 to 100 as specified in ACI 544.3R or ASTM-A820/A820M. Therefore, 0.70 mm diameter GI wire was cut into 37.5mm. pieces to produce GI wire fiber which was used to prepare GWRC with an aim at assessing strength and ductility. Figure 3.5 shows GI wire bundle and GI wire fiber ready-to-use as fiber in GWRC. The specific brand of the wire was '*Apple GI Wire*' which is produced in Narayanganj, Bangladesh. Tensile strength test was performed for a set of local GI wires with diameter of 1.5 mm. Stress-strain curves are plotted in Figure 3.6.The properties of the GI wire indicate that iron used in this wire is mild steel. Properties of the GI wire are as follows-

Yield strength- 340 MPa (49ksi)

Ultimate strength- 500MPa (72.5ksi)

Elongation- 10%

Figure 3.5 (a): GI wire coil

Figure 3.5 (b): GI wire fiber stack

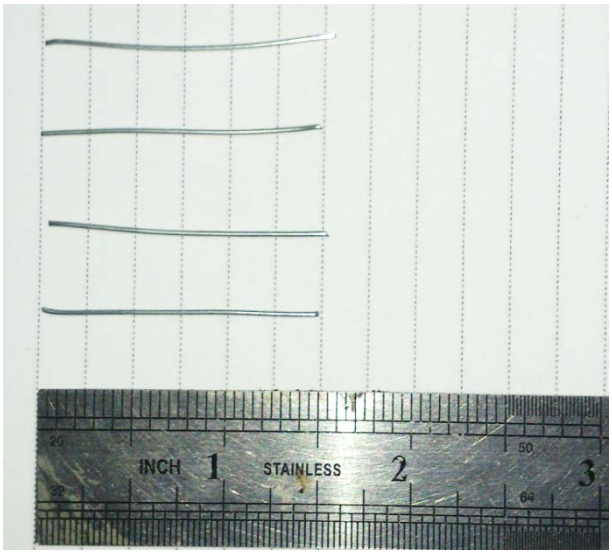

Figure 3.5 (c): GI wire fiber

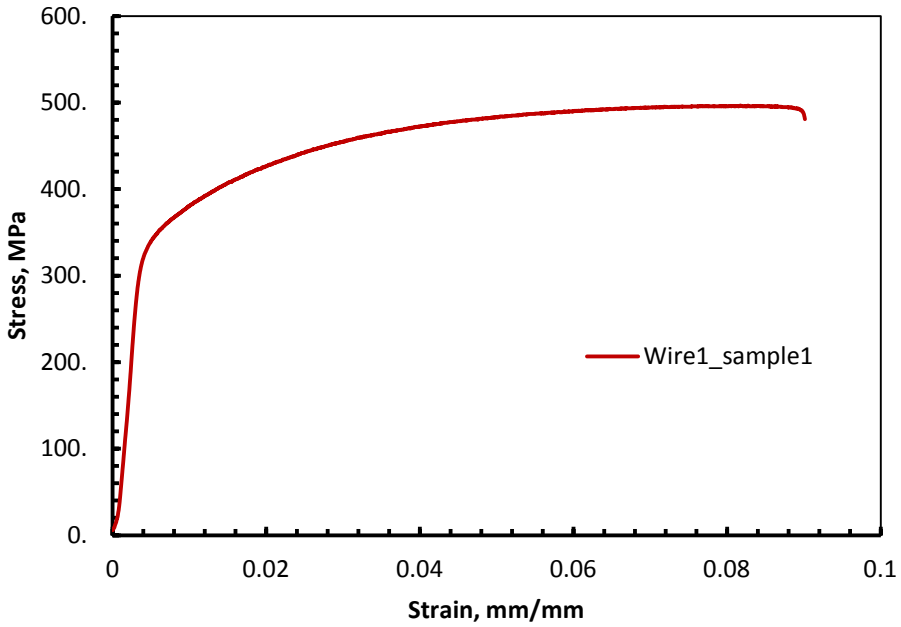

Figure 3.6 (a): Stress-strain curve for wire1 sample 1

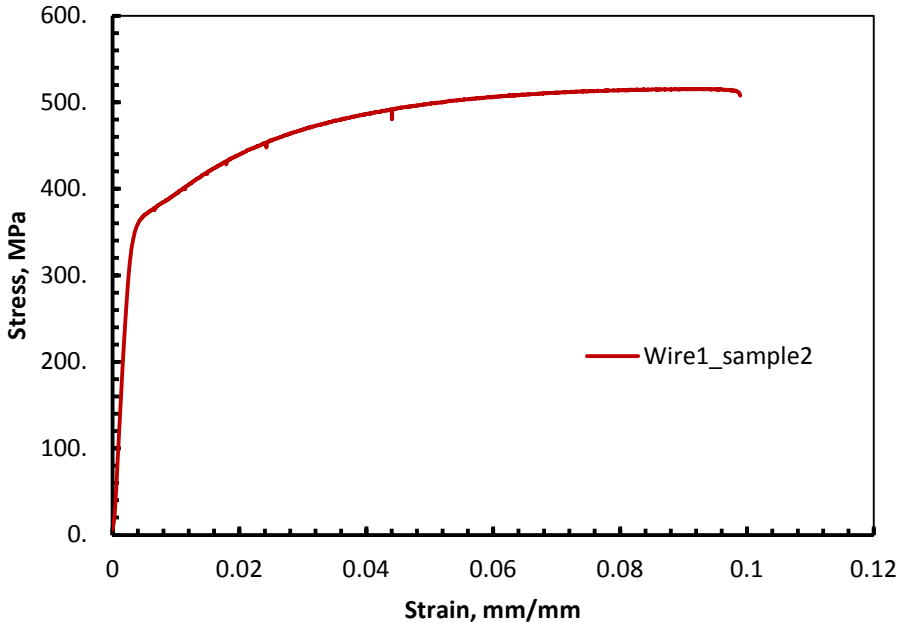

Figure 3.6 (b): Stress-strain curve for wire1 sample 2

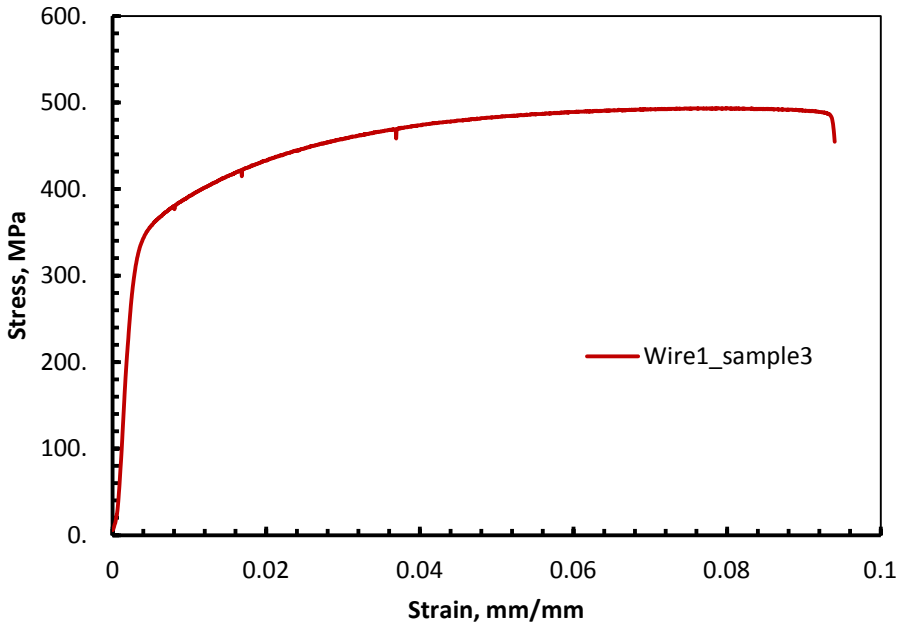

Figure 3.6 (c): Stress-strain curve for wire1 sample 3

3.3.6 Mild Steel Deformed Bar

For the construction of test beams, conventional main reinforcements in the form of longitudinal reinforcement and stirrups were provided along with GI wire fibers. The size of the beams was large enough to necessitate use of longitudinal bars

for preventing breakage due to handling stresses during movements. Stirrups are employed so that premature shear failure can be avoided during testing for flexure. *BSRM Xtreme 500W* steel was used as main reinforcement in the test beams. Relevant properties are given below-

Yield strength- 514 MPa(74.5 ksi)

Ultimate strength-592 MPa (85.8 ksi)

Modulus of elasticity-200,000MPa (29,000,000ksi)

Elongation- 18%

CHAPTER 4

Experimental Program

4.1 Objectives

The primary aim of the experiments conducted under the current program is assessing the performance of GI wire fiber reinforced concrete. Performance, literally, refers to a very broad spectrum and it is imperative to narrow down the focus on the specific parameters that are intended to be inspected. Three salient features of concrete with GI fiber reinforcement have been brought under scrutiny in the present study- strength, ductility and durability. Strength itself can attract an open interpretation, and therefore, it is decided that three basic properties that define strength i.e. modulus of elasticity, compressive and tensile strength are going to be considered in this regard. For the evaluation of ductility, flexural analysis and load-deflection behavior of suitable test specimens are studied to determine various parameters such as first cracking load, ultimate load, deflection and crack patterns at various loading stages, toughness etc. that give an indication of ductility as well as flexural characteristics. And finally, durability which is directly related to the pores in the concrete matrix is judged by permeability to water and chloride ions through these pores into concrete. To sum up, the goal of the experimental phase of the research is to perform the following experiments-

- Compressive strength of cylindrical concrete specimens
- Splitting tensile strength of cylindrical concrete specimens
- Determination of Static Modulus of Elasticity of concrete in compression
- Flexural/ductility analysis of concrete beams
- Rapid Chloride Permeability Test (RCPT)
- Measurement of Rate of Absorption of Water by concrete (Sorptivity test)

4.2 Experiment Scheme

The range of tests carried out was quite multidimensional and a carefully thought planning was required to accomplish the work in the stipulated time frame. The tests were conducted in two main phases. In the first phase of the experiments, mechanical properties i.e. modulus of elasticity, compressive and tensile strength were determined for normal concrete and GWRC with various fiber contents. Coarse aggregate used was also three types- crushed stone (stone chips), crushed burnt clay bricks (brick chips) and gravel-crushed stone mixture. Samples were cured for both 7 and 28 days for compressive strength measurement. Splitting tensile strength and modulus of elasticity were determined only for samples cured for 28 days. Second phase of the tests featured flexural test of beams, Rapid Chloride Permeability Test (RCPT) and Sorptivity test. RCPT and Sorptivity tests were performed for samples aged 56 days since durability tests are more reliable for concrete aged more, as stated by Detwiler et al. [39], Cao and Detwiler [40], Tang and Nilsson [41] and Stanish et al. [42]. This also facilitated testing samples cast simultaneously to be tested at different times. However, the test beams were cast and tested at a different time as the testing of beams requires more time. In addition, fabrication of the beams is also a time consuming endeavor. So, jobs related to beam testing were executed during the second phase of the experimentation window, along with durability tests. Therefore, the experimental design comprises of two phases-

- First phase- determination of modulus of elasticity, compressive and splitting tensile strength
- Second phase- evaluation of durability through RCPT and Sorptivity, assessment of flexural/ductility characteristics of test beams

4.3 Mix Design

Appropriate proportioning of constituent materials which is termed as ‘mix-design’ is the key to achieving desired results in concrete. The art of mix design is reliant on quite a lot of factors. For steel fiber reinforced concrete, the factors to be considered are even more. Moreover, types of fibers are very diverse, so are their characteristics. Therefore, the mix proportion and performance of concrete varies with

the use of different fibers. Albeit, there is no specific guideline for GI wire fiber reinforced concrete; standards and codes such as ACI 544.3R [14], ASTM C 1116 [20] etc. are available for steel fiber reinforced concrete. These codes and standards for SFRC can conveniently be considered as a guideline for designing mix proportions of GWRC. For present research interests, ACI 544.3R-'Guide for Specifying, Proportioning, Mixing, Placing, and Finishing Steel Fiber Reinforced Concrete' has been followed as the standard specification for mix-design design related issues and is referred to as 'the code' henceforth. According to the code, following are the factors that influence the mix proportioning procedure of fiber reinforced concrete the most-

a. Workability and consistency
b. Aspect ratio of the fibers, l/d
c. Volume fraction of fiber, V_f
d. Type of fibers-size, shape, strength, modulus of elasticity etc.
e. Balling of fibers
f. Ratio of fine to coarse aggregate etc.

In addition, the aim of the research is to explore the possibilities of using GWRC in Bangladesh. As a result, established construction practices here in Bangladesh also played an important part in determining suitable mix-proportion. Generally, mix-design is specified on weight basis all over the world and measuring weight of the aggregate, cement and other materials is convenient if a suitable weighing facility is available. Large scale productions require huge weighing facilities which are appropriate for batching plants for ready-mix concrete; but for small construction sites, these facilities might incur undue overhead. Moreover, ready-mix concrete is relatively new in Bangladesh and just recently garnering popularity, but majority of construction works are still dependent on small scale mixing and casting method. Due to unavailability of proper weighing facilities, a customary mix-design based on volumetric ratio has been used for construction over the years and it is well established here in Bangladesh. Therefore, basic concrete mix-proportion for the current study is chosen based on a conventional volumetric ratio of the materials. According to this mix-design, ratio of cement to fine aggregate to coarse aggregate is adopted to be 1:1½:3. Mix-design on weight basis corresponding to this criterion is tabulated in Table 4.1 and 4.2 for stone chips and brick chips respectively. All other

mix-design parameters are chosen after Karim et al. [1] and in accordance with the code [14]. It can be noted that, due to low volume fraction of fiber content and relatively high w/c ratio, workability was as required and thereby, use of super-plasticizing admixture was not necessitated.

Table 4.1: Mix-design for concrete with crushed stone chips and Gravel-stone chips mixture

Item	Crushed stone chips (19.5 mm downgraded)	Gravel-stone chips mixture (25 mm downgraded)
Cement, kg/m^3	153	153
Water, kg/m^3	69	69
Coarse Aggregate, kg/m^3	496	518
Fine Aggregate, kg/m^3	260	260
Water Cement Ratio	0.45	0.45
Fiber content, weight percent	1.0%, 1.5%, 2.0% and 2.5%	
Workability, mm	50-100	50-100

Table 4.2: Mix design for concrete with brick chips

Item	Crushed brick chips (19.5 mm downgraded)
Cement, kg/m^3	153
Water, kg/m^3	69
Coarse Aggregate, kg/m^3	386
Fine Aggregate, kg/m^3	260
Water Cement Ratio	0.45
Fiber content, weight percent	1.0%, 1.5%, 2.0% and 2.5%
Workability, mm	50-75

4.4 Compressive Strength Test

4.4.1 Concept

Compressive strength of cylindrical concrete specimens; for example, molded cylinders and drilled cores; is determined according to ASTM C 39/ C 39M-93[43] Concrete should have a unit weight in excess of 50 lb/ft^3 [800 kg/m^3] for this test. This standard test is conducted by applying a compressive axial load to molded cylinders at a rate which is within a prescribed range until failure occurs. The compressive strength of the specimen is calculated by dividing the maximum load attained during the test by the cross-sectional area of the specimen.

As compressive strength is not a fundamental or intrinsic property of concrete made from given materials; care should be exercised in the interpretation of the strength. Obtained values are dependent on the size and shape of the specimen, batching, mixing procedures, the methods of sampling, molding, and fabrication and the age, temperature, and moisture conditions during curing [40].

4.4.2 Methodology and test setup

Compression tests of moist-cured specimens must be done as soon as practicable after removal from moist storage. Test specimens must be kept moist by any convenient method during the period between the removals from moist storage and testing. They need to be tested in the moist condition. All test specimens for a given test age should be broken within the permissible time tolerances prescribed in ASTM C39/C 39M.

Bearing plates were placed at the top and bottom for even distribution of loads. Compressive load was applied by a hydraulically operated machine continuously and without shock. The load should be applied at a rate of movement (platen to crosshead measurement) corresponding to a loading rate on the specimen within the range of 0.15 to 0.35 MPa/s (20 to 50 psi/s) [40]. So, the machine was set for a loading rate of 2500 N/s (560 lb/s) which falls within the stipulated range. Although, a higher rate of loading may be allowed during the application of the first half of the anticipated loading phase, the same rate was maintained from the start to the end of loading. The load is applied until the specimen fails, and the maximum load carried by the

specimen during the test is recorded. The type of failure and the appearance of the concrete are generally noted. Test setup is shown in Figure 4.1.

4.4.3 Significance of results

The results obtained from this test method are used as a basis for quality control of concrete proportioning, mixing, and placing operations; determination of compliance with specifications; control for evaluating effectiveness of admixtures; and similar uses.

Figure 4.1: Test setup for compression test of cylinders

4.5 Test for Splitting Tensile Strength

4.5.1 Concept

The splitting tensile strength of cylindrical concrete specimens, such as molded cylinders and drilled cores, is determined by ASTM C 496/C 496M-04 [44]. According to the standard, a diametral compressive force is applied along the length of a cylindrical concrete specimen to conduct this test method at a rate that is within a prescribed range until failure occurs. Because of this loading, tensile stresses are

induced on the plane containing the applied load and relatively high compressive stresses in the area immediately around the applied load. Tension failure rather than compressive one occurs because the areas of load application are in a state of triaxial compression, thereby allowing them to withstand much higher compressive stresses than would be indicated by a uniaxial compressive strength test result.

The splitting tensile strength is obtained by dividing the maximum load sustained by the specimen by appropriate geometrical factors. The splitting tensile strength of the specimen is calculated as follows-

$$T = 2P/\pi ld \quad \text{.....eq.4.1}$$

Where,

T = splitting tensile strength, MPa (psi),

P = maximum applied load indicated by the testing machine, N (lbf),

l = length, mm (in.) and

d = diameter, mm (in.)

4.5.2 Methodology and test setup

Size, molding, and curing requirements of the test specimens are conformed according to Practice C 192/C 192M [32] (laboratory specimens). Between the removal from the curing environment and testing, moist-cured specimens are kept moist by suitable methods. Diametral lines are drawn on each end of the specimen using a suitable device that will ensure that they are in the same axial plane.

One of the plywood strips is centered along the center of the lower bearing block. The specimen is placed on the plywood strip and aligned so that the lines marked on the ends of the specimen are vertical and centered over the plywood strip. A second plywood strip is placed lengthwise on the cylinder, centered on the lines marked on the ends of the cylinder.

Assembly is positioned to ensure the following conditions:

- The projection of the plane of the two lines marked on the ends of the specimen intersects the center of the upper bearing plate, and

- The center of the specimen is directly beneath the center of thrust of the bearing block.

The load has to be applied continuously without shock, at a constant rate within the range 0.7 to 1.4 MPa/min (100 to 200 psi/min) splitting tensile stress until failure of the specimen. For this research, the rate of loading was maintained at 500 N/s which falls within the instructed range of loading rate. The maximum applied load was recorded, indicated by the testing machine at failure and splitting tensile strength was computed by the formula given in Equation 4.1. The test setup is shown in Figure 4.2.

Figure 4.2: Test setup for splitting tensile strength of cylinders

4.5.3 Significance of result

Determination of splitting tensile strength is simpler and usually greater than direct tensile strength and lower than flexural strength (modulus of rupture). For the evaluation of the shear resistance provided by concrete in reinforced lightweight aggregate concrete members and the determination of the development length of reinforcement; splitting tensile strength is used in the design of structural lightweight concrete members.

4.6 Test for Static Modulus of Elasticity

4.6.1 Concept

Young's modulus of elasticity of molded concrete cylinders and diamond-drilled concrete cores under longitudinal compressive stress are determined by ASTM C 469-02[45]. Stress versus strain curve is plotted with test data and Modulus of Elasticity is calculated to the nearest 344.74 MPa (50,000 psi) as follows:

$$E = (S_2 - S_1) / (e_2 - 0.000050) \quad \text{eq. 4.2}$$

where,

E = chord modulus of elasticity, psi,

S_2 = stress corresponding to 40 % of ultimate load,

S_1 = stress corresponding to a longitudinal strain, e_1 of 0.00005, psi, and

e_2 = longitudinal strain produced by stress S_2.

4.6.2 Methodology and test setup

Specimens are tested within 1 h after removal from the curing or storage room. Specimens, removed from a moist room for test, are kept moist by a wet cloth covering during the interval between removal and test. Specimens' ends are made perpendicular to the axis (± 0.5°) and plane (within 0.002 in.). Planeness is accomplished by capping in accordance with Practice C 617, or by lapping, or by grinding if the specimen as cast does not meet the planeness requirements. Planeness is considered within tolerance when a 0.002 in. (0.05 mm) feeler gage does not pass between the specimen surface and a straight edge held against the surface. Repairing aggregate pop outs that occur at the ends of specimens is not prohibited, provided the total area of pop outs does not exceed 10 % of the specimen area and the repairs are made before capping or grinding is completed.

The specimen is placed, with the strain-measuring equipment attached, on the lower platen or bearing block of the testing machine. The axis of the specimen is carefully aligned with the center of thrust of the spherically-seated upper bearing block. The reading is noted down on the strain indicators. Rotation of the movable

portion of the spherically-seated block which is brought slowly to bear upon the specimen is done gently by hand so that uniform seating is obtained. The test setup is shown in Figure 4.3.

The specimen is loaded at least twice. Data is not recorded during the first loading. Calculations are based on the average of the results of the subsequent loadings. The performance of the gages is observed during the first loading, which is primarily for the seating of the gages, and any unusual behavior is corrected prior to

Figure 4.3: Test setup for Modulus of Elasticity

the second loading. The load is applied continuously and without any sudden variations. Screw type testing machines are set so that the moving head travels at a rate of about 0.05 in. (1.25 mm)/min when the machine is running idle. In hydraulically operated machines, the load is applied at a constant rate within the range 35 ± 5 psi (241 ± 34 kPa)/s. Without interruption of loading, the applied load and longitudinal strain are recorded at the point when the longitudinal strain is 50 millionths and when the applied load is equal to 40 % of the ultimate load. Total longitudinal deformation divided by the effective gage length is defined as longitudinal strain. Readings are taken at two or more intermediate points without

interruption of loading to determine a stress-strain curve. An instrument can be used that makes a continuous record for this purpose. Except the final loading, the load is reduced to zero at the same rate at which it was applied, immediately after reaching the maximum load. No automatic data logger was available and so, data was obtained by taking readings manually for the present study.

The results of each of the two tests are plotted with the longitudinal strain as the abscissa and the compressive stress as the ordinate when the intermediate readings are taken. The compressive stress is calculated by dividing the quotient of the testing machine load by the cross-sectional area of the specimen. Modulus of Elasticity is then determined by equation 4.2.

4.6.2 Significance of result

For sizing of reinforced and non-reinforced structural members, establishing the quantity of reinforcement, and computing stress for observed strains, modulus of elasticity value, applicable within the customary working stress range (0 to 40 % of ultimate concrete strength) is used. Obtained modulus of elasticity values may be less than moduli derived under rapid load application (dynamic or seismic rates, for example), and may be greater than values under slow load application or extended load duration in most cases, given other test conditions being the same.

4.7 Flexural/ductility Test of Concrete Beams

4.7.1 Concept

The influence of steel fibers on flexural strength of concrete and mortar is much greater than for direct tension and compression [46]. To determine flexural strength of fiber reinforced concrete, two flexural strength parameters are commonly reported. These two parameters are first-crack flexural strength and ultimate flexural strength or modulus of rupture. The first-crack flexural strength corresponds to the load at which the load-deformation curve departs from linearity (Point A on Figure 4.8) and the ultimate flexural strength or modulus of rupture corresponds to the maximum load achieved (Point C on Figure 4.4). Strengths are calculated from the corresponding load using the formula for modulus of rupture given in ASTM C

78[19], though the linear stress and strain distribution on which the formula is based no longer apply after the matrix has cracked.

Procedures for determining first-crack and ultimate flexural strengths, as published in ACI 544.2R [18] and ASTM C 1018[17], are based on testing 100x 100 x 350 mm (4 x 4 x 14 in.) beams under third-point loading. Other sizes and shapes give higher or lower strengths, depending on span length, width and depth of cross section, and the ratio of fiber length to the minimum cross-sectional dimension of the test specime

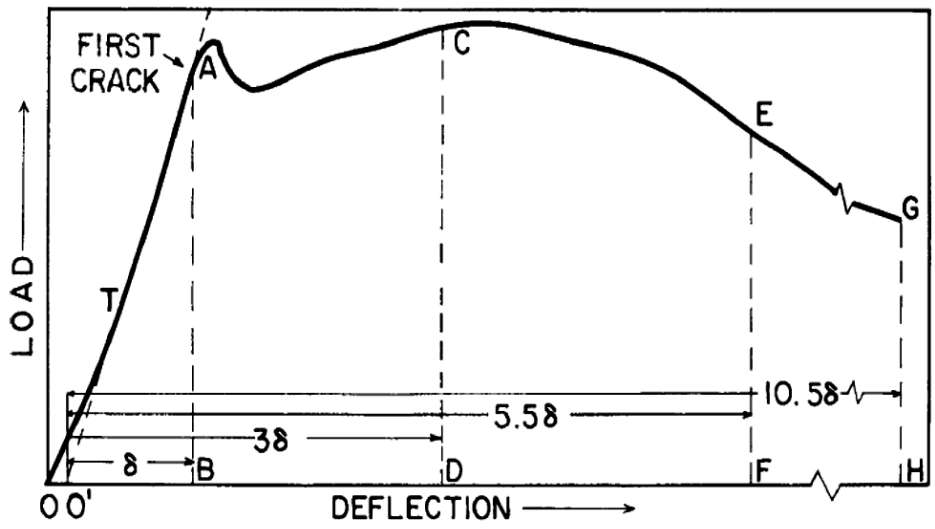

Figure 4.4: Important characteristics of the load-deflection curve [17]

Another significant characteristic that is noted for steel fiber reinforced concrete is Toughness. Under static loading, flexural toughness may be defined as the area under the load-deflection curve in flexure, which is the total energy absorbed prior to complete separation of the specimen [5]. Flexural toughness indexes may be calculated as the ratio of the area under the load-deflection curve for the steel fiber concrete to a specified endpoint, to the area up to first-crack, as shown in Figure 4.1 as per ASTM C 1018[17], or to the area obtained for the matrix without fibers. There are some Index values i.e. $I_{5,}$ $I_{10,}$ $I_{20,}$ I_{30} etc. that can be determined to indicate to flexural strength as well as ductility of the material. These indexes, defined in ASTM C 1018 [17], are obtained by dividing the area under the load-deflection curve, determined at a deflection that is a multiple of the first-crack deflection, by the area under the curve up to the first crack. I_5 is determined at a deflection 3 times the first-crack deflection, I_{10} is determined at 5.5, I_{20} andI_{30} at 10.5 and 15.5 times the first-crack deflection

respectively. Another parameter, residual strength factor,$R_{5,10}$= $20(I_{10} - I_5)$ is computed to provide an impression of amount of strength retained after the first-crack.

The limitation of the above mentioned procedure is that it can be used to a good effect only for concrete without the main reinforcements. ASTM C 1018 stipulates that the procedure can be followed for beams with dimensions varying from the standard 100x 100 x 350 mm (4 x 4 x 14 in.) dimensions [40], but it is understood at the same time that the same methodology shall not apply for beams reinforced with conventional main reinforcements. Notwithstanding this fact, the standard has been followed, after some major and minor modifications, for determination of flexural strength and ductility of full-scale fiber reinforced concrete test beams with main reinforcement for the purpose of the present study. Due to unavailability of standard specification for testing FRC beams with main bars, research by Byung Hwan Oh [9] was consulted for designing the test members and procedures.

4.7.2 Design and fabrication of test beams

Rectangular reinforced concrete beams, with five separate mix-proportions including one normal concrete mix and four GWRC mixes with brick chips as coarse aggregate, were designed in accordance with ACI Design Code (ACI 318-99) [47]. Choice of brick chips as coarse aggregate has been made for studying the effect of fiber reinforcing on lightweight concrete which is the highlight of the research. In addition, brick chips are widely used in Bangladesh for construction of beam and slab.

The overall dimensions of the test beams were the same for all test members, i.e., beam width, b = 150mm (6 in.), beam height, h = 200mm (8 in.), effective depth, d = 169mm (6.76 in.), cover at upper face, d' = 31mm (1.24 in.), and beam length = 1500mm (60 in.). The span length for the test beams was l = 1350 mm (54 in.). Some minor adjustments to the code requirements were made for concrete cover issues since the beams had relatively small dimensions.

No variation was made as far as longitudinal main reinforcement and shear reinforcements are concerned. Only fiber content was varied from 1% to 2.5% on weight basis. The beams were doubly reinforced with longitudinal reinforcement provided at both top and bottom. Minimum reinforcement ratio, $\rho_{min}$for the beams was found to be 0.0028 resulting in a minimum reinforcement, $A_{s,min}$= 70 mm^2 (0.112 in^2).

Balanced reinforcement ratio, ρ_b was 0.016. Two ∅ 10 mm (#3) bars were provided at both top and bottom which furnished 34% of the balanced reinforcement ratio. Consequently, bottom reinforcement ratio, ρ and top reinforcement ratio, ρ' provided in the test beams are both 0.34 ρ_b. To avoid premature shear failure of the beams during loading and handling and to ensure a predominant flexural failure of test subjects, ∅ 8 mm (#2) two-leg vertical stirrups were provided with 150 mm (6 in.) center to center spacing. Details of the beams' fabrication and design are illustrated in Figure 4.5.

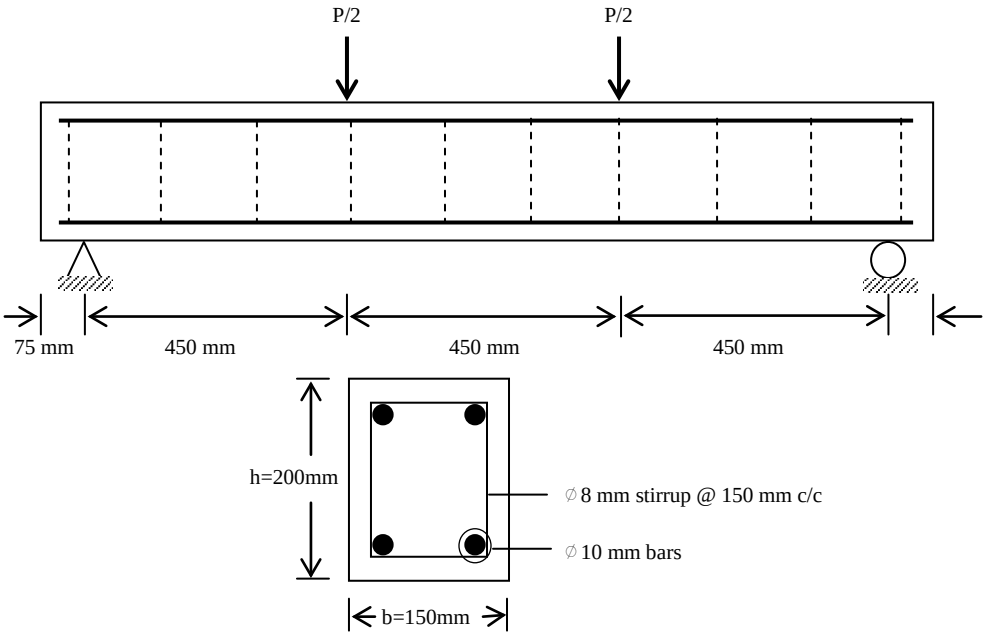

Figure 4.5: Schematic diagram for details of test beams

Careful attention was paid during the mixing process to have the fibers well distributed. The test beams were cured in a wet condition by wrapping them with jute sacks and saturating them regularly with ample amount of water regularly so that continuous curing is ensured. Figures 4.10, 4.11, 4.12 and 4.13 show the beams during concrete placing, compaction by vibrator, finishing and ready beams, respectively.

4.7.3 Methodology and test setup

The beams were subjected to third point loading as shown in Figure 4.9. The beams were mounted on a platform and two steel blocks with semi-circular upper end were placed at the bottom at the points of support so that the beam can deflect as a simply supported beam. Loads were applied at each of the third points by a Tinius Olsen Universal Testing Machine. A constant strain-controlled loading was applied

with the movement rate of the platform being 5 mm/min. Time versus load was continuously monitored and data was saved automatically. Deflection of the beam was also monitored with a video extensometer and time versus deflection data was stored continuously. These data series are then combined to produce load versus deflection curves which are the basis of analysis for flexural strength and ductility. Figure 4.6 displays the overall test setup for beam testing.

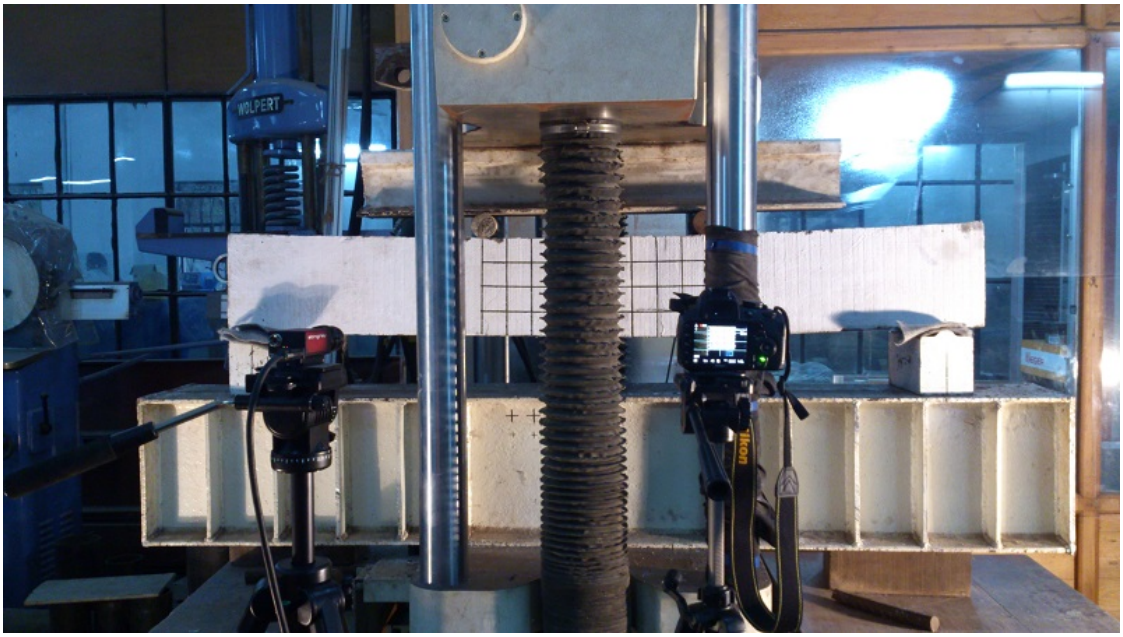

Figure 4.6: Test setup for beam flexure

4.7.4 Significance of test results

Behavior of the fiber-reinforced concrete up to the onset of cracking in the concrete matrix is characterized by the first-crack strength. Toughness up to the first crack indicates to the amount of energy that the member can absorb before the initiation of crack while the toughness indices characterize the toughness there after up to specified end-point deflections. Residual strength factors, which are derived directly from toughness indices, characterize the level of strength retained after first-crack simply by expressing the average post-crack load over a specific deflection interval as a percentage of the load at first-crack [17].

4.8 Test for Concrete's Ability to Resist Chloride Ion Penetration

4.8.1 Concept

The electrical conductance of concrete is determined by ASTM 1202- 97 [48] test method to provide a rapid indication of its resistance to the penetration of chloride ions. Application of this test method is for the types of concrete where correlations have been established between this test procedure and long term chloride ponding procedures such as those described in AASHTO T 259 [49]. The amount of electrical current passed through 50 mm (2 in.) thick slices of 100 mm (4 in.) nominal diameter cores or cylinders during a 6-h period, is monitored through this test method. Across the ends of the specimen, a potential difference of 60 V dc is maintained, one of which is immersed in a sodium chloride solution, the other in a sodium hydroxide solution. The resistance of the specimen to chloride ion penetration is related to the total charge passed, in coulombs.

Because of admixing calcium nitrite into a concrete; this test method may show some error. Test results of such concretes show higher coulomb values, that is, lower resistance to chloride ion penetration, than from tests on identical concrete mixtures (controls) without calcium nitrite. Long-term chloride ponding tests can be a solution in this case which indicate that the concretes with calcium nitrite are at least as resistant to chloride ion penetration as the control mixtures.

As the test results are a function of the electrical resistance of the specimen; test is invalid for specimens containing reinforcing steel (electrically conductive material) positioned longitudinally because of having a significant effect on the results [42]. Nevertheless, the test was carried out for GWRC only to observe if there is any effect of the fiber content on the electrical conductivity that might be supportive to understanding the durability of concrete against chloride penetration.

For calculation, a smooth curve is drawn by plotting current (in amperes) versus time (in seconds) and the area is integrated underneath the curve in order to obtain the ampere seconds, or coulombs, of charge passed during the 6 hour test period. Automatic data processing equipment can alternatively be used to perform the integration during or after the test and to display the coulomb value. Electrical

conductance of the concrete is measured by the total charge passed during the period of the test.

If the current is recorded at 30 min intervals, the following formula, based on the trapezoidal rule, can be used with an electronic calculator to perform the integration-

$$Q = 900\ (I_0 + 2I_{30} + 2I_{60} + \ldots . + 2I_{300} + 2I_{330} + I_{360}\ ) \ldots\ldots\ldots\ldots\ldots \text{eq. } 4.3$$

where:

Q = charge passed (coulombs),

I_0= current (amperes) immediately after voltage is applied, and

I_t = current (amperes) at t min after voltage is applied.

Table 4.3 is used to evaluate the test results. These values were developed from data on slices of cores taken from laboratory slabs prepared from various types of concretes.

Table4.3: Chloride Ion Penetrability Based on Charge Passed

Charged Passed (coulombs)	Chloride Ion Penetrability
>40000	High
2000 - 4000	Moderate
1000 - 2000	Low
100 - 1000	Very Low
<100	Negligible

4.8.2 Methodology and test setup

The specimens are, at first, conditioned by the specified process. Water is boiled and then cooled in a sealed container to obtain de-aerated water. The curved surfaces of the samples are then sealed properly using enamel paint and cured till the paint dry out. The specimens were directly placed in a vacuum desiccator with both end faces of specimen exposed. Sealing the desiccator, the vacuum pump was started that declined the pressure to less than 1 mm Hg (133 Pa) within a few minutes. The vacuum was maintained for three hours continuously. Then de-aerated water, prepared earlier, is poured into the desiccator through the separatory funnel.

Specimens were then removed from water, blotted off excess water, and transferred to a sealed can or other container which maintains the specimen in 95 % or higher relative humidity. A 100 mm outside diameter by 75 mm inside diameter by 6 mm (4in. outside diameter by 3in. inside diameter by 1⁄4in.) circular vulcanized rubber gasket was placed in each half of the test cell. Samples were inserted and the two halves of the test cell were clamped together to seal.

Side of the cell containing the top surface of the specimen was filled with 3.0% NaCl solution. This side of the cell would be connected to the negative terminal of the power supply. The other side of the cell which would be connected to the positive terminal of the power supply was filled with 0.3 N NaOH solution. Lead wires were attached to cell banana posts. Electrical connections were made to voltage application and data readout apparatus appropriately. Power supply was turned on, set to 60.0 ± 0.1 V, and initial current reading was recorded. Specimen temperature, applied voltage cell, and solutions was set at 68 to 77°F (20 to 25°C) at the time of commencement of the test, that is, when the power supply is turned on. Air temperature around the specimens was maintained in the range of 68 to 77°F (20 to 25°C). In case of very high current, temperature of the solution may rise to alarming proportions and therefore, tests were terminated as soon as temperature of any cell reached close to 194°F (90 °C). A schematic diagram of test setup is shown in Figure 4.7.

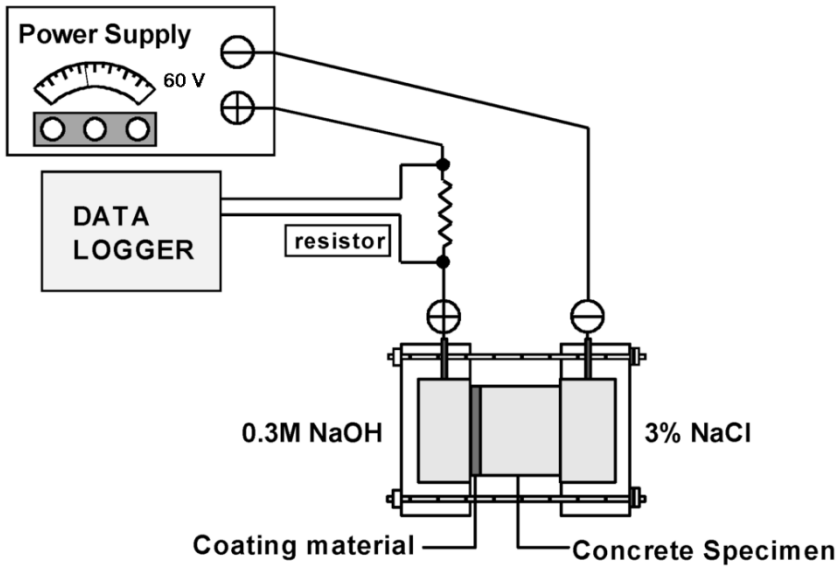

Figure 4.7: Schematic diagram of RCPT setup

Current was read and recorded at the interval of every 30 min. For the entire period of the test, each half of the test cell was kept filled with the appropriate solution. Finally, after 6 hours of test, total charge passed was calculated using equation 4.3 and conductivity was interpreted from Table 4.3.

4.8.3 Significance of result

Electrical conductance of concrete samples can be evaluated by laboratory procedures to provide a rapid indication of their resistance to chloride ion penetration through this test method. Results indicate that the electrical conductance has a good correlation with chloride ponding tests in most cases, such as AASHTO T259, on companion slabs cast from the same concrete mixture. Evaluation of materials and material proportions obtained from this test method is suitable for design purposes and research and development.

Obtained numerical results (total charge passed, in coulombs) from this test method must be used with caution, especially when applying for quality control and acceptance testing.

Results can be significantly affected by age of sample, depending on the type of concrete and the curing procedure. In most of the cases, properly cured concrete, become progressively and significantly less permeable with time.

4.9 Test for Rate of Absorption of Water

4.9.1 Concept

Penetrability of the pore system affects the performance of concrete greatly, especially where concrete is subjected to aggressive environments. Rate of ingress of water or other liquids through this porous system is largely controlled by absorption in unsaturated concrete due to capillary action. This phenomenon is termed as ‘water sorptivity’ by Hall [50] who proposed a test procedure for measuring rate of absorption (sorptivity) of water by concrete. The methodology was adopted by ASTM and it was introduced as a standard test; under the designation ASTM C 1585-04 [51]; for determining the rate of absorption of water by hydraulic cement concrete by measuring the increase in the mass of a specimen resulting from absorption of water

as a function of time when only one surface of the specimen is exposed to water. Dominated by capillary suction during initial contact with water; the exposed surface of the specimen remains immersed in water and water ingress of unsaturated concrete.

Absorption is calculated by dividing the change in mass by the product of the cross-sectional area of the test specimen and the density of water. Temperature effect on the density of water is neglected and a value of 0.001 g/mm^3 is used for this test. The units of *I* is mm.

$$I = m_t/(ad) \quad \text{eq. 4.4}$$

where,

I = the absorption,

m_t= the change in specimen mass in grams, at the time *t*,

a = the exposed area of the specimen, in mm^{2}and

d = the density of the water in g/mm^3.

Slope of the line that is the best fit to *I* plotted against the square root of time (s$^{1/2}$) is defined as the initial rate of water absorption (mm/s$^{1/2}$). This slope can be obtained by using least-squares, linear regression analysis of the plot of *I*versus time$^{1/2}$. Regression analysis is done by using all the points from 1 min to 6 h, excluding points for times after the plot shows a clear change of slope. Data between 1 min and 6 h must follow a linear relationship and show a systematic curvature to determine the initial rate of absorption.

Slope of the line that is the best fit to *I* plotted against the square root of time (s$^{1/2}$) using all the points from 1 d to 7 d is defined as the secondary rate of water absorption (mm/s$^{1/2}$). The slope is determined by using least-square linear regression. Data between 1 d and 7 d must follow a linear relationship (a correlation coefficient of less than 0.98) and show a systematic curvature to determine the secondary rate of water absorption.

4.9.2 Methodology and Test setup

Conditioning of sample before the start of the absorption procedure is very important for this test. Samples were conditioned by processing them through suitable temperatures (50 ± 2°C for 3 days in a desiccator), humidity and storage procedures (at 23 ± 2°C for 15 days in a sealable container).

Specimens were removed from the storage container and mass of the conditioned specimens were recorded to the nearest 0.01 g before sealing of side surfaces. Four diameters of the specimen were measured at the surface to be exposed to water. Diameters are measured to the nearest 0.1 mm and the average diameter is calculated to the nearest 0.1 mm. Side surface of each specimen was sealed with a suitable sealing material which was electrician's plastic tape in this case. The end of the specimen that is not exposed to water is supposed to be sealed by using a loosely attached plastic sheet.

The absorption procedure was conducted at 23 ± 2°C with tap water conditioned to the same temperature to determine water absorption as a function of time. Sealed specimen mass was measured to the nearest 0.01 g and it was recorded as the initial mass for water absorption calculations. At the bottom of the pan, support device was placed and then the pan was filled with tap water. Through the duration of the test, the water level was maintained at 1 to 3 mm above the absorbing surface by means of an inverted bottle filled with water. The test setup is shown in Figure 4.8.

Figure 4.8: Test setup for Rate of water absorption (sorptivity)

After starting the timing device, the test surface of the specimen was immediately placed into the water on the support device. Time and date of initial contact with water were recorded. According to the intervals listed in Table 4.4, mass is recorded after first contact with water.

Table 4.4 Times and Tolerances for the Measurements Schedule

Time	60 sec	5 min	10 min	20 min	30 min	60 min	Every hour up to 6 h	Once a day up to 3 days	Day 4 to 7 (3 readings 24 h apart)	Day 7 to 9 One reading
Tolerance	2 s	10 s	2 min	2 min	2 min	2 min	5 min	2 h	2 h	2 h

When a test specimen was removed from the pan, timing device was stopped when the contact time is less than 10 min, and any surface water was blotted off with a dampened paper towel for every mass determination. The mass is measured to the nearest 0.01 g within 15 seconds of removal from the water. The timing device is started again immediately after replacing the specimen in the water on the support device.

4.9.3 Significance of result

Water absorption of a concrete surface is largely dependent on many factors including: *(a)* concrete mixture proportions; *(b)* the presence of chemical admixtures and supplementary cementitious materials; *(c)* the composition and physical characteristics of the cementitious component and of the aggregates; *(d)* the entrained air content; *(e)* the type and duration of curing; *(f)* the degree of hydration or age; *(g)* the presence of micro-cracks; *(h)* the presence of surface treatments such assealers or form oil; and *(i)* placement method including consolidation and finishing. Moisture condition of the concrete also strongly affects water absorption at the time of testing.

Determination of the susceptibility of an unsaturated concrete to the penetration of water is the prime function of this test method. Differences are visualized between the rate of absorption of concrete at the surface and the rate of absorption of a sample taken from the interior. Because of less curing; exterior surface becomes exposed to the most potentially adverse conditions. Using this test method,

both the concrete surface and interior concrete water absorption rate can be measured. Absorption at different distances from the exposed surface can be evaluated by drilling a core horizontally and cutting it transversely at selected depths.

CHAPTER 5

Result and Discussion

In this chapter, test results from all the experiments and their analysis with proper explanations and illustrations will be presented.

5.1 Compressive Strength

Compressive strength is the most important property of concrete since the purpose that concrete is always supposed to serve is taking compressive stress. Compressive strength is the strong suit of concrete. Compressive strengths of GWRC specimens were evaluated and the test results with analysis are presented in this section.

5.1.1 Results

Compressive strength was determined for control samples (samples without GI wire) and four GWRC mixes with weight percentage of fiber varying from 1 to 2.5 percent in accordance with ASTM C 39[40]. Three types of coarse aggregate have been used, crushed stone (stone chips), crushed burnt clay bricks (brick chips) and gravel/ stone chips mixture. Properties of the aggregates and other materials have already been presented in Chapter 3. Characteristic compressive strength was determined with cylindrical concrete samples for both 7 and 28 days of curing.The results of compressive strength tests are presented in the following sections.

Charts in Figures 5.1, 5.2 and 5.3 show compression test results of samples brick chips, stone chips and gravel/stone chips mixture, respectively. Figures 5.4 and 5.5 present the comparison of compressive strengths of samples (both control and GWRC) based on coarse aggregate type measured at 7 and 28 days, respectively. Finally, increase in compressive strength in GWRC with respect to control samples is shown in the charts of Figures 5.6 and 5.7 for 7 to compare the effect of fiber content in GI wire reinforced concrete.

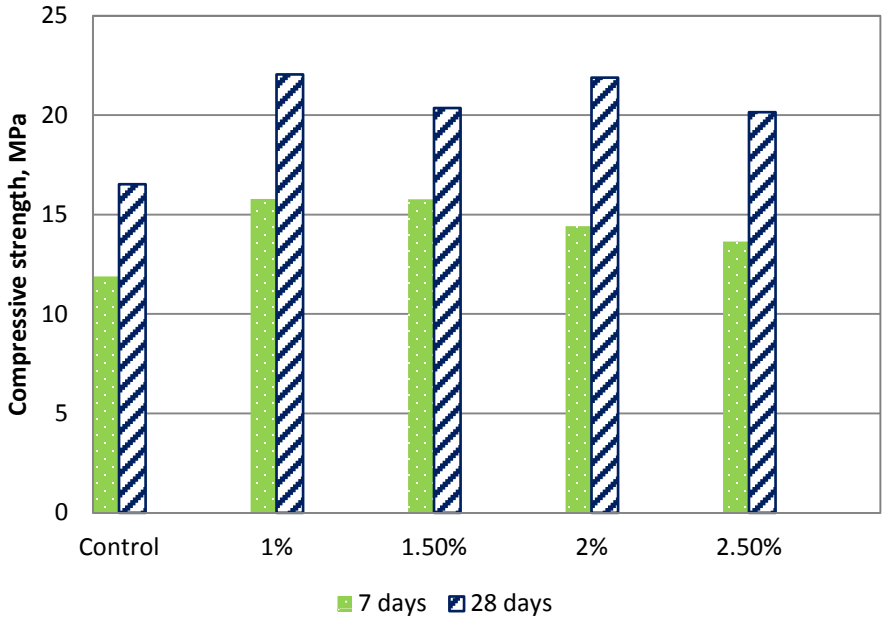

Figure 5.1: Compressive strength with BC

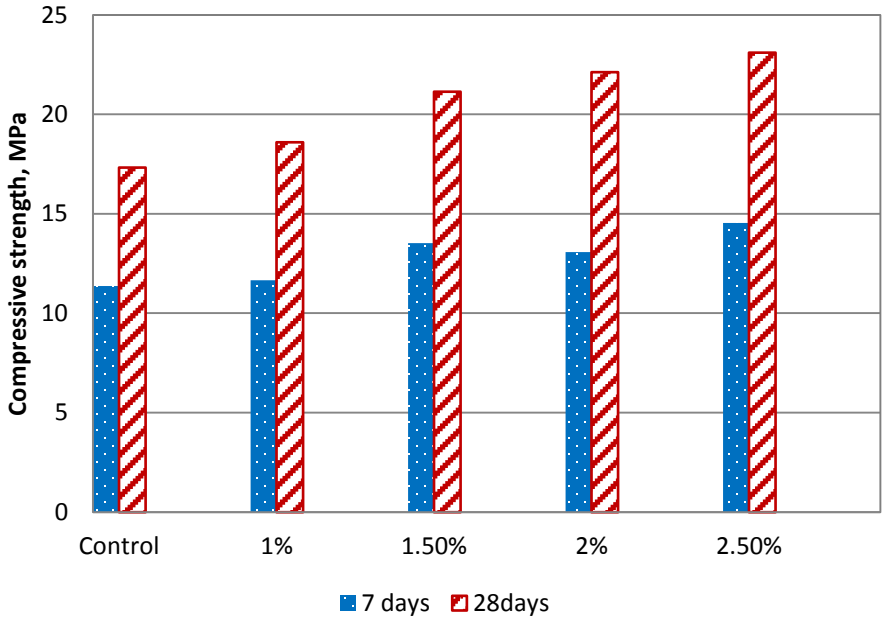

Figure 5.2: Compressive strength with SC

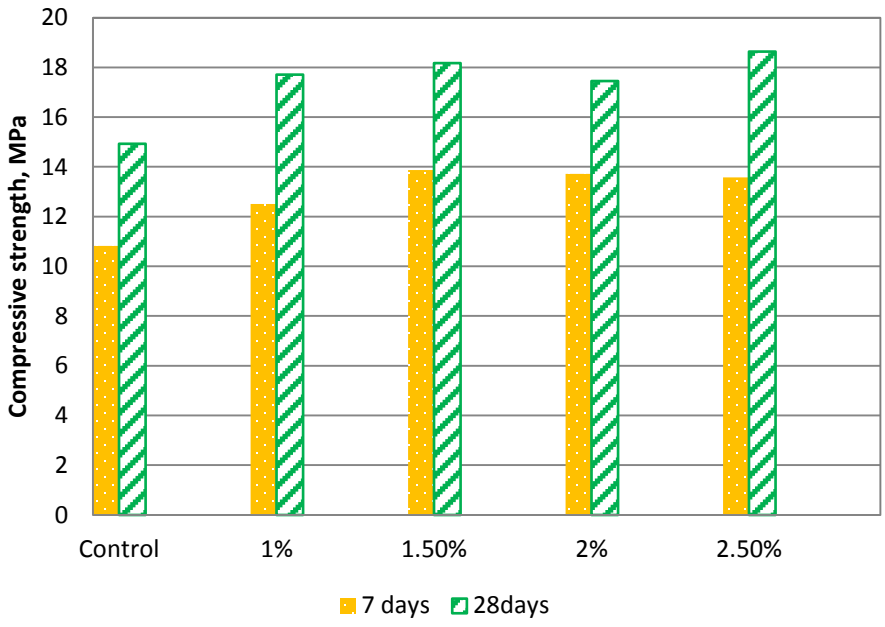

Figure 5.3: Compressive strength with Gravel/SC mix

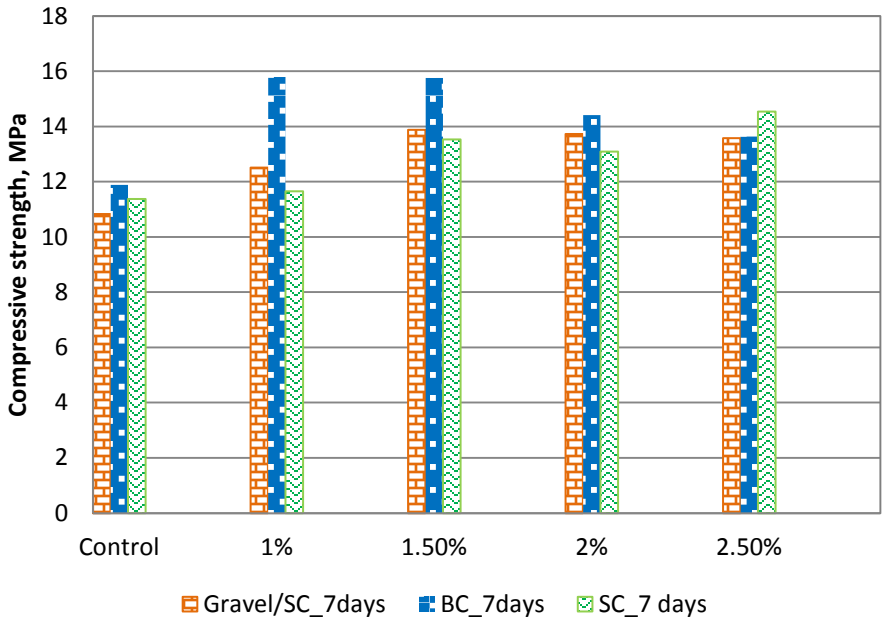

Figure 5.4: Compressive strength at 7 days

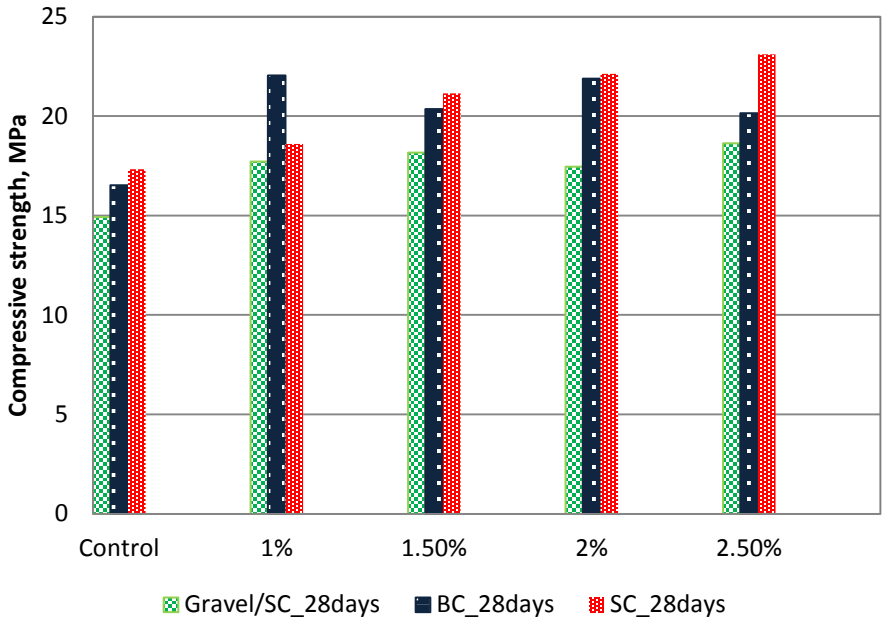

Figure 5.5: Compressive strength at 28 days

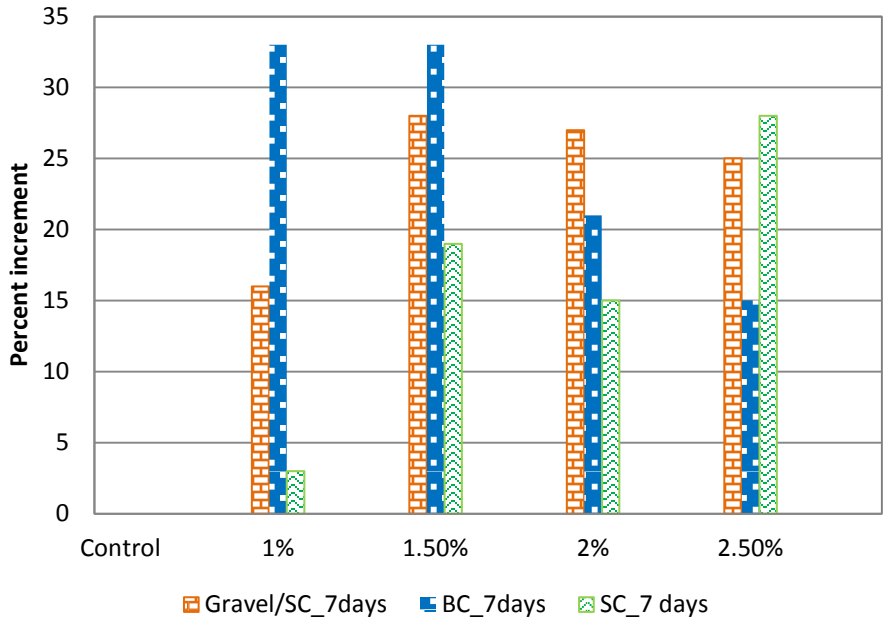

Figure 5.6: Increase in Compressive strength at 7 days due to GI fibers

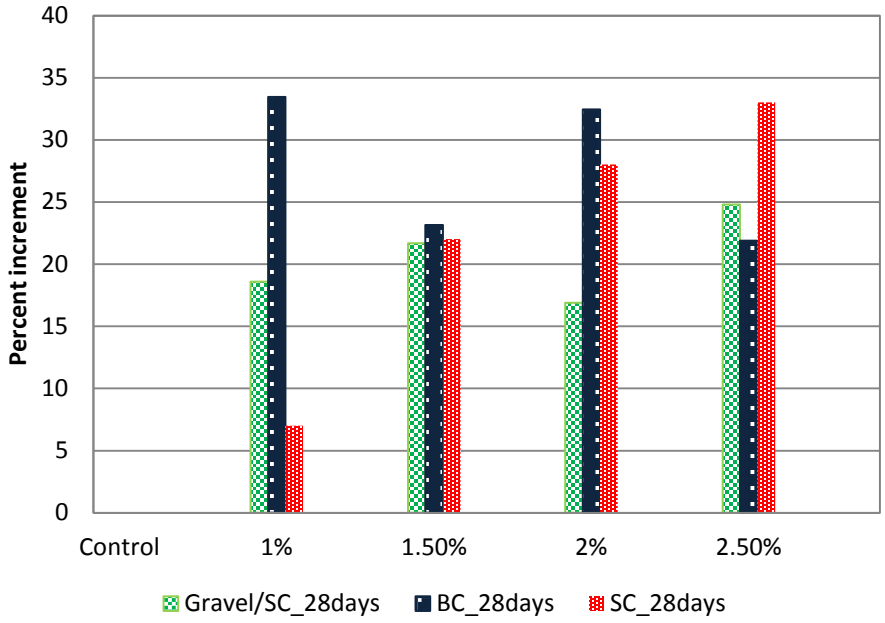

Figure 5.7: Increase in Compressive strength at 28 days due to GI fibers

5.1.2 Discussion

Concrete is a composite material and consequently, its strength depends on properties of all its constituent ingredients. Not only the materials, size and shape of the specimen, batching and mixing procedures; sampling, molding, and fabrication methods; and the age, temperature, and moisture conditions during curing etc. or even the rate of loading influences the results of the compressive strength test. On top of all these, when fibers are added to the concrete matrix, the list of influencing factors even grows longer. Different characteristics of added fibers and their dosage come to play vital roles in inducing deviation, better or worse,in concrete's behavior and eventually the performance.

Fiber content and attributes do not have direct influence on compressive strength properties of fiber reinforced concrete; nonetheless, they can passively contribute to augmentation of compressive strength as observed from a lot of previous studies [6, 8,26] with steel fibers in concrete. This phenomenon can be attributed to the confining effect of fibers that tend to hold the materials together and countering effect to the lateral tension. But the extent of these effects depend largely on

preferential orientation of the fibers which is impracticable to control in such case of randomly distributed discrete fibers in concrete matrix. Consequently, contribution to static compressive strength due to randomly dispersed fibers cannot be predicted and foreseen. Figure 5.8, showing two cylinders after failure, can provide an idea of the confining effect of GI wire fibers can impart into concrete matrix. Furthermore, fibers can significantly escalate the post-cracking ductility or, in other words, energy absorption of concrete [6]. Figure 2.5 presented in Chapter 2 shows the stress-strain curves of normal concrete and SFRC clearly manifests ductility in SFRC under compressive loading.

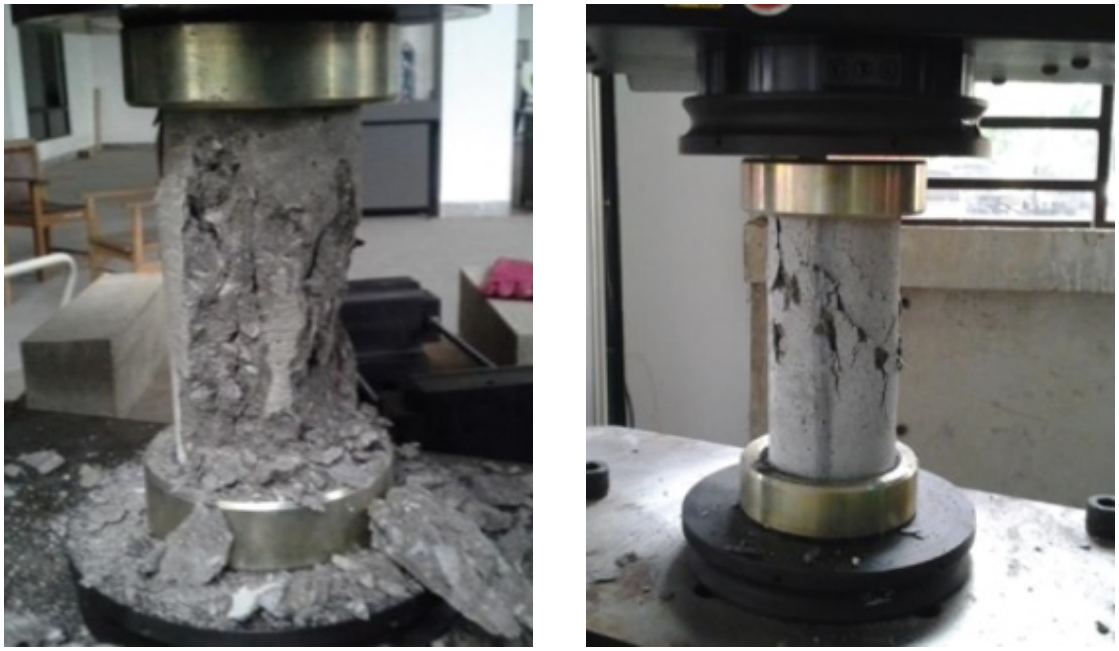

Figure 5.8: (a) Normal concrete failure (b) GWRC failure[1]

Figures 5.1, 5.2 and 5.3 presented compressive strengths at 7 and 28 days for three types of aggregates in concrete- brick chips, stone chips and gravel/stone chips mixture, respectively. Typical increment of strength from 7 days to 28 days was apparent for all types of concrete. Charts in Figures 5.4 and 5.5 are helpful in comparing performances of GWRC with three different coarse aggregates. From Figure 5.4, it is observed that, after 7 days of curing, concrete with stone chips and gravel mix gained almost similar strength while concrete with brick chips grew relatively stronger. At these early ages, failure is generally governed by mortar failure

and therefore effect of coarse aggregate is not supposed to be the dominant factor for strength, unless a quick hardening cement is used in the mix. In this case, samples with stone aggregates had predominantly mortar failure whereas, samples with brick chips showed, to an extent, combined failure characteristics. This can be the reason for some additional strength of the concrete with brick chips. After 28 days of curing, all the samples had combined failure in compression and therefore, much less variation was observed. Stone chips had slightly better performance than brick chips in concrete which is expected due to the fact that stone chips isthe stronger of the two. Another observation is that concrete with Gravel mix as coarse aggregate was weaker than the other two. This can be the result of the coarse aggregate being gap-graded as the gradation curve in Figure 3.6 in Chapter 3 suggests. Another reason can be the smooth texture of the aggregates that does not contribute to the interlocking of mixture elements in the overall matrix.

Figure 5.6 shows increment of compressive strength at 7 days due to GI wire fiber addition for all three types of aggregate. Maximum increase in strength observed is up to 33%. Strengths at 28 days are presented in Figure 5.7. Again, the maximum increment is recorded at 33%.

5.2 Tensile Strength

Split-cylinder tensile strength is the easiest method of determining tensile strength capacity of concrete. In order to understand the effect of GI wire fiber on tensile strength of concrete, splitting cylinder test was performed on normal concrete and GWRC. The test results are provided in this section and also the analysis of results.

5.2.1 Results

Splitting tensile strength of normal concrete and GWRC was determined at 28 days only for concrete with all three types of coarse aggregates according to ASTM C 496/ C 496M-04 [44]. The test provides an indication to tensile capacity of concrete. Column charts in Figures 5.9, 5.10 and 5.11 present tensile strength results for concrete with different coarse aggregates and volume fraction of GI wire fiber in GWRC. Charts in Figures 5.12, 5.13 and 5.14exhibit the augmentation of splitting

tensile strength due to incorporation of various GI wire fiber content for concrete with brick chips, stone chips and gravel/ stone chips respectively.

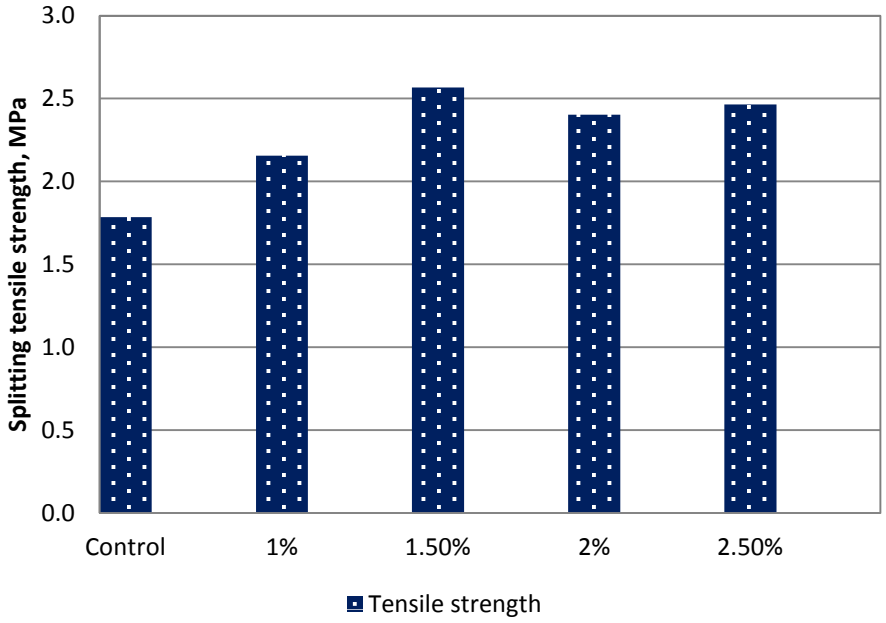

Figure5.9: Tensile strength of GWRC with brick chips

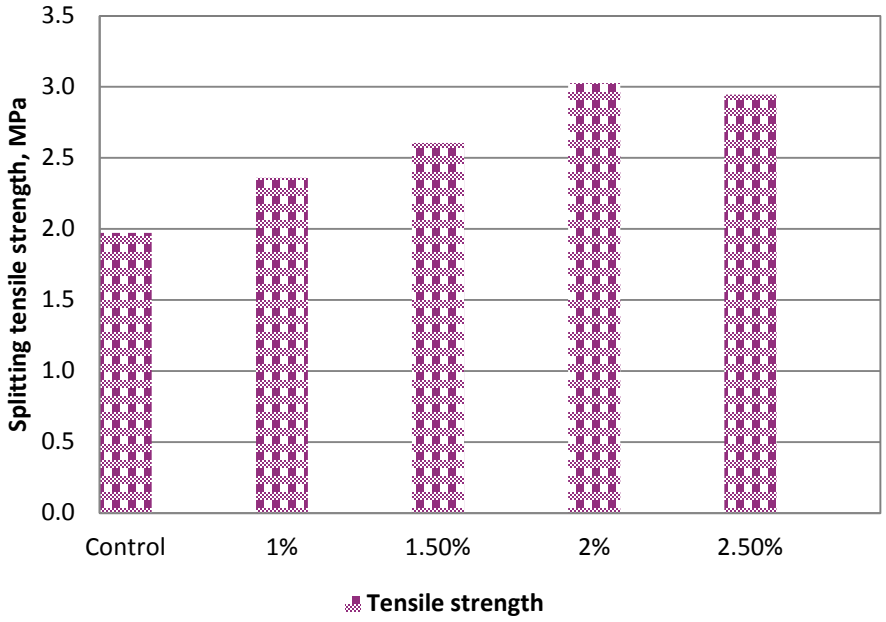

Figure 5.10: Tensile strength of GWRC with stone chips

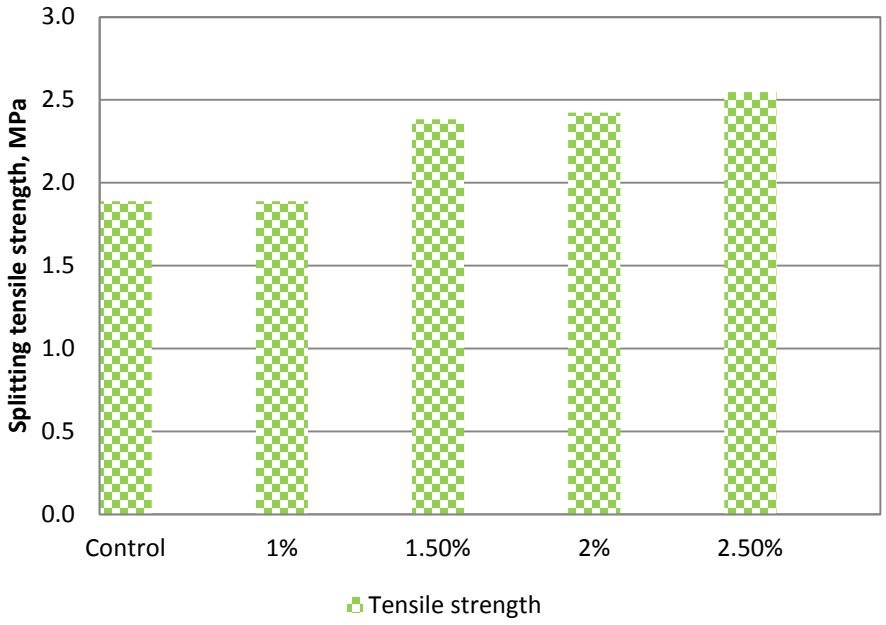

Figure 5.11: Tensile strength of GWRC with gravel/stone chips mix

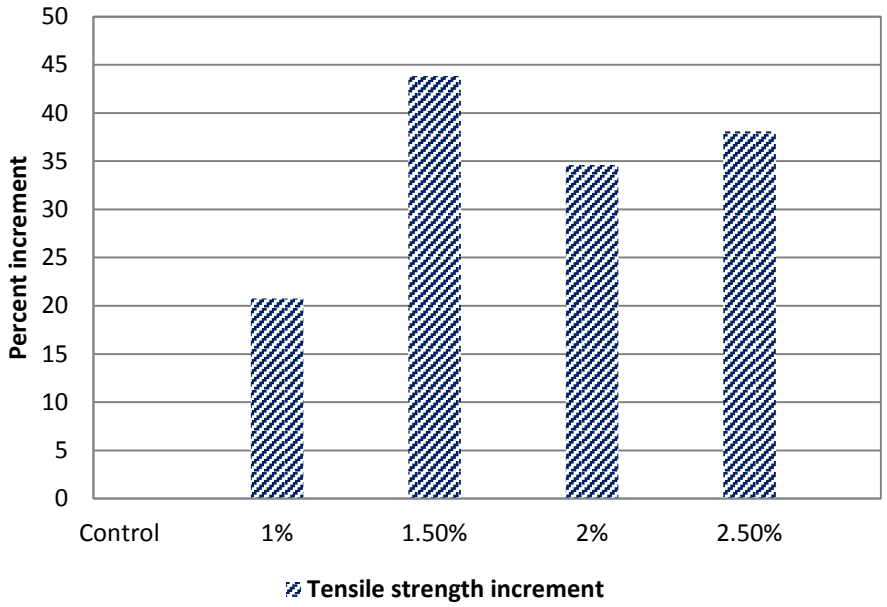

Figure 5.12: Increase in tensile strength for concrete with brick chips

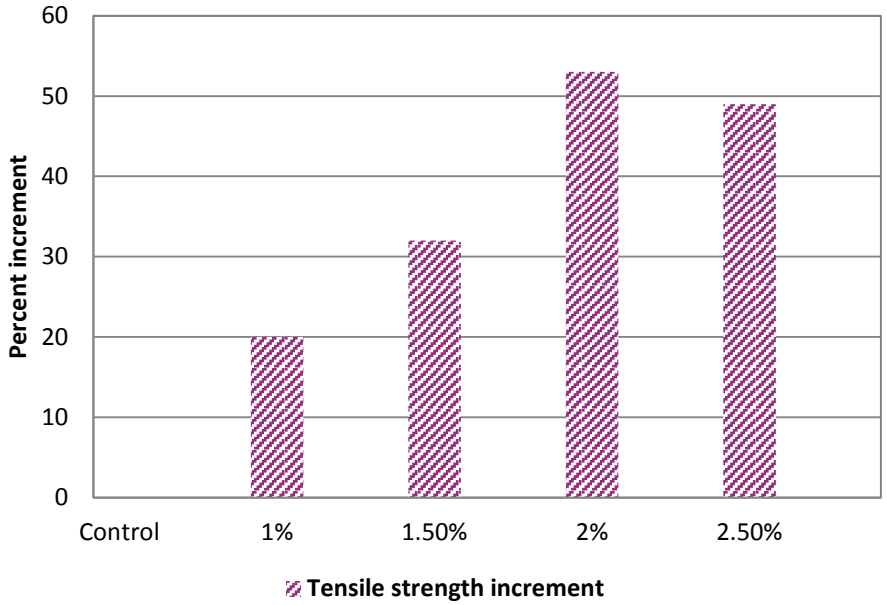

Figure 5.13: Increase in tensile strength for concrete with stone chips

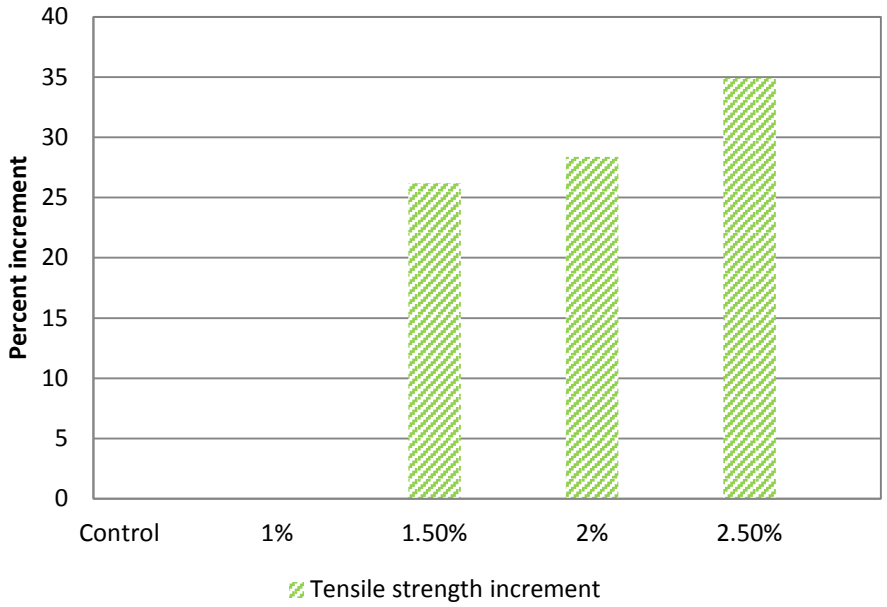

Figure 5.14: Increase in tensile strength for concrete with gravel/stone chips mixed

5.2.2 Discussion

The results are indicative of tensile strength of concrete. Values from splitting tensile strength tests are generally lower than direct tensile strength and higher than flexural strength (Modulus of rupture) [44]. But this test is the simplest way of evaluating tensile capacity of concrete since it requires special arrangements for neither sample preparation nor testing the specimens.

Figures 5.9, 5.10 and 5.11 show tensile strengths from split-cylinder tests. All concrete samples fall in the category of normal-weight concrete. According to Nilson et al. [33], approximate range of split cylinder strength of concrete is from $6\sqrt{f'c}$ to $8\sqrt{f'c}$. All the samples apparently have tensile strength within the range.

From Figure 5.12, it is evident that maximum increase in tensile strength is 44 percent. The highest increment was observed for 1.5% fiber content. Again, from Figure 5.13, for stone chips, it is found that increment varies from 20 to 53 percent with the largest gain being for 2% fiber content. Conversely, for gravel/stone chips mixture, the greatest increase was 35 percent for 2.5% fiber content, as indicated by Figure 5.14. Therefore, it is obvious that addition of GI wire fibers definitely contributed to increment of tensile strength. It is also evident from Figures 5.12, 5.13, 5.14 that with higher fiber content, strength increment tends to be higher though this trend cannot be relied upon completely. This increase is tensile capacity can be credited to the fibers aligned in the direction of the tension developed. With the increase in fiber content, probability of fibers to be aligned in this direction also increases. This explains the reason for the trend observed. For randomly distributed steel fibers, the increase can be nil to 60%. Therefore, GI wire fiber has produced similar results as steel fibers even though this increase is a bit arbitrary in nature. However, fibers contribute to major post cracking strength or toughness as found in case of compression.

5.3 Modulus of Elasticity

Modulus of Elasticity of a material is an important property to analyze load-deflection behavior. Modulus of elasticity of GWRC specimens were determined as a

part of the experimental work and this section presents and analyses the results of the tests.

5.3.1 Results

Modulus of Elasticity of concrete is determined according to ASTM C 469-02 [45]. Due to heterogeneous nature of concrete, it can always show significant aberrations in results of Modulus of Elasticity test. The test was conducted to determine if added GI fibers have any effect on this parameter.

Typical stress-strain curves for control sample and 1%, 1.5%, 2%, 2.5% GI wire fiber content with brick chips as coarse aggregate is shown in Figures 5.16 through 5.20. Stress-strain curves for concrete samples with stone chips are presented in Figures 5.21 through 5.25. Curves for the rest of the samples are provided in Appendix A.

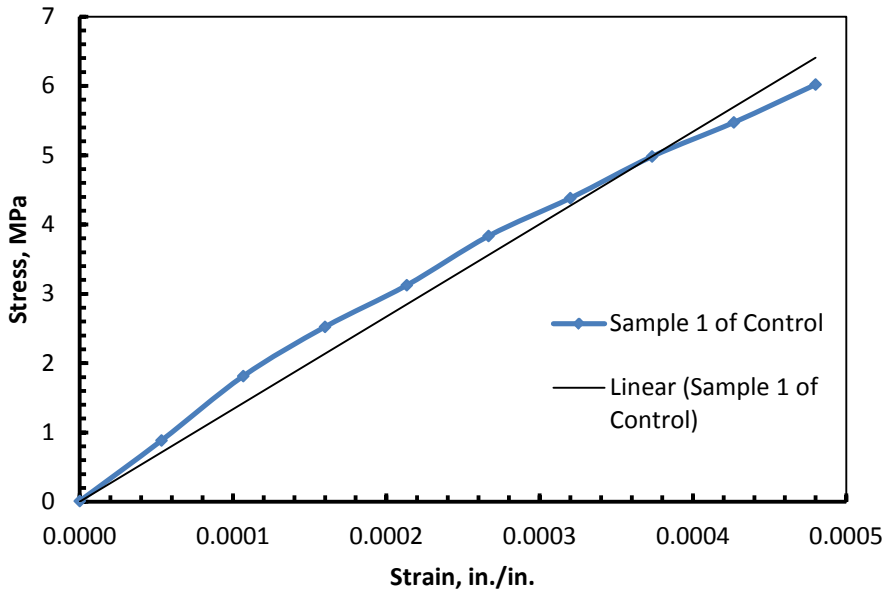

Figure 5.16: Stress-strain curve for control sample with brick chips

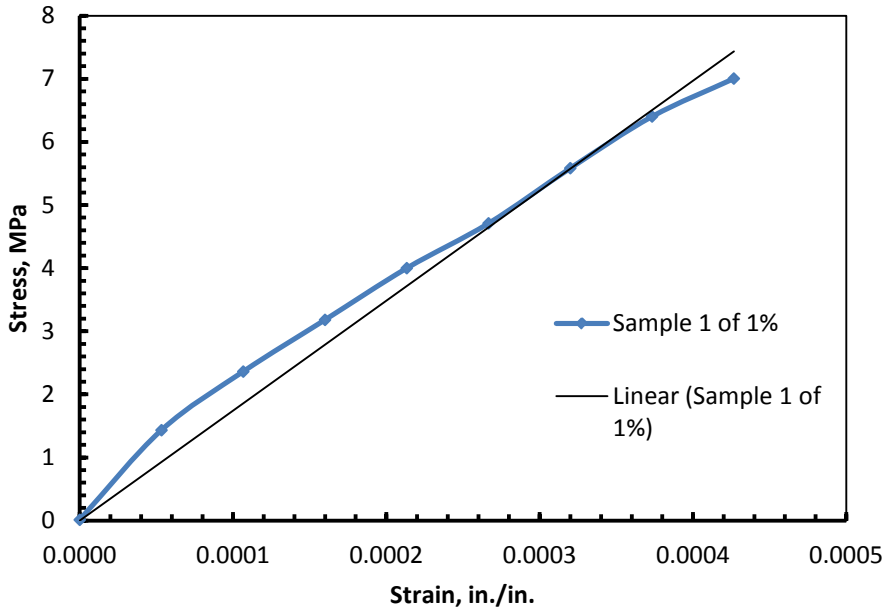

Figure 5.17: Stress-strain curve for 1% GWRC sample with brick chips

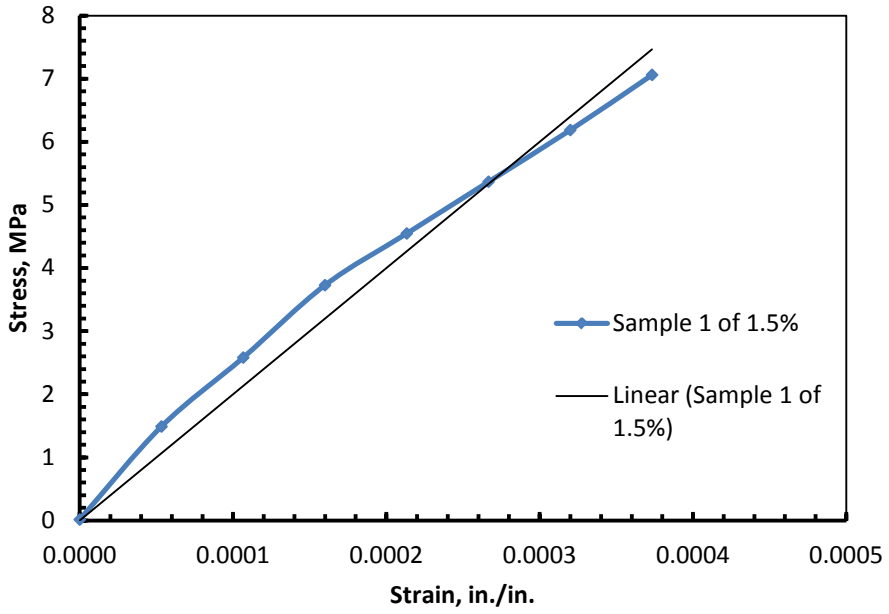

Figure 5.18: Stress-strain curve for 1.5% GWRC sample with brick chips

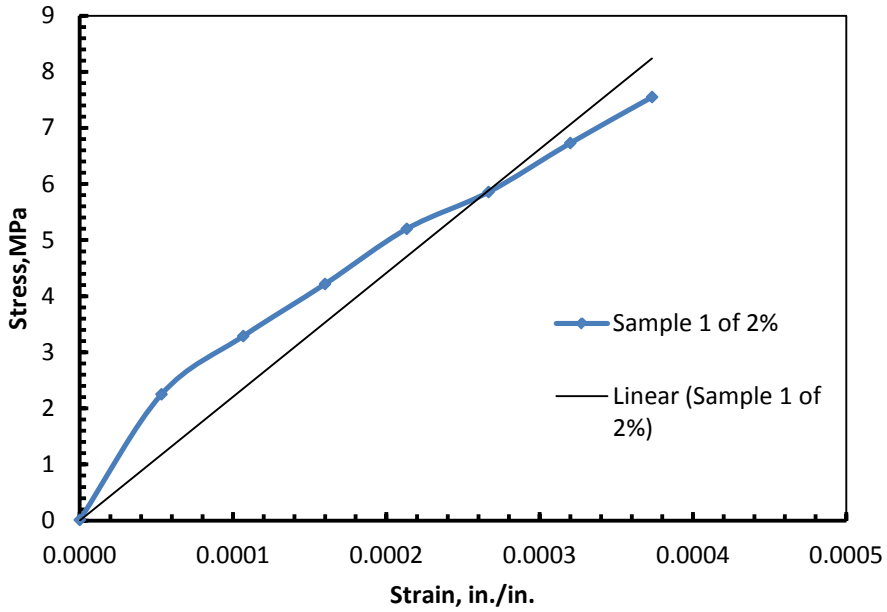

Figure 5.19: Stress-strain curve for 2% GWRC sample with brick chips

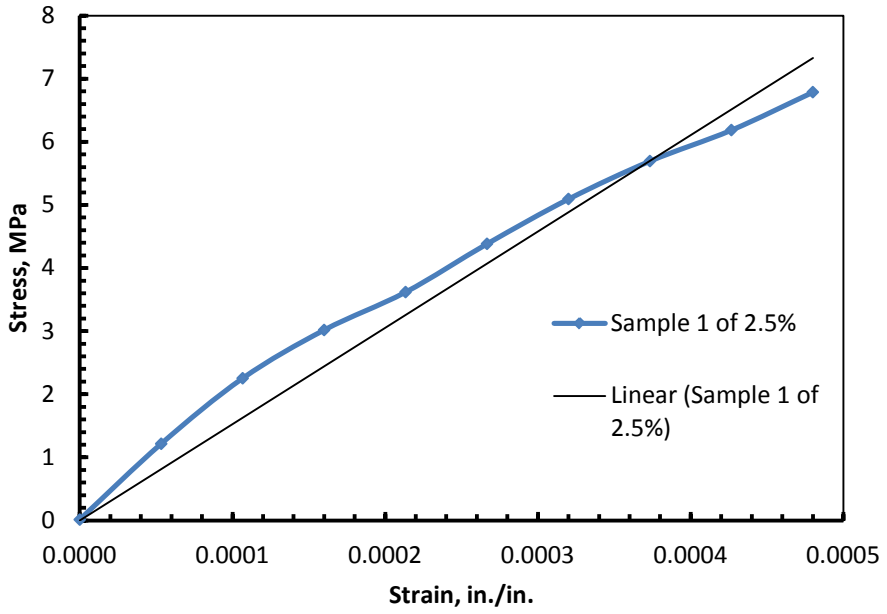

Figure 5.20: Stress-strain curve for 2.5% GWRC sample with brick chips

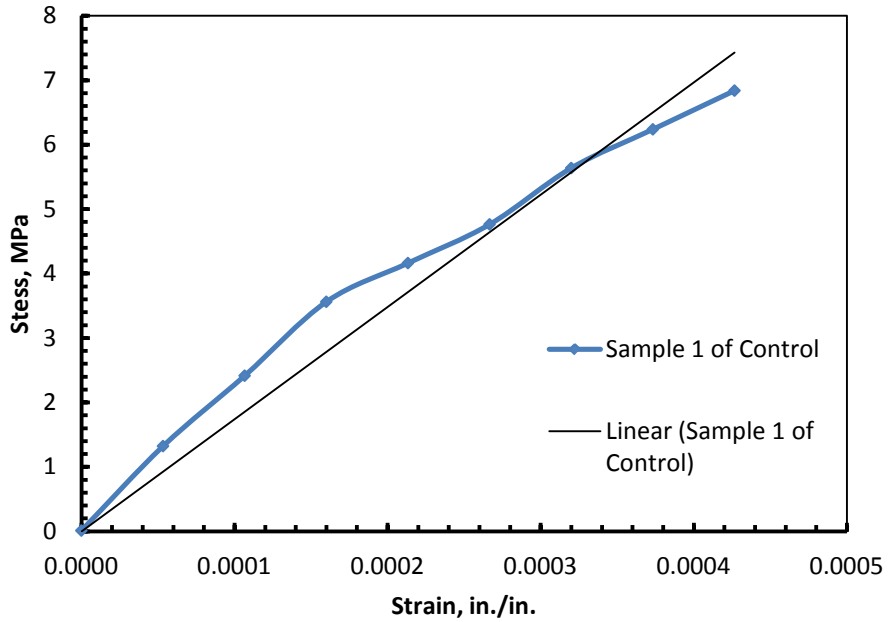

Figure 5.21: Stress-strain curve for control sample with stone chips

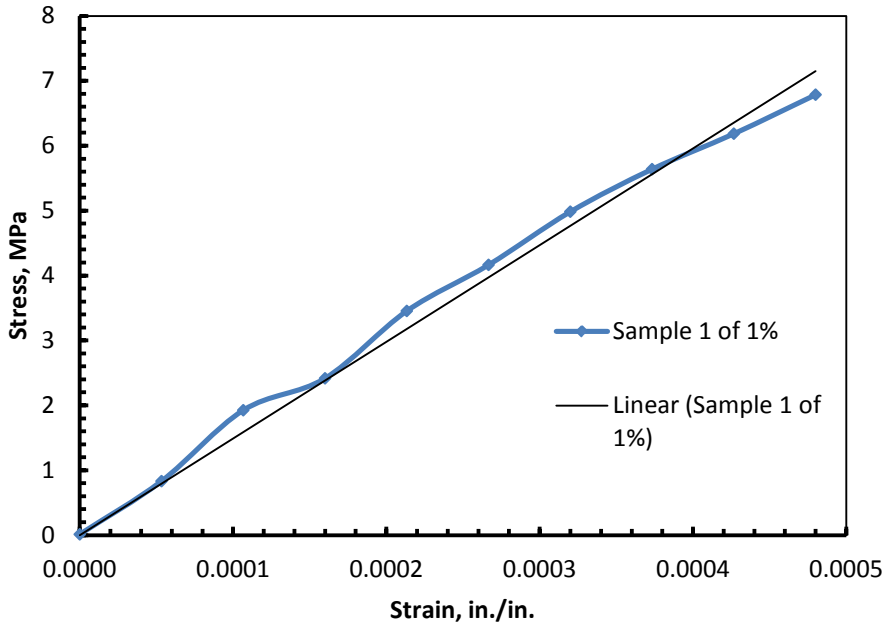

Figure 5.22: Stress-strain curve for 1% GWRC with stone chips

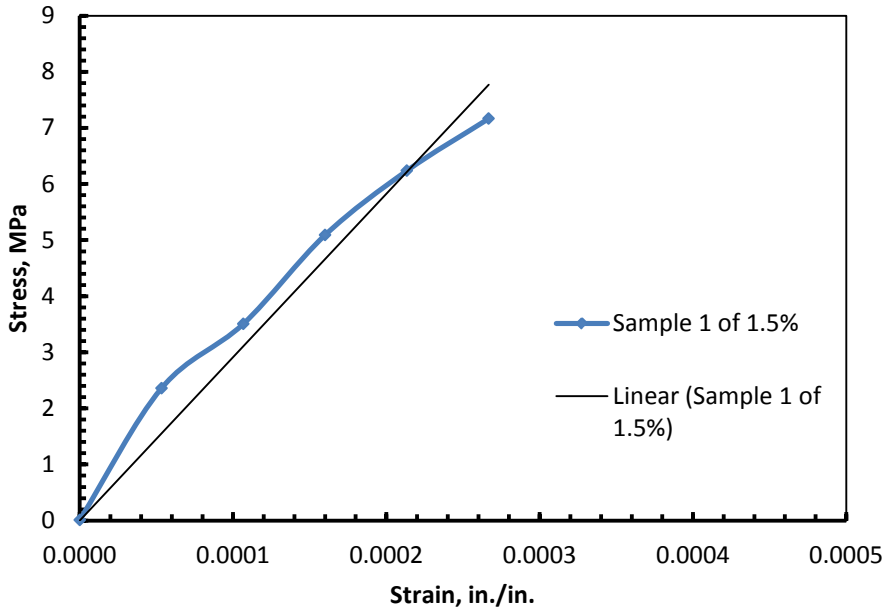

Figure 5.23: Stress-strain curve for 1.5% GWRC with stone chips

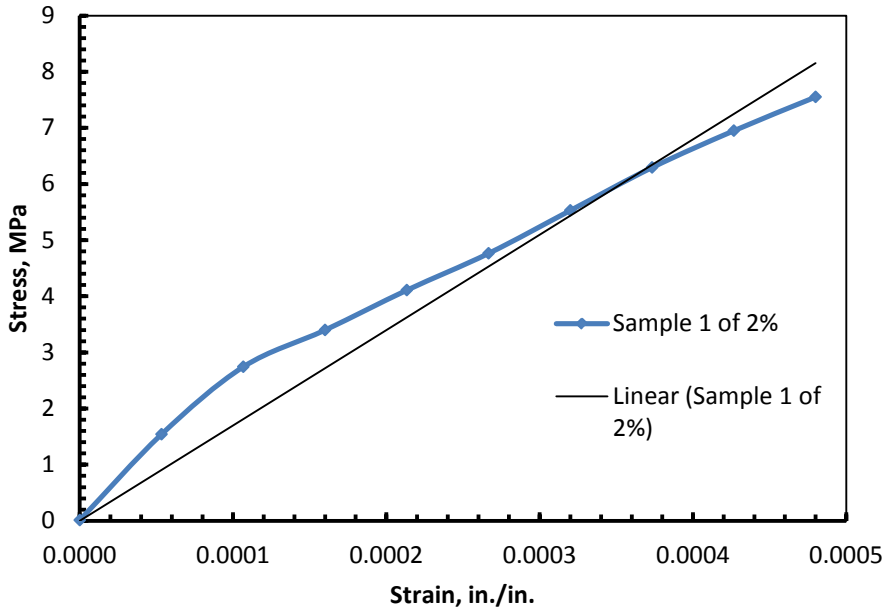

Figure 5.24: Stress-strain curve for 2% GWRC with stone chips

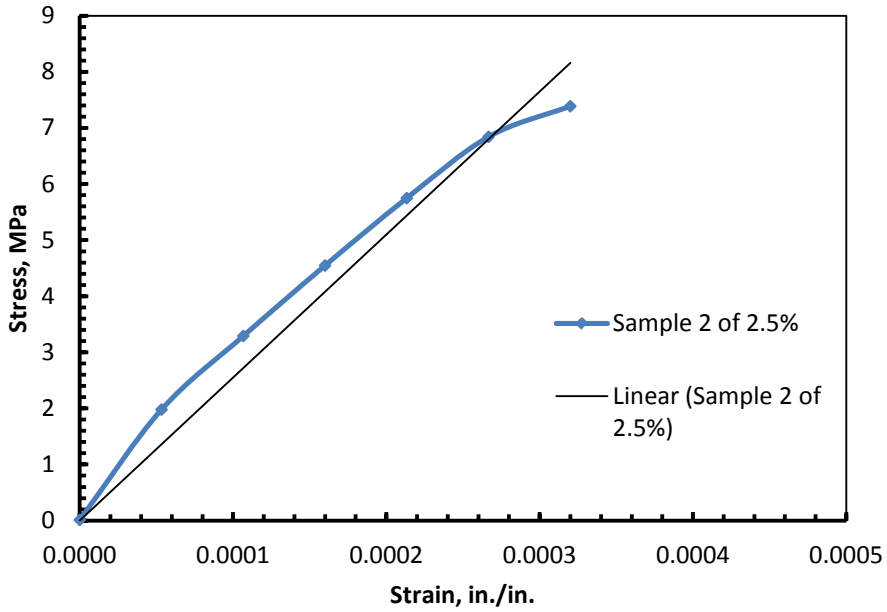

Figure 5.25: Stress-strain curve for 2.5% GWRC with stone chips

Average Modulus of Elasticity values are presented in column charts on Figures 5.26 and 5.27 for an overall comparison. Figure 5.28 and 5.29 shows increase of Modulus of elasticity due to fiber addition.

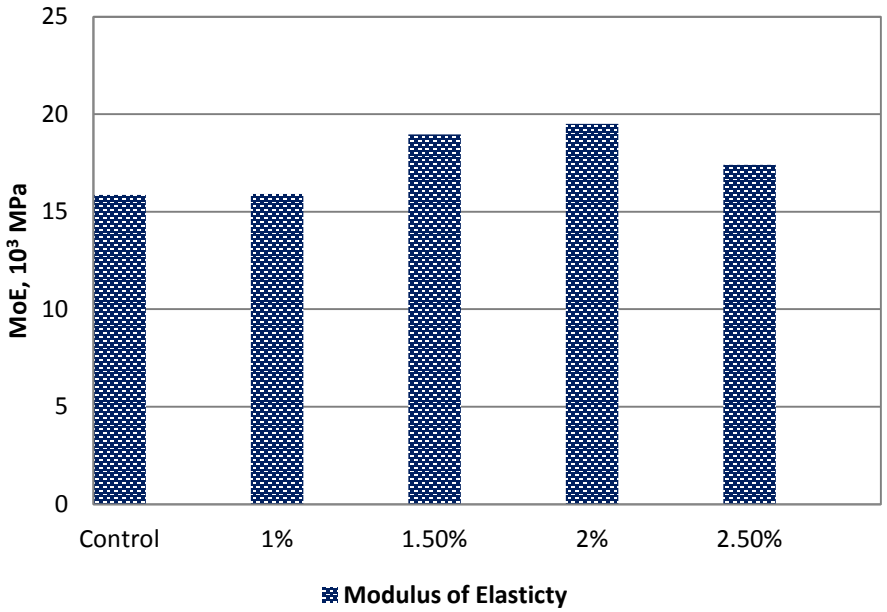

Figure 5.26: Modulus of Elasticity of normal concrete and GWRC with brick chips

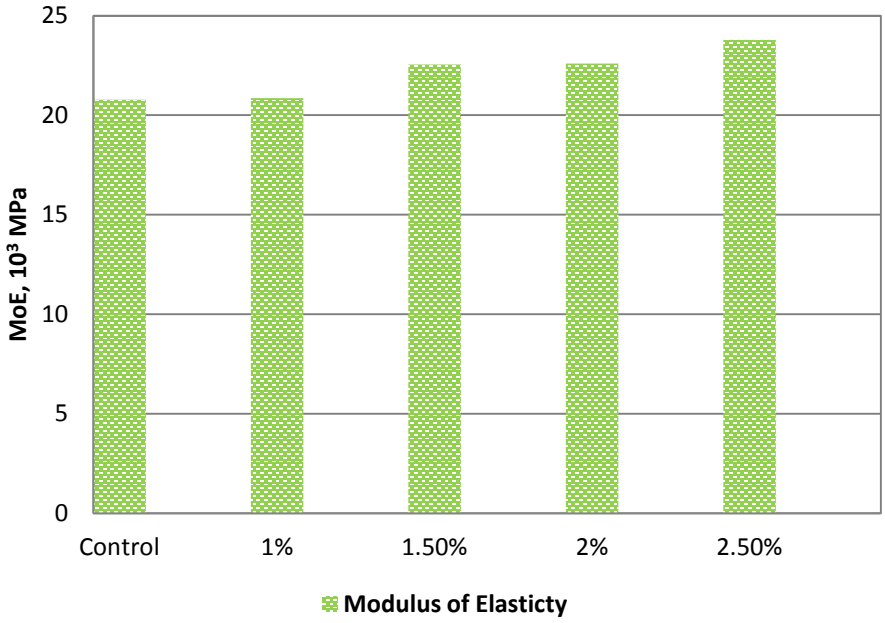

Figure 5.27: Modulus of Elasticity of normal concrete and GWRC with stone chips

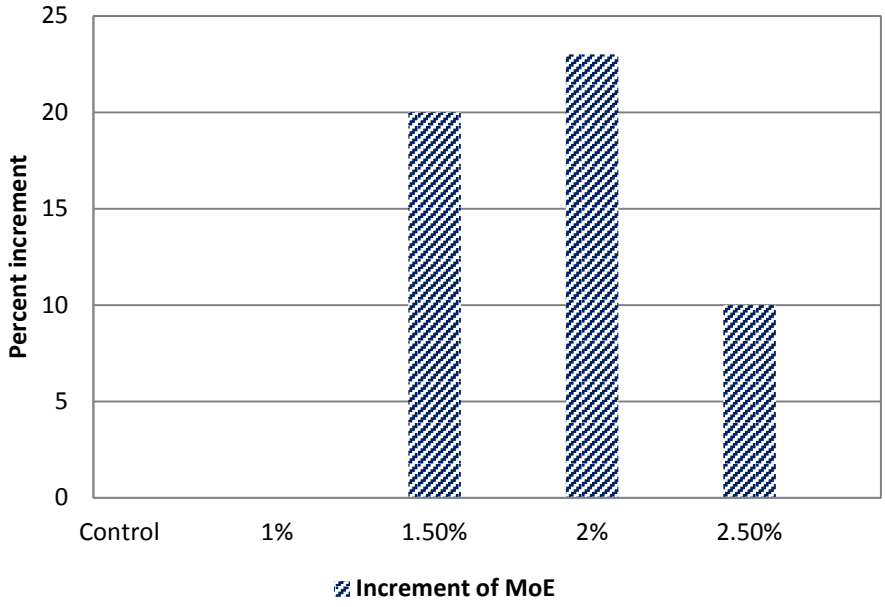

Figure 5.28: Increase in MoE due to GI fiber addition with brick chips

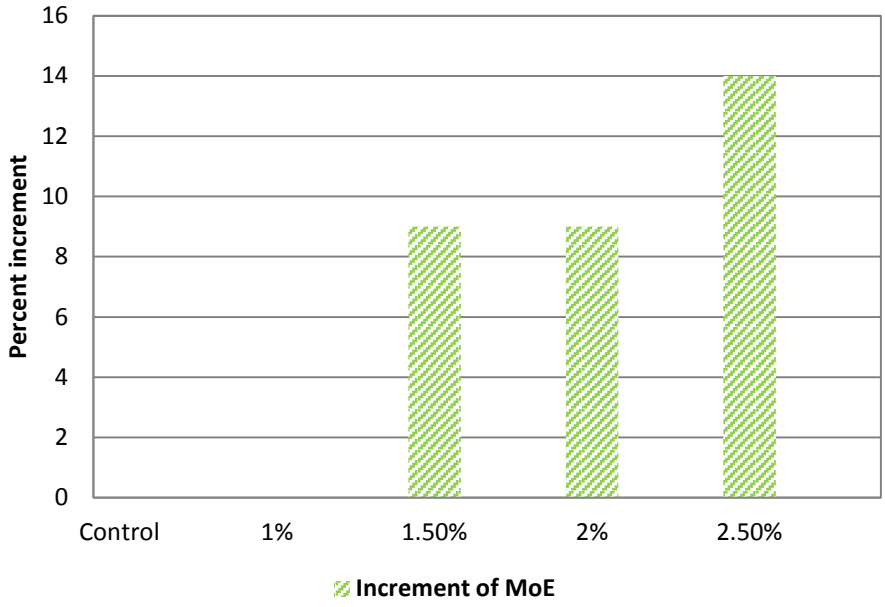

Figure 5.29: Increase in MoE due to GI fiber addition with stone chips

5.3.2 Discussion

Modulus of Elasticity helps to predict stress-strain relationship within elastic limit. Deflection under certain loading depends primarily on this parameter. As a result, for sizing reinforced and non-reinforced structural members, modulus of elasticity value is used. Moreover, for establishing the quantity of reinforcement, and computing stress for observed strains within the conventional working stress range which is upto 40% of ultimate concrete strength, modulus of elasticity is very useful. One point must be noted that, Obtained modulus of elasticity values may be less than moduli derived under rapid load application (dynamic or seismic rates, for example), and may be greater than values under slow load application or extended load duration in most cases, given other test conditions being the same[45].

From Figures 5.26 and 5.27, it is evident that effect of GI wire fiber is not very obvious, the variation being very small. Charts in Figures 5.28 and 5.29 reveal that for 1% fiber content, there is literally no effect on Modulus of elasticity. With increasing fiber content, value of the parameter increases. For brick chips in concrete, the maximum increase was 23% for 2% fiber content. With stone chips, though, the maximum increase was about 14% for 2.5% fiber content. Therefore, it can be assumed that addition of GI fiber in concrete has no negative effect of Modulus of

Elasticity values; rather it can increase, though not very pronounced, the value of the modulus.

5.4 Beam Flexure/Ductility test

This section of the chapter focuses on the third-point loading test performed on the test beams. For the test members, brick chips was used as a lightweight coarse aggregate. Brick chips were chosen because slabs and beams are cast with brick chips for majority of the buildings in Bangladesh in order to reduce self-weight, low cost and availability. Stone chips are also used for comparison with previous studies. Results from the tests are presented in the next section and analysis of the results follows.

5.4.1 Results

The beams were tested as described in Chapter 4. A total number of 25 beams were tested for the research. Three beams were prepared for concrete without fiber and three each for four different GWRC mixes up to 2.5% fiber content with brick chips. Two samples each was prepared for 3% and 3.5 % fiber content. Two more mixes with 3% and 3.5% fiber content and stone chips were prepared. Light-weight concrete with brick chips is the main focus of the study. Samples with stone chips were used for comparison with previous works with mild steel fibers. Third point loading was applied. The load deflection curves derived from the tests are presented in Figures 5.30 through 5.36. Mean load deflection curve for all five concrete mixes is shown in Figure 5.37 for comparison of performances of GWRC with respect to normal concrete. Table 5.1 summarizes the test results. Several new terms have been used in the results table. The terms are explained right after the table is presented.

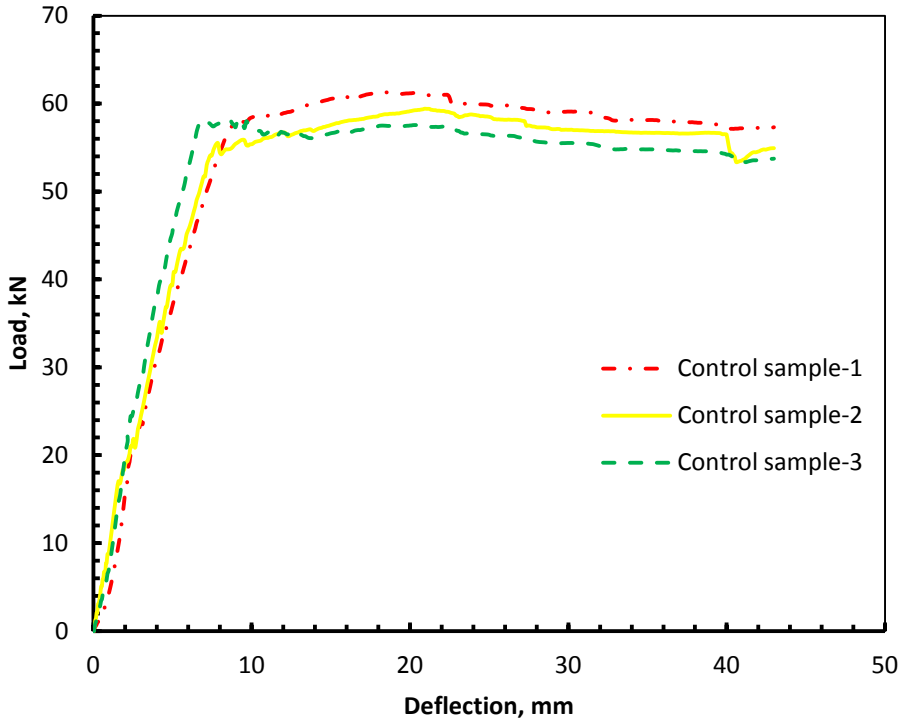

Figure 5.30: Load-deflection curve for control samples

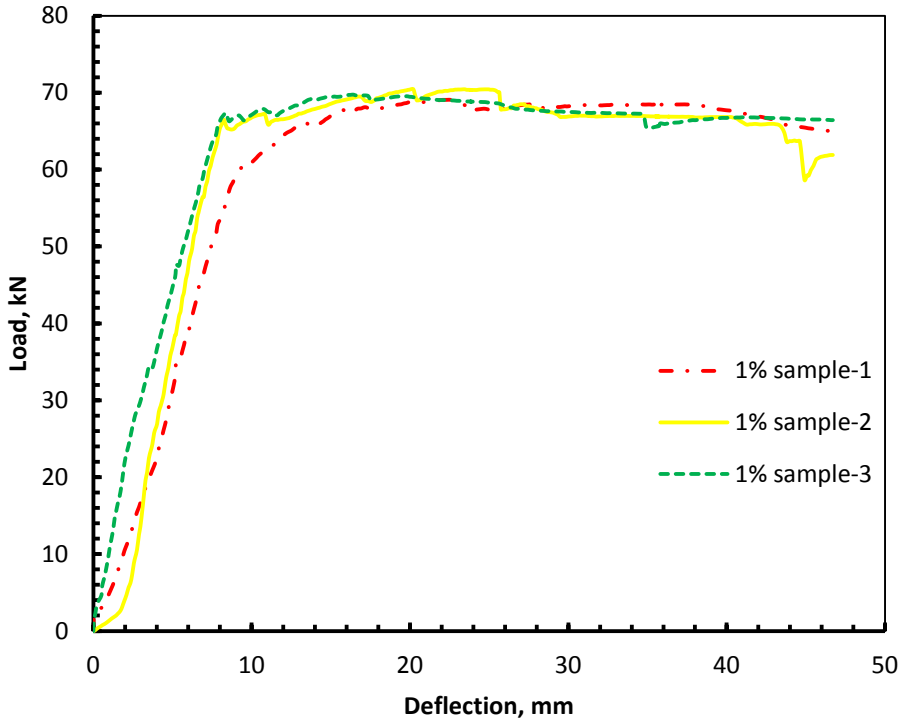

Figure 5.31: Load-deflection curve for 1% GWRC samples

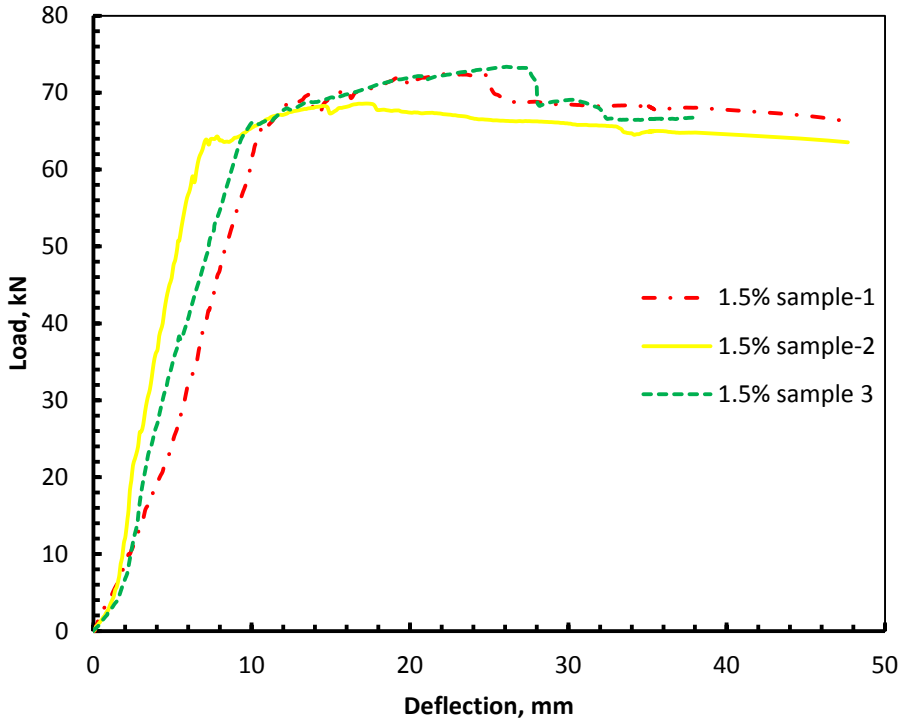

Figure 5.32: Load-deflection curve for 1.5% GWRC samples

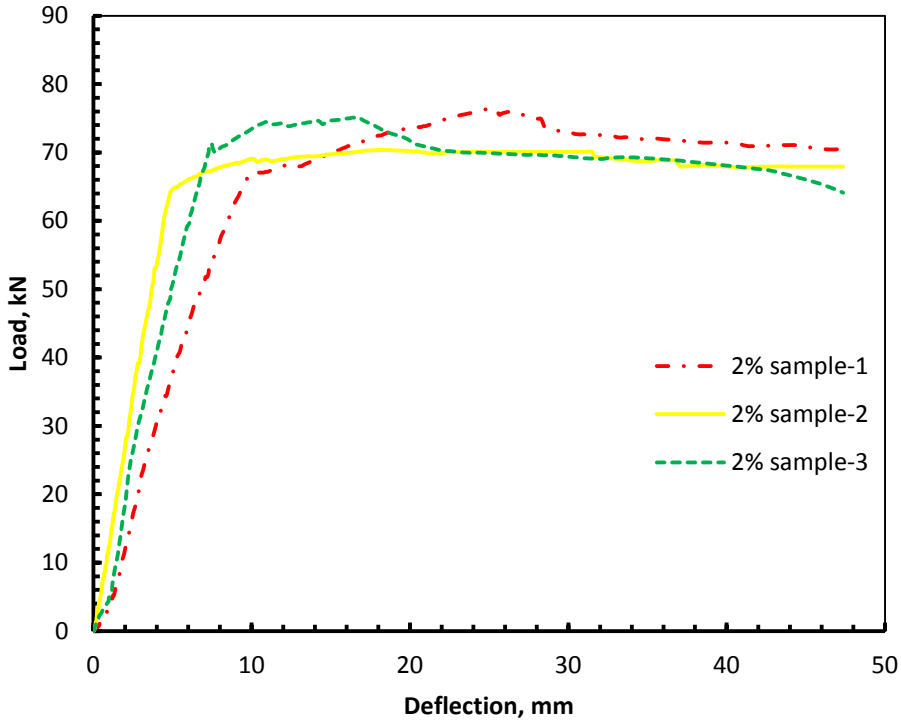

Figure 5.33: Load-deflection curve for 2% GWRC samples

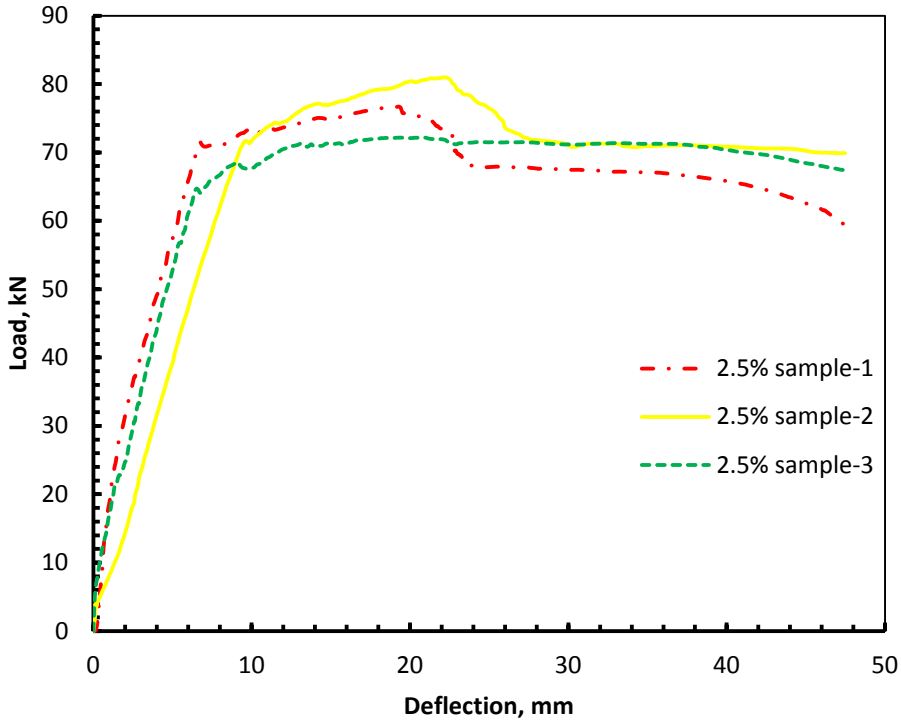

Figure 5.34: Load-deflection curve for 2.5% GWRC samples

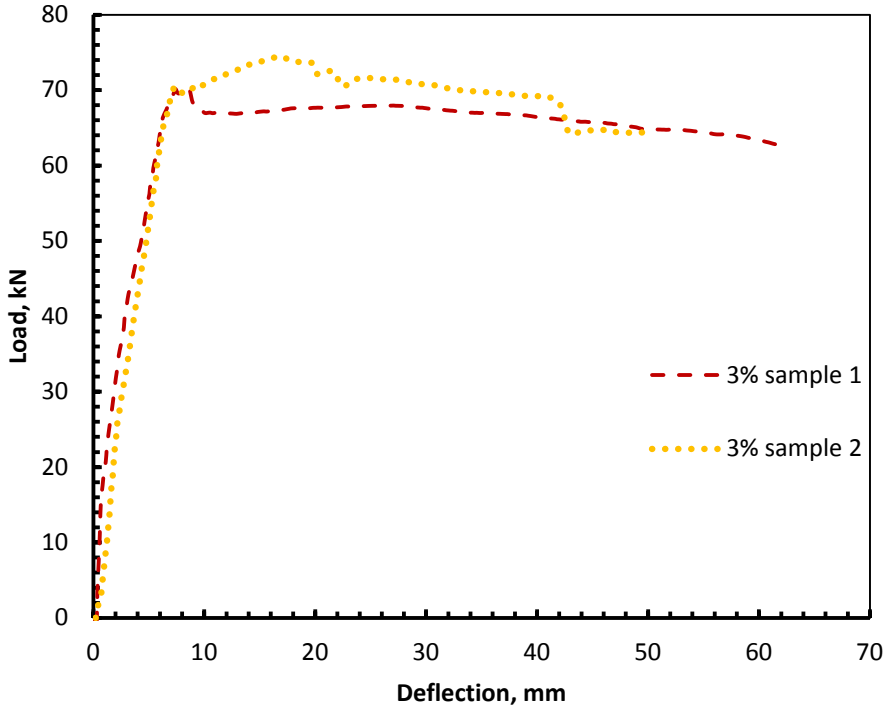

Figure 5.35: Load-deflection curve for 3.0% GWRC samples

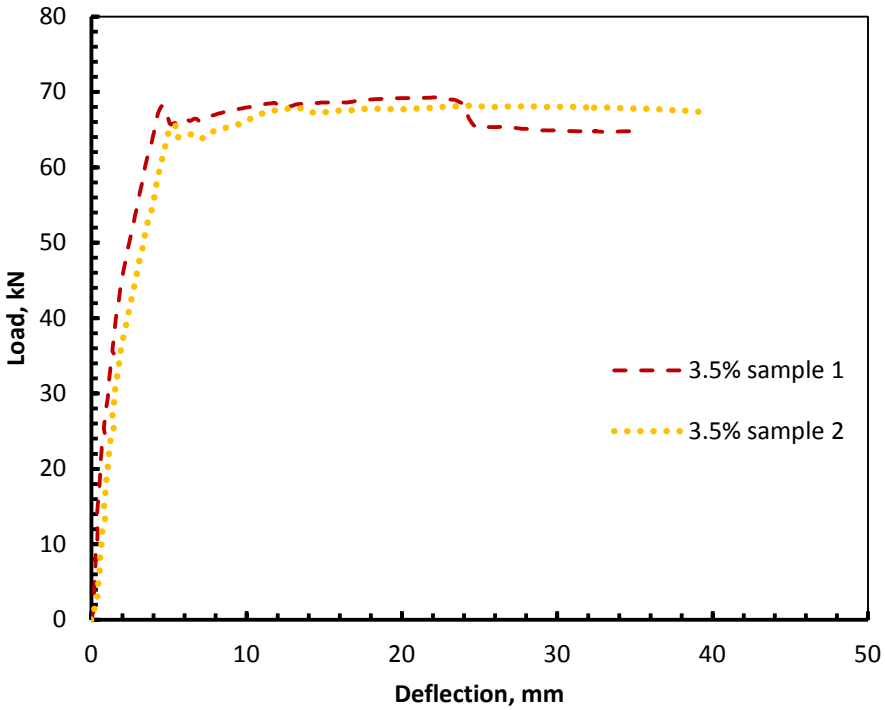

Figure 5.36: Load-deflection curve for 3.5% GWRC samples

Table 5.1: Summary of flexural tests on test beams

Concrete	Sample ID	Micro-crack load	Average load for Micro-crack	Visible hairline crack load	Macro-crack load(assumed first crack)	Average Macro-crack load	First-crack mid-span deflection	First crack Toughness	Average Toughness	Ultimate Load	Average Ultimate Load
		kN	kN	kN	kN	kN	mm	N.m	N.m	kN	kN
Control	Sample-1	23.843	23.8	37	58.222	57.4	9.180	304.80	260.2	61.22	60.3
	Sample-2	23.756		41	55.493		7.806	250.08		59.4	
	Sample-3	25.337		40	58.378		8.582	270.23		60.33	
1% GWRC	Sample-1	36.666	33.2	54	66.028	66.2	8.262	245.28	282.7	70.46	70.5
	Sample-2	30.506		49	67.412		8.322	320.14		69.76	
	Sample-3	32.498		52	65.274		8.293	281.58		71.21	
1.5% GWRC	Sample-1	34.222	44	41	65.837	65	10.666	321.46	327.9	72.36	71.4
	Sample-2	59.083		61	64.216		7.169	231.80		68.58	
	Sample-3	38.549		58	66.070		10.017	334.27		73.34	
2% GWRC	Sample-1	-	-	46	67.217	68.6	10.095	372.46	324	76	73.8
	Sample-2	-		38	67.246		7.416	320.39		70.15	
	Sample-3	-		69	71.338		7.461	279.08		75.14	
2.5% GWRC	Sample-1	-	-	71	71.489	69.2	6.728	282.87	303.3	76.72	76.6
	Sample-2	-		69	71.714		9.668	375.58		81	
	Sample-3	-		57	64.51		6.557	251.33		72.14	
3.0% GWRC	Sample-1	-	-	67	66.322	68.0	7.469	307.61	289.0	70.12	72.3
	Sample-2	-		64	69.710		7.388	270.36		74.50	
3.5% GWRC	Sample-1	-	-	65	68.672	68.2	4.557	283.20	286.0	69.3	68.7
	Sample-2	-		69	64.375		5.392	288.88		68.1	

In the table above, micro-crack means the very first start of cracking which is only noted by sudden yet very small decrease in loading where load was supposed to steadily rise in the elastic zone. Elastic deformation zone can be defined up to this point. A micro-crack cannot be discerned with eye. The crack needs to grow a little more to the minimum width for the eyes to notice. The minimum load when this crack is detectable with an unaided eye is called 'visible hairline crack load'. Macro-crack is the initiation of sudden widening of cracks without much increase in load. This phenomenon is a little similar to 'yielding' which is observed for mild steel. This point is also similar to the crack termed as 'first-crack' in ASTM 1018 [17] which is a test for FRC without main reinforcement. Therefore, these two points have different meaning and significance. But for similarity of their nature, the macro-crack will be mentioned as the first-crack henceforward. The load corresponding to the first-crack is called first-crack load. Toughness calculated up to first-crack is the first-crack toughness. Ultimate strength is the maximum load recorded.

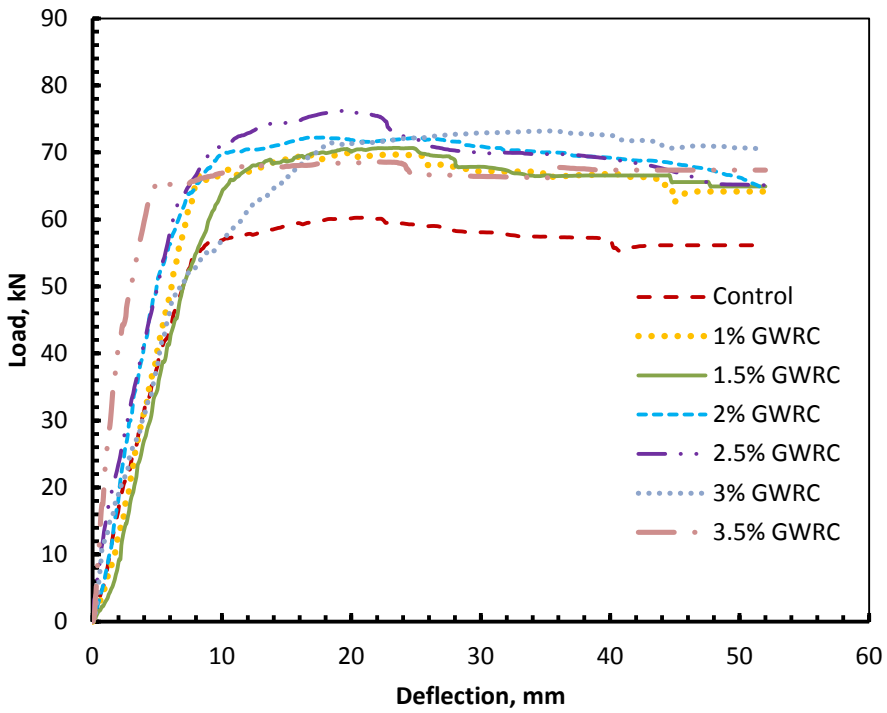

Figure 5.37: Mean load-deflection curves for five different mix-designs

5.4.2 Discussion

Load-deflection curves under flexural loading are generally utilized to assess flexural capacity as well as ductility and toughness. Therefore, three beams for each mix-design were prepared to evaluate the flexural performance of locally available GI wire reinforced concrete beams. Load-deflection curves in Figures 5.30 through 5.36 demonstrate that all the curves for the same mix design are almost identical. Therefore, results can be assumed to be reliable since same results are obtained for a number of samples. The pattern of the curves are similar, an elastic portion prior to crack formation followed by plastic deformation region.

From Figure 5.37, it is obvious that all the GWRC samples had much higher strength than the control samples. The initial elastic deformation region was similar for all the mixes including control mix. But the initiation of plastic deformation was greatly delayed by added fibers. Difference between the performances of GWRC samples is difficult to discern by visual assessment. From the shape of the curves it is evident that up to 2% to 2.5% fiber addition, there is an increasing trend in ultimate strength of the beams. However, this observation is subject to numerical analysis which follows in the subsequent sections.

From Table 5.1, average micro cracking load for control, 1% and 1.5% GWRC are 23.8, 33.2 and 44 kN respectively. No micro-crack was observed with samples with more than 2% fiber content. This indicates that 1.5% fiber content has increased the micro-crack load by 85% where fiber content more than that has resisted formation of micro-crack in the elastic deformation zone. This is a significant contribution of GI wire fibers in delaying micro-crack formation. This phenomenon can be the result of GI fibers taking tension away from concrete through crack bridging action. Yet, it should be noted that, this action will be intensified with the fibers aligned in the direction of tension and downsized if the fibers are aligned perpendicular to tension developed.

Visible hairline crack is a little less reliable parameter since detection of the crack with open eyes is largely dependent on the efficiency of the observer. Moreover, coatings on the members may conceal the crack until the cracks grow sufficiently large to be visible. Therefore, it is difficult to make any concrete judgment on the basis of this parameter.

Macro-crack load or the first-crack load can be considered as a reliable measure for the flexural strength of the beams. This is the initiation of the plastic deformation region. From column 7 in the table 5.1, it is obvious that the average first-crack load for control samples is 57.4 kN whereas, for 2.5% GWRC samples, it is 69.2 kN. The increase by about 22 percent can be accredited to the contribution by GI wire fibers. The crack arresting mechanism of the distributed fibers in the concrete matrix helps the members not only to sustain a larger load, but also to absorb more energy before rupture. Figure 5.38 shows fibers in the beams after failure. These fibers are, supposedly, the source of added strength. Figure 5.39 presents the increase of first-crack loads due to fiber addition.

Figure 5.38: GI wire fibers spanning across the crack

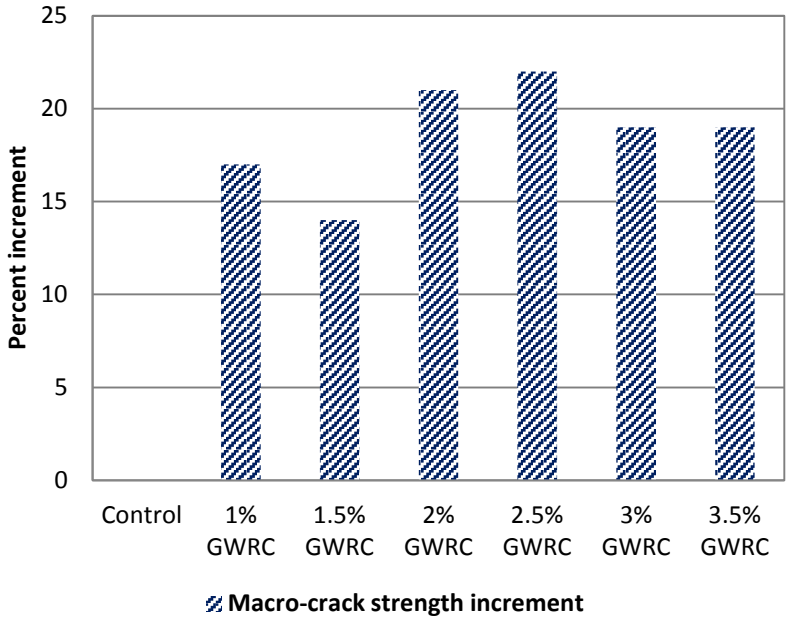

Figure 5.39: Increase in macro-crack strength due to fiber addition

First-crack toughness and ultimate strength also show marked increase, as Figures 5.40 and 5.41 demonstrate. From the charts, it can be seen that increase of toughness is maximum for 1.5 to 2% fiber content. On the other hand, maximum increase in ultimate strength is observed for GWRC with 2.5% fiber content. The indices described in Chapter 3 were determined and are tabulated in Table 5.2.

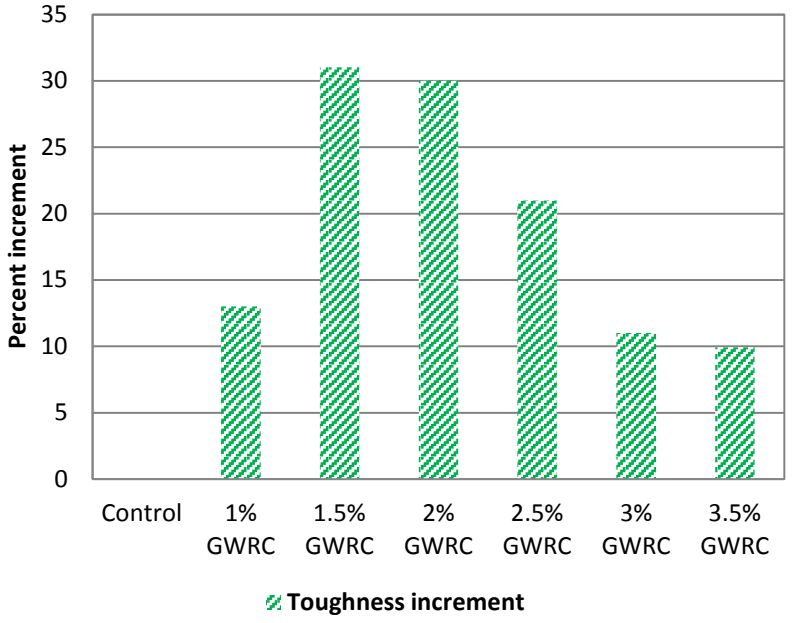

Figure 5.40: Increase in Toughness up to first-crack due to fiber addition

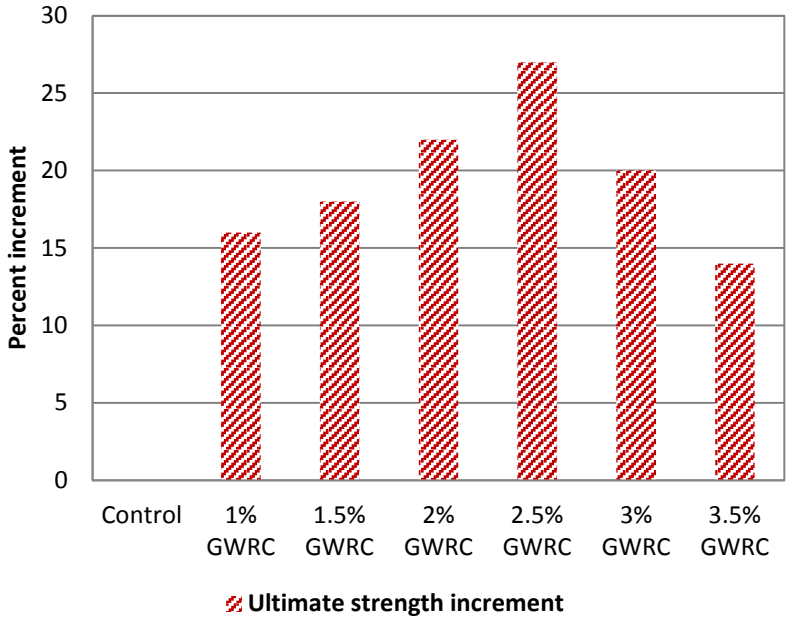

Figure 5.41: Increase in Ultimate strength due to fiber addition

Table 5.2: Indices relevant to ASTM 1018[17]

Concrete	Sample ID	I_5	Average I_5	I_{10}	Average I_{10}	$R_{5,10} = 20(I_{10} - I_5)$	Average $R_{5,10}$
Control	Sample-1	4.6	4.5	8.9	8.9	86	86
	Sample-2	4.6		9		88	
	Sample-3	4.2		8.8		85	
1% GWRC	Sample-1	5.6	5	11.2	10	112	97
	Sample-2	4.6		8.9		86	
	Sample-3	4.8		9.8		93	
1.5% GWRC	Sample-1	5.7	5.4	11.1	10.4	108	101
	Sample-2	5.2		10.2		100	
	Sample-3	5.2		10		96	
2% GWRC	Sample-1	4.9	4.7	9.7	9.2	96	90
	Sample-2	4.3		8.3		80	
	Sample-3	4.9		9.6		94	
2.5% GWRC	Sample-1	4.5	4.7	8.6	9.1	82	89
	Sample-2	4.9		9.4		90	
	Sample-3	4.7		9.4		94	
3% GWRC	Sample-1	4.8	4.6	9.1	9.1	86	90
	Sample-2	4.4		9.1		94	
3.5% GWRC	Sample-1	2.9	3.1	5.7	6.1	56	60
	Sample-2	3.3		6.5		64	

The indices in Table 5.2 are more relevant to ASTM 1018 tests as the test specimens are made without main reinforcement. Concrete without fibers shows brittle failure and these indices become zero. But for FRC, these indices can be utilized to evaluate toughness with respect to first-crack toughness and also the amount of energy that the member can absorb after the crack. As test beams for the current research was doubly reinforced, the samples without fibers also shows some degree of ductility due to main reinforcement. As a result, the increase in the indices is the contribution of the fibers on top of the input by the main reinforcement. Thus, value of the absolute toughness is better suited rather than the indices in this context, as first-crack toughness of the GWRC samples are higher than that of normal concrete.

One more characteristic behavior was studied. From the design data, load vs. crack width graphs (shown in Figure 5.42) were plotted which gives a clear idea about the effectiveness of fibers in reducing crack width. Crack pattern is also an important aspect of the test. Only the major crack was considered for the graphs. Crack patterns for different mix-designs are shown in Figures 5.43 through 5.47.

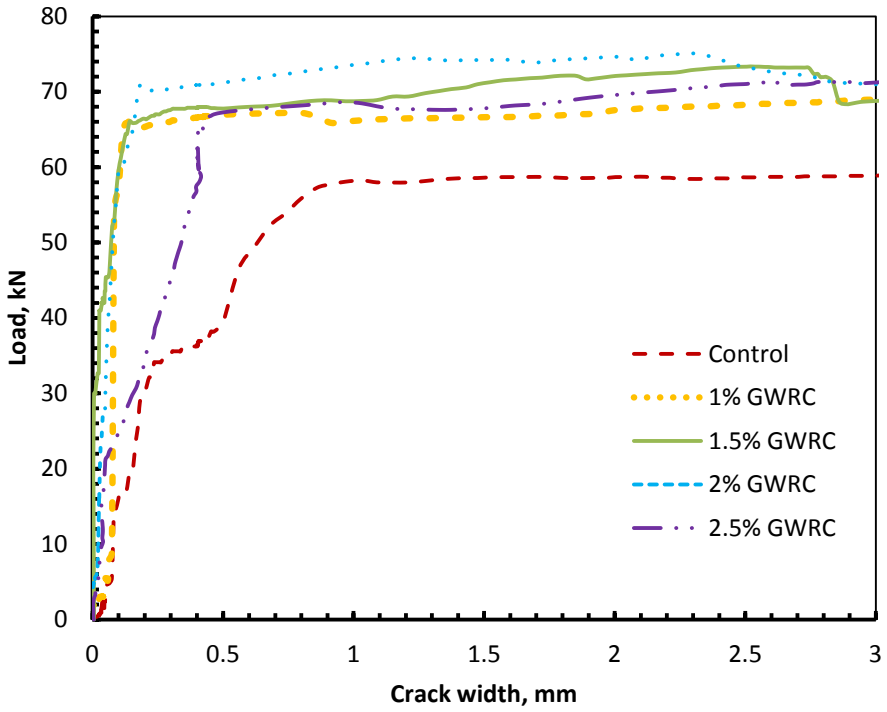

Figure 5.42: Load vs. crack width

Figure 5.43: Crack-pattern for control specimen

Figure 5.44: Crack-pattern for 1% GWRC specimen

Figure 5.45: Crack-pattern for 1.5% GWRC specimen

Figure 5.46: Crack-pattern for 2% GWRC specimen

Figure 5.47: Crack-pattern for 2.5% GWRC specimen

From the crack width vs. load curves, it is evident that for the same load, crack width of the control specimen is considerably larger than those of GWRC samples. This is because fibers bridge across the cracks and help the segments from pulling apart. After failure, crack width is of little interest. But the graphs also showed that the failure loads for GWRC specimens are substantially higher than that of control specimen which is the indication of greater flexural strength in GWRC. Crack patterns in Figures 5.43 to 5.47 show that number of cracks in control specimen is greater than those in GWRC specimens. One important observation from the study of crack patterns is that control specimens developed diagonal shear-flexure cracks unlike GWRC specimens that mainly failed through vertical flexural crack. This may be an indication that fiber reinforcement induced better shear capacity in the GWRC members. This can only be confirmed after studying shear strength of GWRC, but that is out of scope for the present research.

5.4.3 Comparison of result with previous studies

Test beams with stone chips as coarse aggregate in GWRC were prepared in order to compare the performance with commercially available steel fiber reinforced concrete. Fiber contents in the current study were 3% and 3.5% by weight which is 0.93% and 1.10% by volume respectively. The curves from the present tests are well in congruence with the curves produced from previous experiments. Figure 5.48 and 5.49

show the load-deflection curve for 3 and 3.5 percent GWRC samples, respectively. Figure 5.50 presents the corresponding curve as produced by Byung Hwan Oh [8].Comparing the stress-stress curves, it is evident that performance of locally available GI wire is close to commercially available steel fiber in concrete.

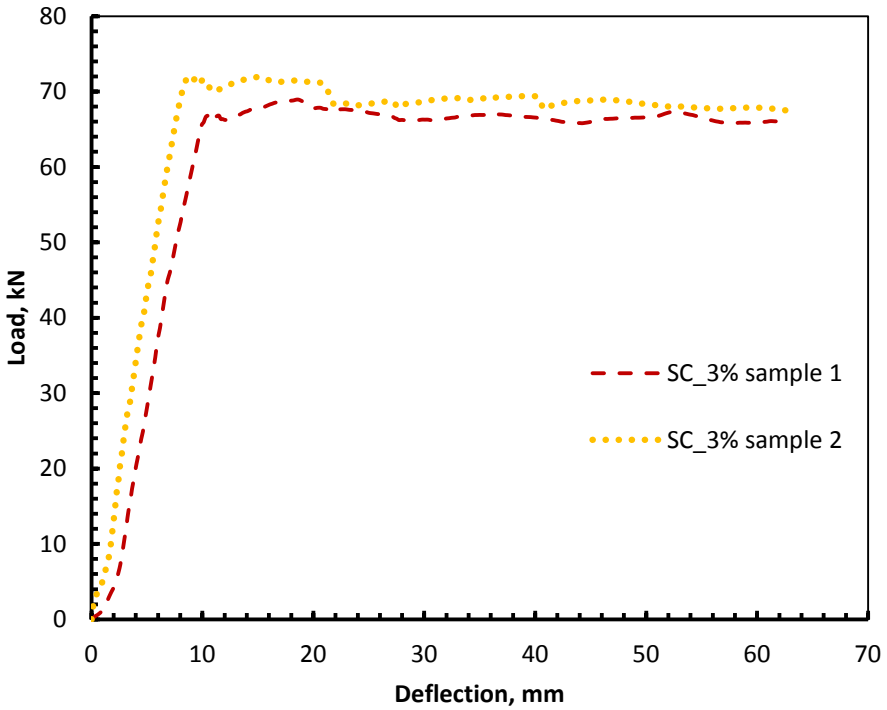

Figure 5.48: Load-deflection curve for 3% GWRC with stone chips

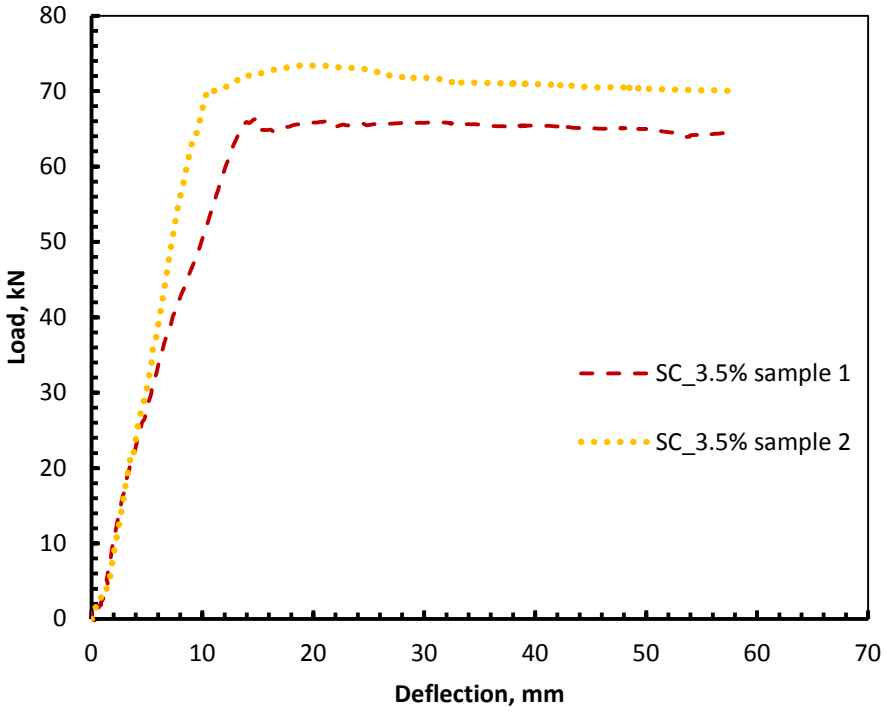

Figure 5.49: Load-deflection curve for 3% GWRC with stone chips

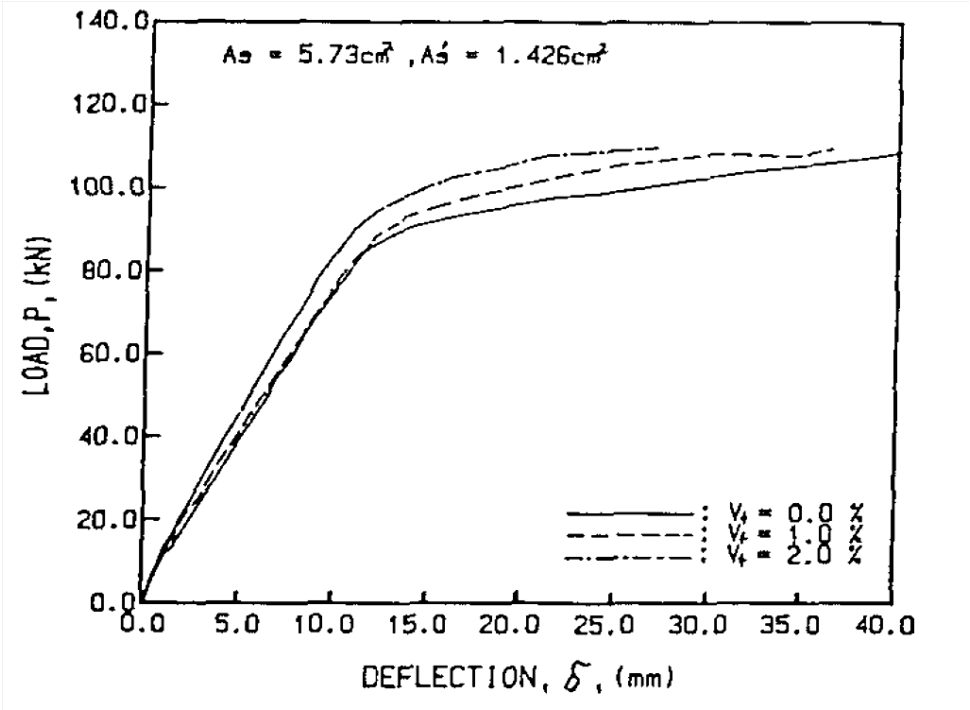

Figure 5.50: Load deflection curve for doubly reinforced beams

5.4.4 Recommendation

Based on the result and discussion presented above, it is understood that for GWRC beams with burnt clay brick chips as coarse aggregate, overall performance is significantly better when fiber content is around 2 to 2.5 percent by weight (0.74 to 0.93 percent by volume). Moreover, with higher fiber contents, workability of the concrete mix degrades and as a result, casting becomes difficult. This also affects the strength of the concrete. Since, the focus was on conventional concrete mixes without water reducing admixtures; mixing, placing and compacting GWRC with fiber content more than 3 percent by weight will not be feasible. Therefore, considering the overall performance, GI wire fiber content of 2 to 2.5 percent can be recommended for use without admixture for the stated mix design with brick chips.

5.5 Rapid Chloride Permeability Test

This section presents and discusses the results of the rapid chloride permeability tests performed on samples with both brick chips and stone chips. The RCPT test was conducted on samples aged 56 days as opposed to 28 days for previously discussed tests since RCPT results are more reliable for specimens aged more as discussed in Chapter 4.

5.5.1 Result and Discussion

This test was carried out in order to confirm if this test is applicable for determining durability of GWRC. The target of the test was to see if there is any correlation of charge passed with fiber content. The results from the tests are tabulated in Table 5.3.

Table 5.3: Results from Rapid Chloride Permeability Tests

Coarse Aggregate type	Sample ID	Total Charge passed (Q), Coulombs	Comments
Brick chips	Control-1	2016	Moderate
	Control-2	2916	Moderate
	1%_sample 1	20286	Extremely high, Ammeter threshold reached
	1%_sample 2	6606	High
	1.5%_sample 1	2115	Invalid, discontinued due to high temperature
	1.5%_sample 2	9612	High
	2%_sample 1	21312	Extremely high, Ammeter threshold reached
	2%_sample 2	1152	Invalid, discontinued due to high temperature
	2.5%_sample 1	21204	Extremely high, Ammeter threshold reached
	2.5%_sample 2	19350	Extremely high, Ammeter threshold reached
Stone chips	Control-1	0	Negligible
	Control-2	0	Negligible
	1%_sample 1	4149	High
	1%_sample 2	1620	Low
	1.5%_sample 1	2304	Invalid, discontinued due to high temperature
	1.5%_sample 2	7650	High
	2%_sample 1	5733	High
	2%_sample 2	15426	Extremely high, Ammeter threshold reached
	2.5%_sample 1	21384	Extremely high, Ammeter threshold reached
	2.5%_sample 2	3744	Invalid, discontinued due to leakage

From the table, it is seen that the control samples have good results. But samples with GI wire fibers show erratic results which is very logical as they contain conductors within the cement matrix. An alternative interpretation can be that higher current indicates even distribution of fibers which facilitated the flow of charge. However, no correlation of current with fiber content could be established. Detailed current readings are provided in Appendix B.

5.6 Sorptivity Test

As RCPT did not provide any concrete results on durability of GWRC, Sorptivity test was then carried out for determining the durability of GWRC. This section presents and analyses the results from Sorptivity test performed on 56 days old samples with both brick chips and stone chips. The results and discussion on Sorptivity test is presented in this section.

5.6.1 Results

Determination of the susceptibility of an unsaturated concrete to the penetration of water and thereby harmful substances is the prime function of this test method. The samples are conditioned for about 18 days before the commencement of the test procedure as described in Chapter 4. Water absorption is plotted against the square root of time in seconds. The slopes of the best fit curves represent the rate of absorption. Initial rate of absorption, S_i is the slope of the curve up to 6 hours of the start of absorption. Secondary rate of absorption, S_s is the slope of the curve plotted with the data from day 1 to day 7 from the beginning of absorption. Typical graphs from the tests are presented below. In the designation of the samples, first number represents fiber content by weight percent, then BC or, SC means brick chips or stone chips respectively. In the parentheses, a and b means sample number 1 and 2 respectively and IA and SA means Initial and Secondary Absorption respectively.

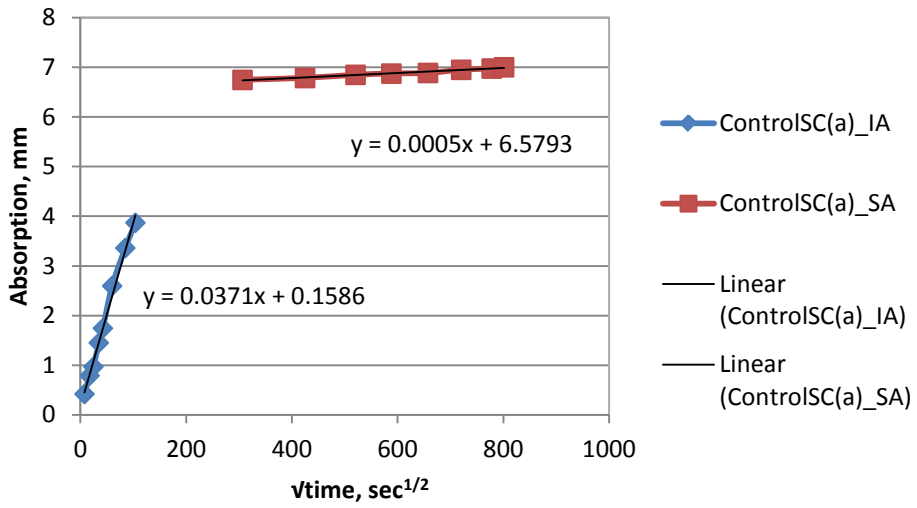

Figure 5.51: Absorption curve for Control sample-1 with stone chips

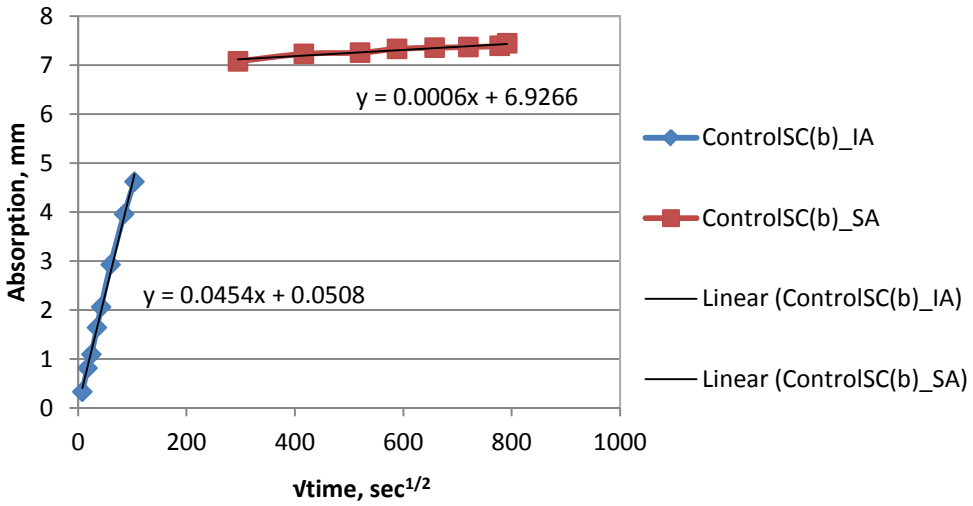

Figure 5.52: Absorption curve for Control sample-2 with stone chips

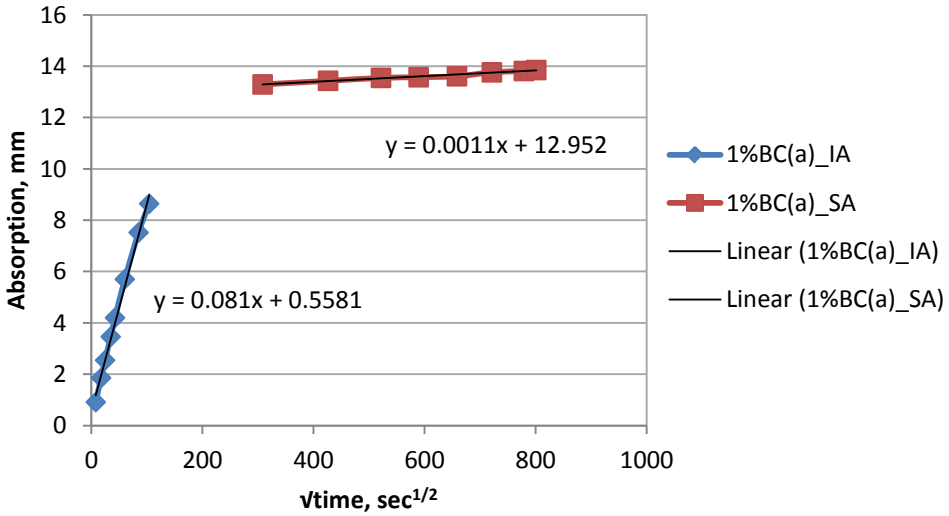

Figure 5.53: Absorption curve for 1% GWRC sample-1 with brick chips

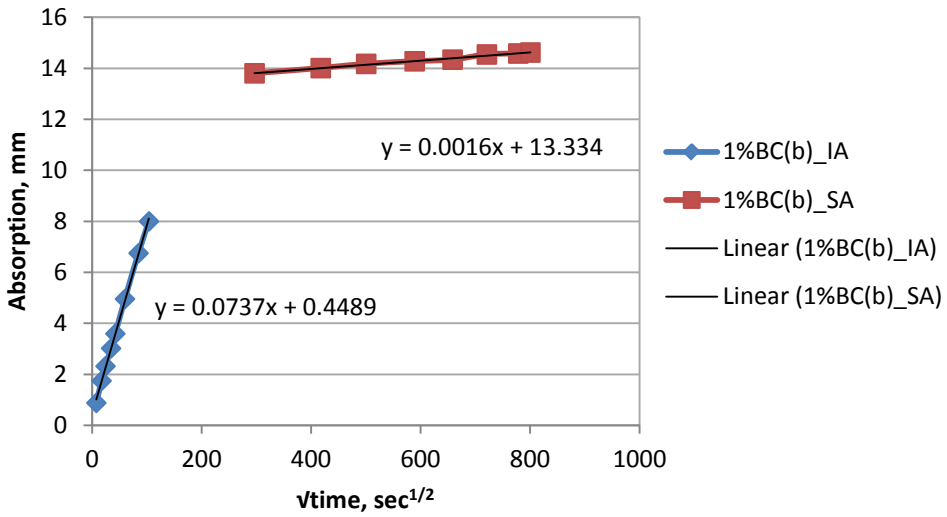

Figure 5.54: Absorption curve for 1% GWRC sample-2 with brick chips

5.6.2 Discussion

Water absorption of concrete is dependent on the pore structure of the matrix. The higher the pore content, the higher the rate of absorption. And porous concrete allows more ingress to deleterious ions along with water. Therefore, higher rate of absorption indicates weaker concrete with respect to durability. The results from the test are summarized in Table 5.4.

From the table, it can be seen that initial absorption rate of concrete without fiber is higher than those of GWRC samples for both brick chips and stone chips. But for secondary absorption rate, the results show that GWRC samples have higher absorption rate. It must be noted that the initial rate is more important because the pores in the concrete matrix stay unsaturated initially. As a result, initial rate of absorption is always higher than secondary rate. Initial rates of absorption of GWRC samples are slightly less than that of control samples, which means GWRC specimens have shown comparable performance in terms of permeability with respect to control samples. In addition, the secondary absorption rates of GWRC composites are also very close to the values of control samples.

Table 5.4: Summary of Sorptivity test results

Specimen	Initial Absorption (S_i), mm/s$^{1/2}$	Average Initial Absorption (S_i), mm/s$^{1/2}$	Secondary Absorption (S_s), mm/s$^{1/2}$	Average Secondary Absorption (S_s), mm/s$^{1/2}$
Control_SC (a)	0.0371	0.04125	0.0005	0.00055
Control_SC (b)	0.0454		0.0006	
1%SC (a)	0.0367	0.0402	0.0006	0.00065
1%SC (b)	0.0437		0.0007	
1.5%SC(a)	0.0412	0.0375	0.0005	0.00055
1.5%SC(b)	0.0338		0.0006	
2%SC(a)	0.0398	0.0356	0.0006	0.00055
2%SC(b)	0.0314		0.0005	
2.5%SC(a)	0.0405	0.03695	0.0006	0.00065
2.5%SC(b)	0.0334		0.0007	
Control_BC(a)	0.0817	0.08505	0.0012	0.0012
Control_BC(b)	0.0884		0.0012	
1%BC(a)	0.081	0.07735	0.0011	0.00135
1%BC(b)	0.0737		0.0016	
1.5%BC(a)	0.0513	0.0578	0.0033	0.00285
1.5%BC(b)	0.0643		0.0024	
2%BC(a)	0.061	0.056	0.0033	0.00385
2%BC(b)	0.051		0.0044	
2.5%BC(a)	0.0702	0.07135	0.0016	0.0015
2.5%BC(b)	0.0725		0.0014	

5.7 Cost Study:

For bulk purchase, locally produced GI wire costs about BDT 75,000-90,000 ($950-1150) per ton here in Bangladesh. Retail price for a kg in local market varies from BDT 80 to 100 ($ 1.00 to 1.25). Additional cost for processing of wire into fibers is about BDT 10,000 ($125) per ton. On the other hand, steel fiber for use in FRC is not produced in Bangladesh and importing fiber from China costs around BDT 120,000-200,000 ($1500-2500) per ton including shipment costs. Estimated cost analysis of materials for GWRC and SFRC with the mix design stipulated in Table 2 and 1% fiber content (weight basis) is presented in Table 4. It is found that GI wire fiber, if used as a substitute of steel fiber, can save BDT 1380 ($17.2), which means a

cost reduction of almost 14%, per cubic meter of concrete when fiber dosage is 1% on weight basis. With higher dosage of fiber, reduction in cost increases proportionately.

Table 5.5: Cost estimation for GWRC and SFRC

Item	Amount (kg/m^3)	Unit Price	GWRC Cost (per m^3)	SFRC Cost (per m^3)
Cement	440	BDT 500 ($ 6.5) per bag	BDT 4400 ($55.0)	BDT 4400 ($55.0)
Coarse Aggregate (Crushed stone)	735	BDT 150 ($1.90) per cft	BDT 2600 ($32.5)	BDT 2600 ($32.5)
Fine Aggregate (Sylhet sand)	898	BDT 40 ($ 0.5) per cft	BDT 840 ($10.5)	BDT 840 ($10.5)
GI Wire Fiber (1% wt)	23	BDT 100 ($ 1.25) per kg	BDT 2300 ($28.8)	-
Steel fiber (1% wt)	23	BDT 160 ($ 2.0) per kg	-	BDT 3680 ($46)
Total			BDT 10,140 ($126.80)	BDT 11,520 ($144.00)

CHAPTER 6

Conclusion

6.1 General

An attempt for incorporating locally available GI wire fiber as a substitute for commercially available steel fiber in concrete in Bangladesh has been made in this study. However, the behavior and performance of such GI wire reinforced concrete (GWRC) are yet to be explored. Therefore, this research made an effort to discover several basic characteristics of GWRC chiefly related to strength, ductility and durability. However, the central focus of the study was on the effect of fiber content on the aforementioned properties of GWRC. As a result, fiber dosage was varied within low volume content while the mix design and fiber properties, in effect, were kept unchanged. Strength properties considered in the study are static compressive strength, splitting tensile strength and modulus of elasticity under compressive loading. For assessment of flexural capacity and ductility, test beams were prepared that were subjected to third-point loading and their load-deflection and toughness behavior were studied and analyzed. Lastly, Rapid Chloride Permeability and Sorptivity tests were carried out in order to gauge the effect of GI wire fiber addition on durability of concrete. One of the prime focuses of the study is on the behavior of concrete with lightweight brick chips as coarse aggregate since these are very common in the country. Stone chips are also used for comparing the results with previously conducted studies.

6.2 Conclusions

After completion of the tests and analysis of the results regarding strength, ductility and durability of GI wire fiber reinforced concrete, following are the conclusions that can be deduced-

- Compressive strength tests at 28 days on GWRC samples showed a maximum increase of 33%.

- Splitting tensile strength tests at 28 days on GWRC samples displayed a maximum of 53% increment.
- A maximum increase of about 23% was observed in the value of Modulus of Elasticity of GWRC with respect to normal concrete
- Flexural test of beams has produced excellent findings that GI wire inclusion increased the first-crack load, toughness and ultimate load by a significant margin of about 15 to 30%.
- Water absorption (Sorptivity) tests revealed that GI wire fiber reinforced concrete has analogous permeability characteristics compared to normal concrete.

6.3 Major Finding

The beam flexure tests have shown some significant results for GWRC with lightweight aggregate i.e. burnt clay bricks. . The comparisons have been done with respect to the values of control beams (beams without GI wire fibers). Various strength properties such as toughness, first-crack load, and ultimate load increase significantly by addition of GI wire fiber. Increase of strength by such proportions despite the presence of main reinforcements ensures a major contribution by GI wire fibers. Considering overall performance, it is recommended that fiber content within 2 to 2.5 percent should be suitable for use in conventional concrete mix (i. e. 1 : 1.5 : 3 volumetric mix) with burnt clay bricks without use of any additives.

6.4 Recommendations

During the course of the experiments and analysis, there was always an urge to expand the scope of the study in order to gather some more information and to achieve some better results. Moreover, as this is a relatively new field in construction sector of the country, opportunities for future researches are numerous. Some of these future research prospects are recommended below-

- To study performance of GWRC with higher fiber contents up to 6 % by weight with appropriate mix design.

- To study the effect of GI wire fiber reinforcement on shear resistance of concrete since GWRC specimens did not form shear-flexure crack as opposed to control specimens.
- To investigate application of GWRC as a suitable retrofitting material
- To investigate the response of GWRC under cyclic loading.
- To conduct experiments on any particular property of GWRC with a large sample size in order to establish a statistically significant relationship between various characteristic properties.
- To study effect of aspect ratio of GI wire fiber on various properties of GWRC

References

[1] Karim, M. Z., Mamun, A. A., and Rahman, M. S. (2013), "Investigation on the Feasibility of GI Wire Reinforced Concrete in Bangladesh", *B. Sc. Thesis*, Military Institute of Science and Technology, Dhaka, Bangladesh.

[2] Bentur, A., and Mindess, S. (2006), 'Fibre Reinforced Cementitious composites', CRC Press, Taylor & Francis, Madison Avenue, New York, USA.

[3] ccanz (2009), 'Fiber Reinforced Concrete', Information Bulletin : IB 39, Cement and Concrete Association of New Zealand, 142 Featherston Street, PO Box 448, Wellington, NZ.

[4] Naaman, A. E. (2003), 'Engineered steel fibers with optimal properties for reinforcement of cement composites', Journal of advanced concrete technology, 1(3).

[5] ACI Committee 544 (1996), 'State-of-the-art report on fiber reinforced concrete: ACI 544.1R-96', American Concrete Institute, Farmington Hills, MI.

[6] Bencardino, F., Rizzuti, L., Spadea, G., and Swamy, R. N. (2008), 'Stress-strain behavior of steel fiber-reinforced concrete in compression', Journal of Materials in Civil Engineering, 20(3), pp. 255-263.

[7] Chanh, N.V. (2005), 'Steel Fiber Reinforced Concrete', Proceedings of JSCE-VIFCEA Joint Seminar on Concrete Engineering, pp. 108-116.

[8] Musmar, M. (2013), 'Tensile Strength of Steel Fiber Reinforced Concrete', Contemporary Engineering Sciences, 6(5), pp. 225 – 237.

[9] Oh, B. H. (1992), 'Flexural Analysis Of Reinforced Concrete Beams Containing Steel Fibers', Journal of Structural Engineering, ASCE, 118(10), Paper No. 1970, pp. 2821-2835.

[10] Otter, D., and Naaman, A. E. (1988), 'Properties of steel fiber reinforced concrete under cyclic loading', ACI Materials Journal, 85(4), pp. 254-261.

[11] Ou, Y., Tsai, M., Liu, K., and Chang, K. (2012), 'Compressive Behavior of Steel-Fiber-Reinforced Concrete with a High Reinforcing Index', Journal of Materials in Civil Engineering, 24(2), pp. 207–215.

[12] Foster, S. J., and Attard, M. M. (2001), “Strength and ductility of fiber reinforced high-strength concrete columns”, Journal of Structural Division, 127(1), pp. 28–34.

[13] Kimura, H., Ishikawa, Y., Kambayashi, A., and Takatsu, H. (2007), “Seismic behavior of 200 MPa ultra-high-strength steel-fiber reinforced concrete columns under varying axial load”, Journal of Advanced Concrete Technology, 5(2), pp. 193–200.

[14] ACI Committee 544 (1993), ‘Guide for Specifying, Proportioning, Mixing, Placing, and Finishing Steel Fiber Reinforced Concrete: ACI 544.3R-93’, American Concrete Institute, Farmington Hills, MI.

[15] ASTM A820/ A820M (2004), ‘Standard Specification for Steel Fibers for Fiber-Reinforced Concrete’, ASTM International, West Conshohocken, PA, USA.

[16] BS EN 14889-1 (2006), ‘Fibres for concrete – Part1: Steel fibres – Definitions, specifications and conformity’, British Standards Institution, London, UK.

[17] ASTM C 1018/ C1018M (1997), ‘Standard Test Method for Flexural Toughness and First-Crack Strength of Fiber Reinforced Concrete (Using Beam with Third-Point Loading)’, ASTM International, West Conshohocken, PA, USA.

[18] ACI Committee 544 (1989), ‘Measurement of Properties of Fiber Reinforced Concrete: ACI 544.2R-89’, American Concrete Institute, Farmington Hills, MI.

[19] ASTM C 78/ C78M (2002), ‘Standard Test Method for Flexural Strength of Concrete (Using Simple Beam with Third-Point Loading)’, ASTM International, West Conshohocken, PA, USA

[20] ASTM C 1116/ C1116M (2002), ‘Standard Specification for Fiber Reinforced Concrete and Shotcrete’, ASTM International, West Conshohocken, PA, USA

[21] Tatro, and Brent, S. (1987), ‘Performance of Steel Fiber Reinforced Concrete Using Large Aggregates’, Transportation Research Record1110, Transportation Research Board, Washington, D.C., pp. 127-129.

[22] Rettburg, and William, A. (1986), “Steel-Reinforced Concrete Makes Older Dam Safer, More Reliable”, HydroReview, Spring, pp. 18-22.

[23] Schrader, and Ernest, K. (1989), “Fiber Reinforced Concrete”, *ICOLD Bulletin* 40, International Committee on Large Dams, Paris, pp. 22.

[24] Schrader, E. K. and Munch, A. V. (1976), ‘Deck Slab Repaired by Fibrous Concrete Overlay’, Journal of the Construction Division, 102(1), pp. 179-196.

[25] Ounanian, Douglas, W., and Kesler, Clyde E. (1976), “Design of Fiber Reinforced Concrete for Pumping”, *Report No.* DOT-TST 76T-17, Federal Railroad Administration, Washington, D.C., pp. 53

[26] Johnston, C. D. (1982), ‘Steel fiber reinforced mortar and concrete’, A review of mechanical properties in fiber reinforced concrete, ACI-SP-Detroit.

[27] Johnston, C.D. (1982), “Definition and measurement of flexural toughness parameters for fiber reinforced concrete”, Cement Concrete Aggregate.

[28] Craig, R. (1987). "Flexural behavior and design of reinforced fiber concrete members." *ACI SP105,* American Concrete Institute, pp. 517-563.

[29] Henager, C. H., and Doherty, T. J. (1976), "Analysis of reinforced fibrous concrete beams", Journal of Structural Engineering, ASCE, 102(1), pp. 178-188

[30] Swamy, R. N., and Al-Ta'an, S. A. (1981), "Deformation and ultimate strength in flexure of reinforced concrete beams made with steel fiber concrete", ACI Materials Journal, 78(5), pp. 395-405.

[31] Holt, J. M. (2000), ‘Uniaxial Tension Testing’, ASM Handbook Vol. 8: Mechanical Testing and Evaluation (ASM International), pp. 124-142.

[32] ASTM C192/ C192M (2007), ‘Standard Practice for Making and Curing Concrete Test Specimens in the Laboratory’, ASTM International, West Conshohocken, PA, USA

[33] Nilson, A. H., Darwin, D., and Dolan C. W. (2003), ‘Design of Concrete Structures’, 13th Edition, McGraw-Hill, New York, USA.

[34] Kosmatka, S. H., Kerkhoff B., and Panarese, W. C. (2002), 'Design and Control of Concrete Mixtures', 14th Edition, PCA Engineering Bulletin 001, Portland Cement Association, Illinois, USA.

[35] ASTM C 29/29M (1991), 'Standard Test Method for Bulk Density (Unit Weight) and Voids in Aggregate', ASTM International, West Conshohocken, PA, USA.

[36] ASTM C 127 (1988), 'Standard Method of Test for Specific Gravity and Absorption of Coarse Aggregate', ASTM International, West Conshohocken, PA, USA.

[37] ASTM C 136 (2001), 'Standard Test Method for Sieve Analysis of Fine and Coarse Aggregates', ASTM International, West Conshohocken, PA, USA.

[38] http://www.metalwiresupplier.com/ (2014), Anping Galvanized Wire Factory, Anping County, Hebei, China

[39] Detwiler, R. J., Kjellsen, K. O., and Gjorv, O. E. (1991), "Resistance to Chloride Intrusion of Concrete Cured at Different Temperatures", ACI Materials Journal, 88(1), pp. 19-24.

[40] Cao, Y., and Detwiler, R. J. (1995), "Backscatter Electron Imaging of Cement Pastes Cured at Elevated Temperatures", Cement and Concrete Research, 25(3), pp. 627-638.

[41] Tang, L. and Nilsson, L. O. (1992), "Chloride Diffusivity in High Strength Concrete", Nordic Concrete Research, 11(119), pp. 162-170.

[42] Stanish, K. D., Hooton R. D. and Thomas, M. D. A. (1997), 'Testing The Chloride Penetration Resistance Of Concrete: A Literature Review', FHWA Contract DTFH61-97-R-00022: "Prediction of Chloride Penetration in Concrete", Department of Civil Engineering, University of Toronto, Canada.

[43] ASTM C 39/ C39M (2003), 'Standard Test Method for Compressive Strength of Cylindrical Concrete Specimens', ASTM International, West Conshohocken, PA, USA.

[44] ASTM C 496/ C496M (2011), ‘Standard Test Method for Splitting Tensile Strength of Cylindrical Concrete Specimens’, ASTM International, West Conshohocken, PA, USA.

[45] ASTM C 469/ C469M (2002), ‘Standard Test Method for Static Modulus of Elasticity and Poisson’s Ratio of Concrete in Compression’, ASTM International, West Conshohocken, PA, USA.

[46] ACI Committee (1988), ‘Design Considerations for Steel Fiber Reinforced Concrete: ACI 544.4R-88’, American Concrete Institute, Farmington Hills, MI.

[47] ACI Committee 318 (1999), ‘Building code requirements for structural concrete: ACI 318-99’, American Concrete Institute, Farmington Hills, MI.

[48] ASTM C 1202/ C1202M (1986), ‘Standard Test Method for Electrical Indication of Concrete's Ability to Resist Chloride Ion Penetration’, ASTM International, West Conshohocken, PA, USA.

[49] AASHTO T 259 (2002), ‘Resistance of Concrete to Chloride Ion Penetration’, AASTHO, 444 N Capitol St. NW Suite 249 Washington, DC 20001, USA.

[50] Hall, C. (1989), “Water Sorptivity of Mortars and Concretes: A Review,” Magazine of Concrete Research, 41(147), pp. 51-61.

[51] ASTM C 1585/ C1585M (2006), ‘Laboratory Comparison of Several Tests for Evaluating the Transport Properties of Concrete’, ASTM International, West Conshohocken, PA, USA

APPENDIX A

Stress-strain Plots for Modulus of Elasticity

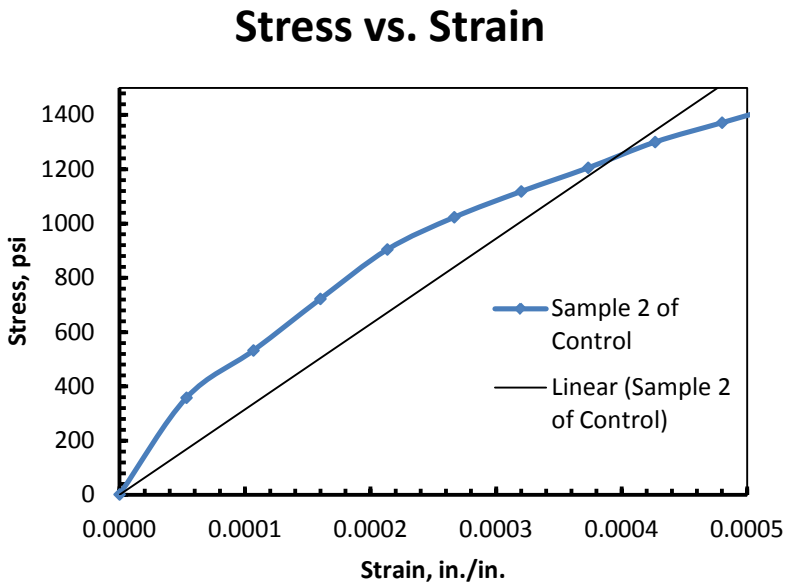

Figure A-1: Stress-strain curve for control sample-2 with stone chips

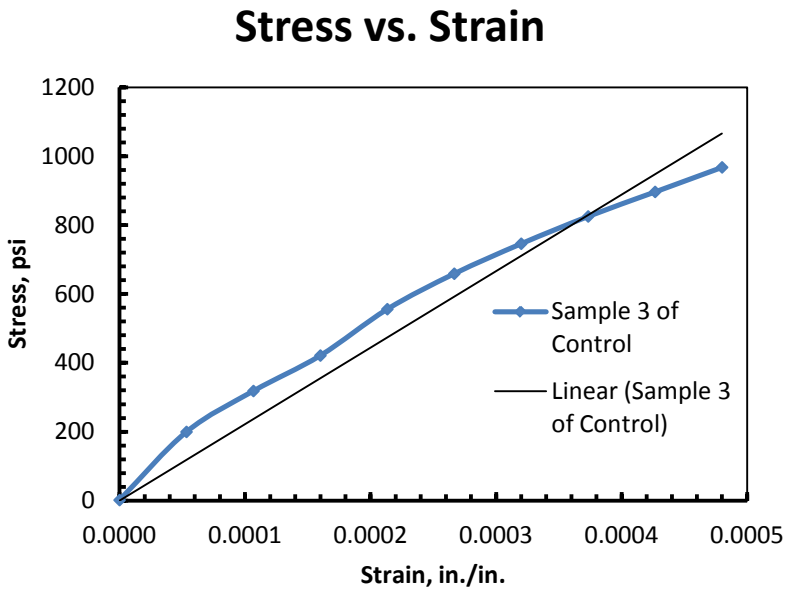

Figure A-2: Stress-strain curve for control sample-3 with stone chips

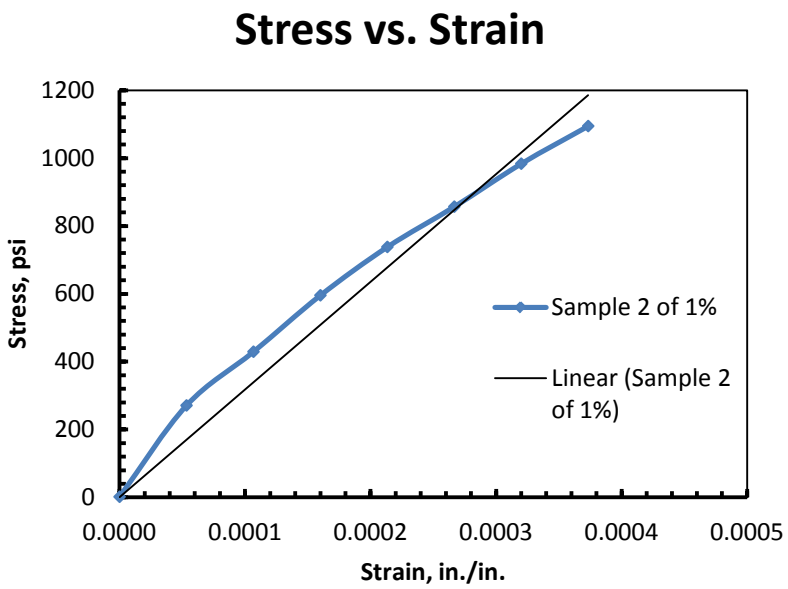

Figure A-3: Stress-strain curve for 1% GWRC sample-2 with stone chips

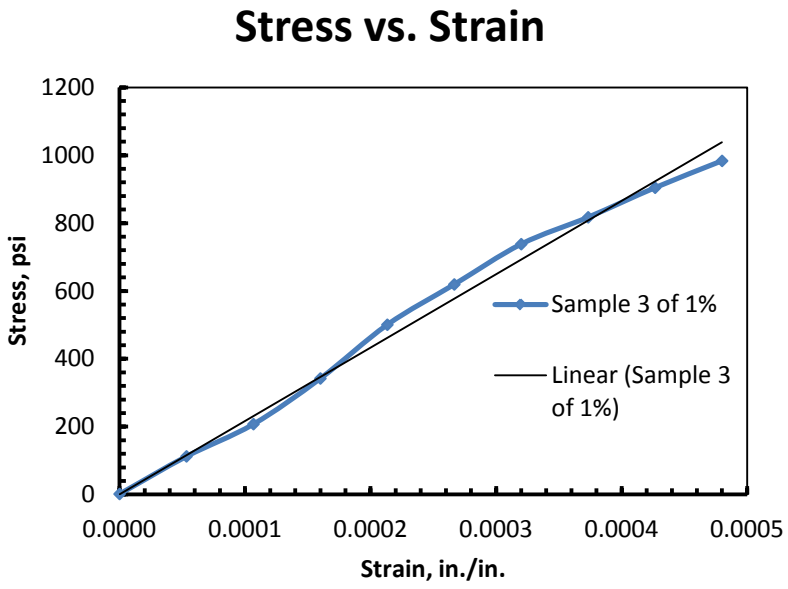

Figure A-4: Stress-strain curve for 1% GWRC sample-3 with stone chips

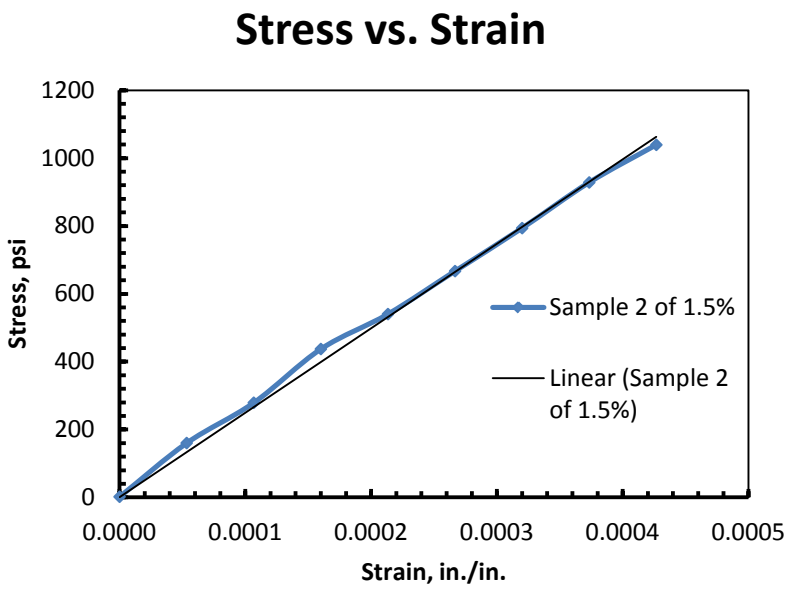

Figure A-5: Stress-strain curve for 1.5% GWRC sample-2 with stone chips

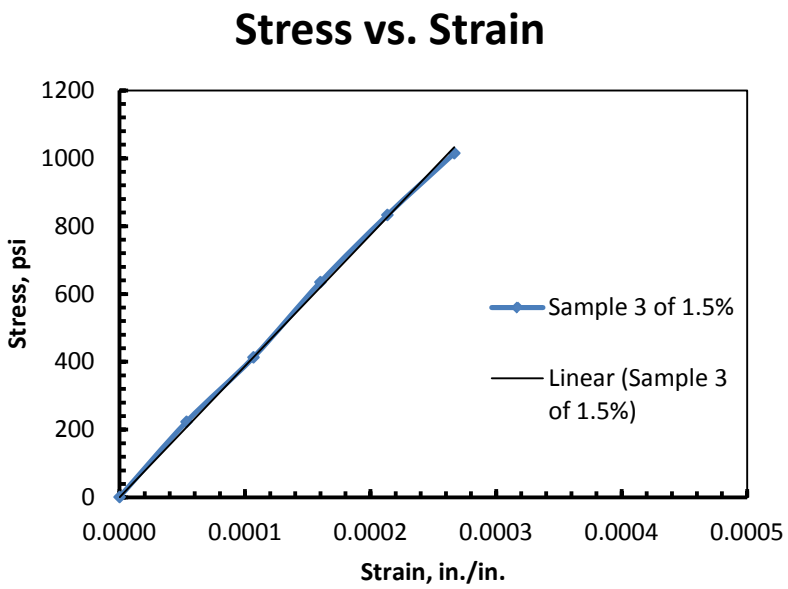

Figure A-6: Stress-strain curve for 1.5% GWRC sample-3 with stone chips

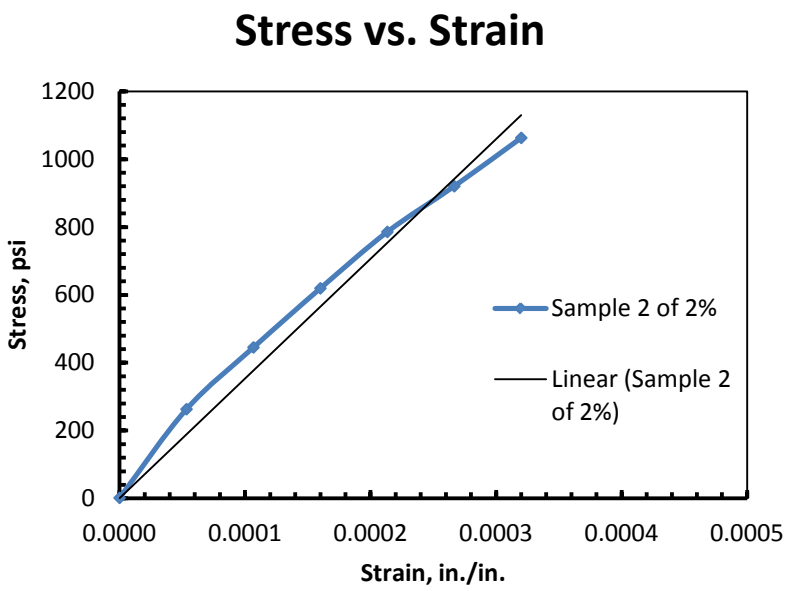

Figure A-7: Stress-strain curve for 2% GWRC sample-2 with stone chips

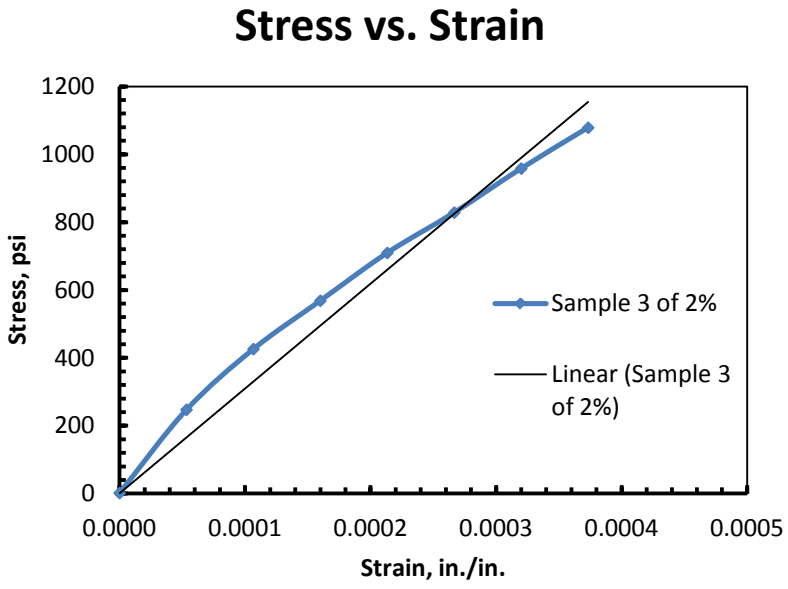

Figure A-8: Stress-strain curve for 2% GWRC sample-3 with stone chips

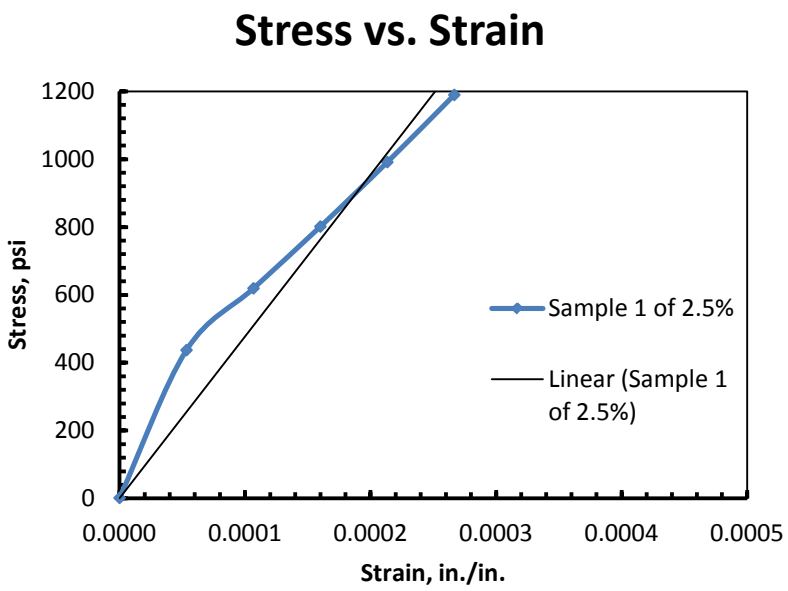

Figure A-9: Stress-strain curve for 2.5% GWRC sample-1 with stone chips

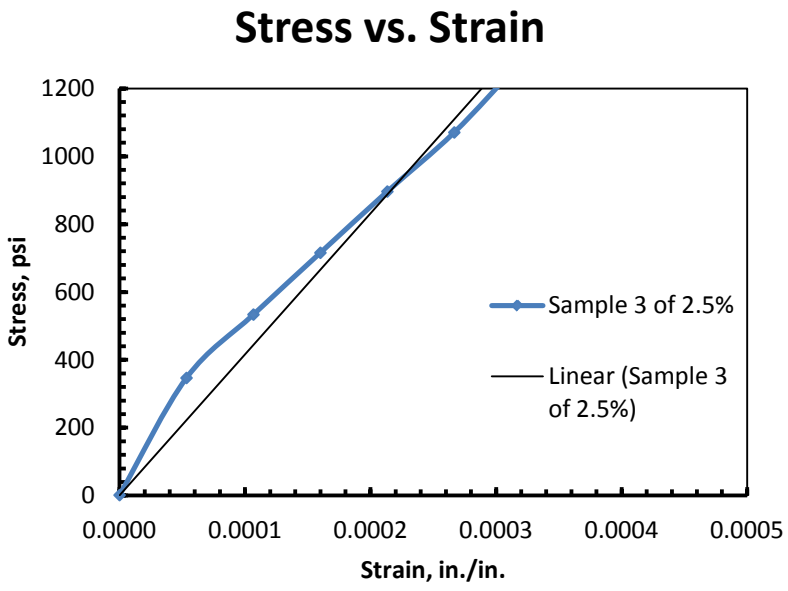

Figure A-10: Stress-strain curve for 2.5% GWRC sample-3 with stone chips

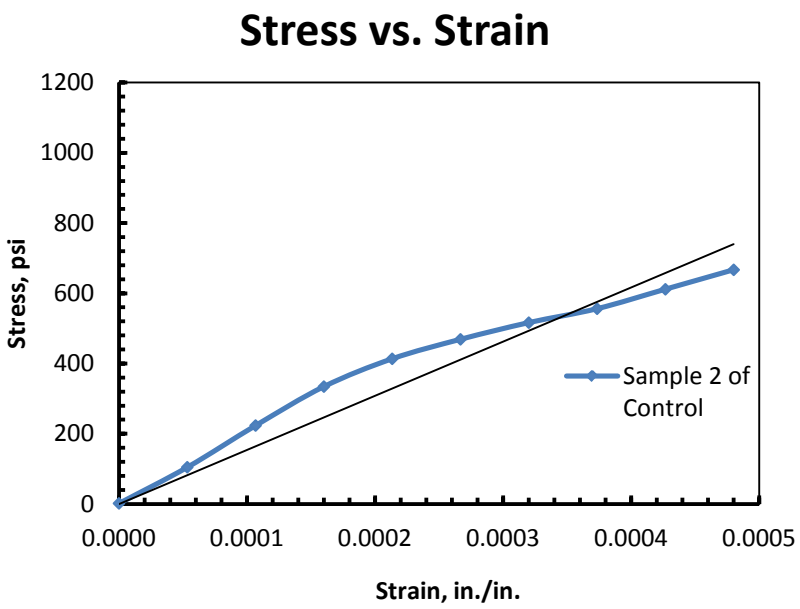

Figure A-11: Stress-strain curve for control sample-2 with brick chips

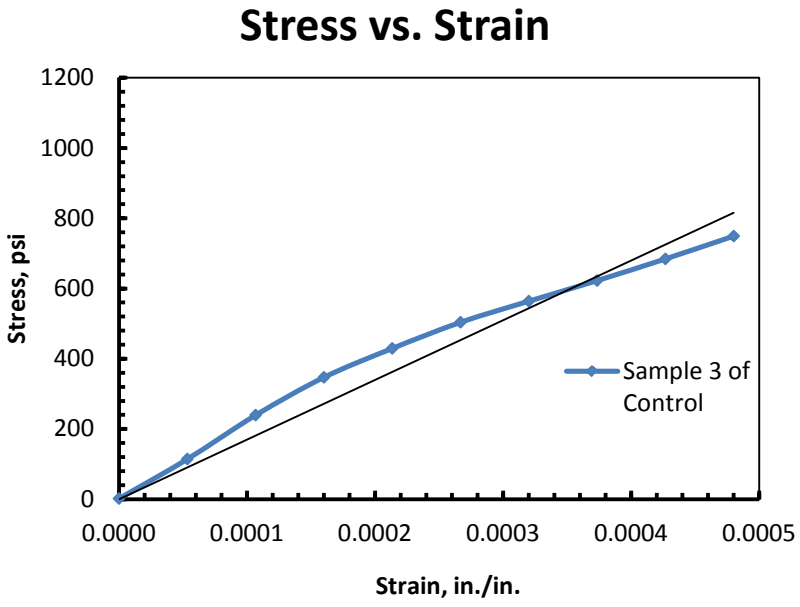

Figure A-12: Stress-strain curve for control sample-3 with brick chips

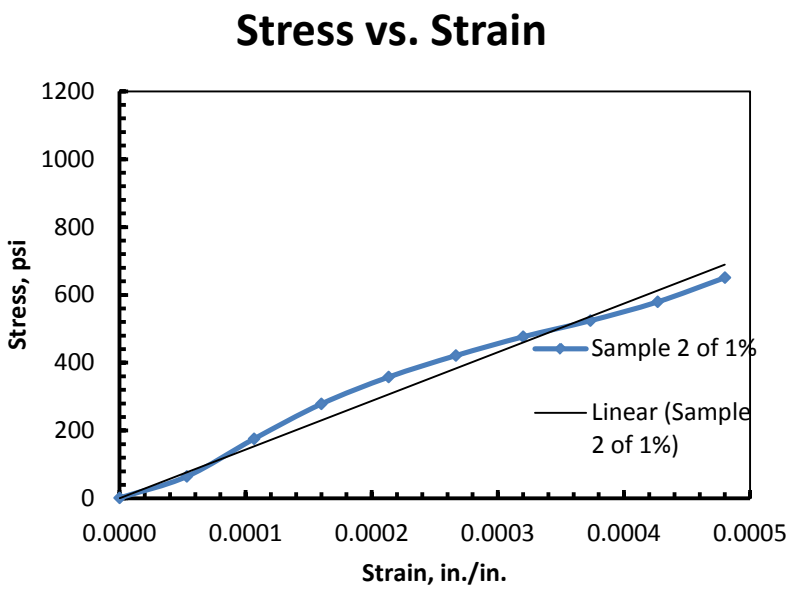

Figure A-13: Stress-strain curve for 1% GWRC sample-2 with brick chips

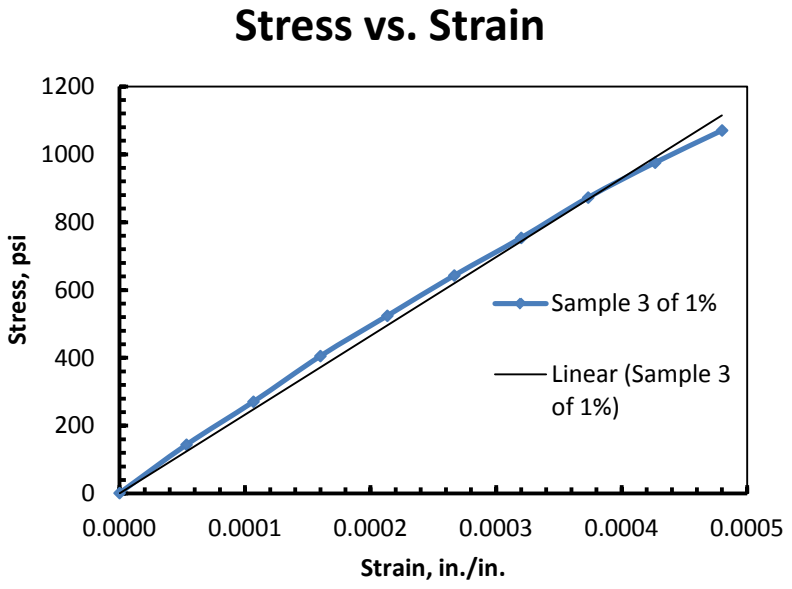

Figure A-14: Stress-strain curve for 1% GWRC sample-3 with brick chips

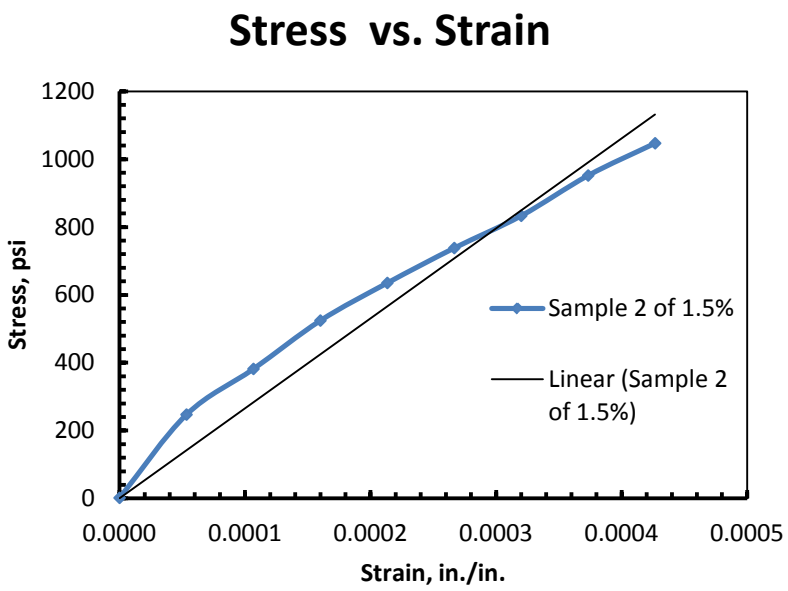

Figure A-15: Stress-strain curve for 1.5% GWRC sample-2 with brick chips

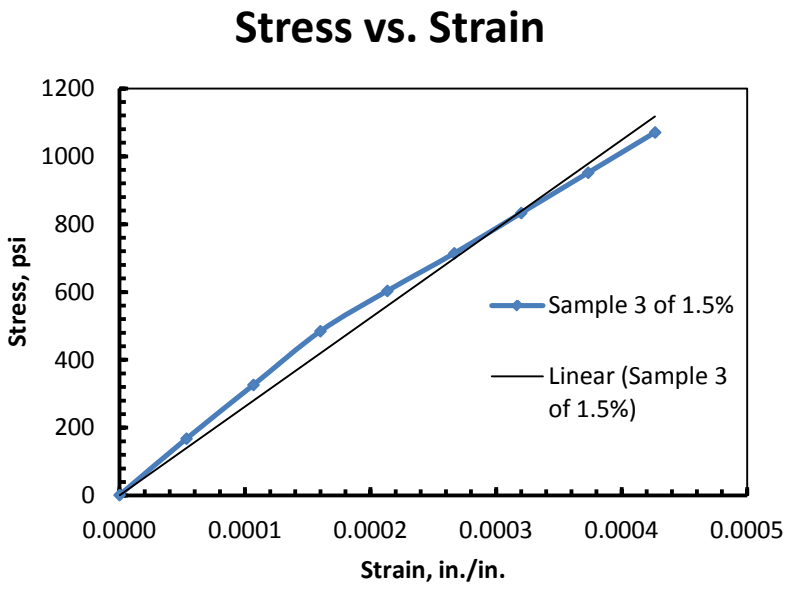

Figure A-16: Stress-strain curve for 1.5% GWRC sample-3 with brick chips

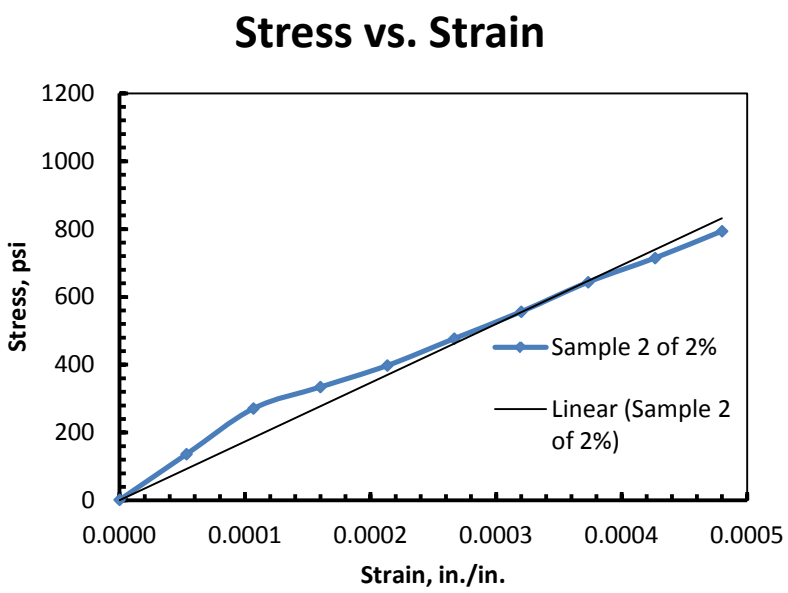

Figure A-17: Stress-strain curve for 2% GWRC sample-2 with brick chips

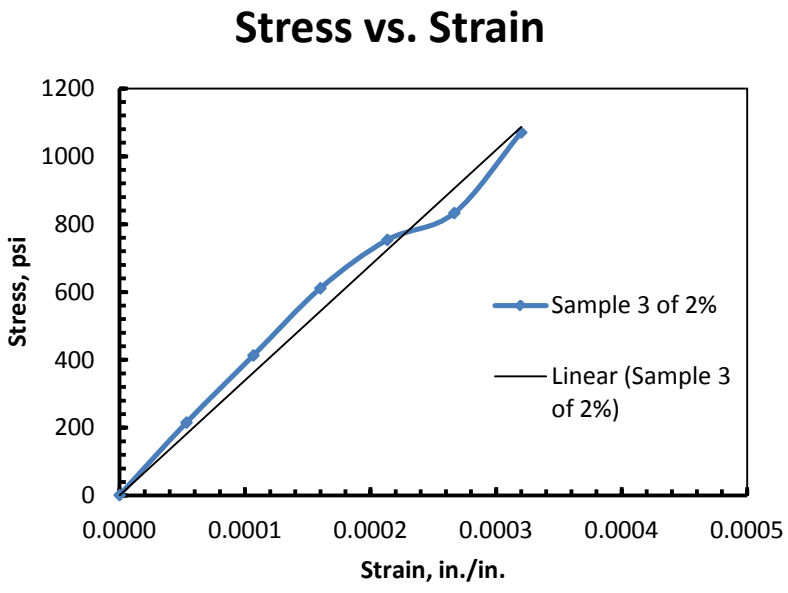

Figure A-18: Stress-strain curve for 2% GWRC sample-3 with brick chips

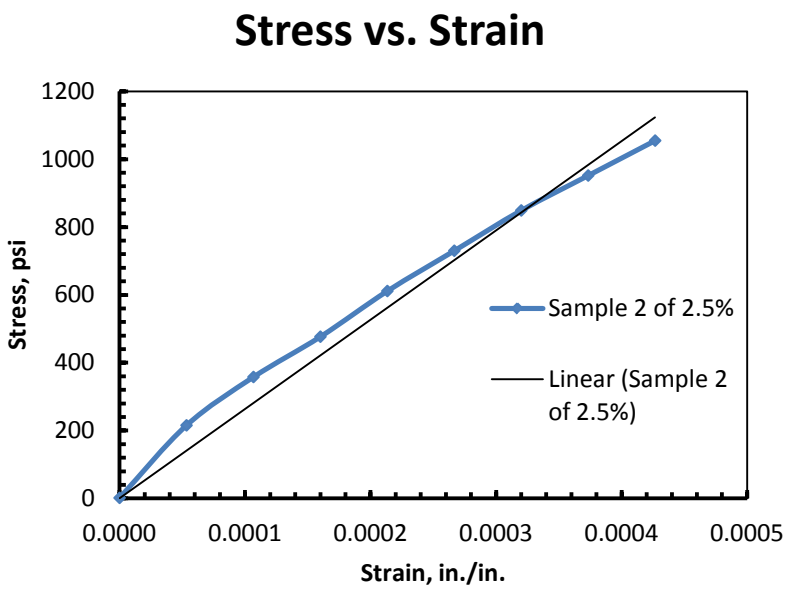

Figure A-19: Stress-strain curve for 2.5% GWRC sample-2 with brick chips

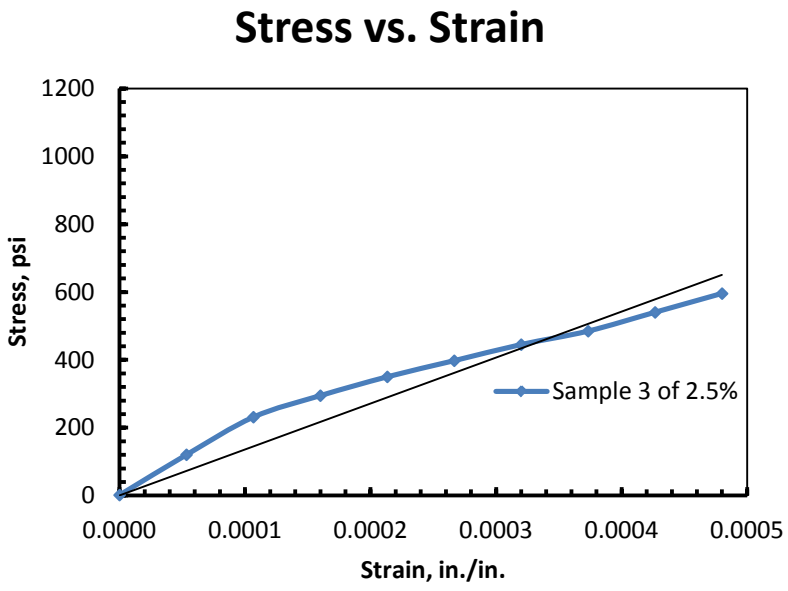

Figure A-20: Stress-strain curve for 2.5% GWRC sample-3 with brick chips

APPENDIX B

Table B-1: Raw Data of RCPT

Coarse Aggregate type	Sample ID	$I_{0,}$ amp	I_{30} ,amp	$I_{60,}$ amp	$I_{90,}$ amp	$I_{120,}$ amp	I_{150} ,amp	I_{180} ,amp	$I_{210,}$ amp	I_{240} ,amp	$I_{270,}$ amp	$I_{300,}$ amp	$I_{330,}$ amp	$I_{360,}$ amp	Total Charge passed (Q), Coulombs
Brick chips	Control-1	0.06	0.06	0.08	0.1	0.1	0.1	0.1	0.1	0.1	0.1	0.1	0.1	0.1	2016
	Control-2	0.06	0.08	0.1	0.12	0.12	0.15	0.15	0.15	0.16	0.16	0.16	0.16	0.16	2916
	1%_sample 1	0.52	0.72	0.79	1	1	1	1	1	1	1	1	1	1	20286
	1%_sample 2	0.26	0.32	0.32	0.37	0.35	0.32	0.31	0.3	0.29	0.29	0.27	0.27	0.26	6606
	1.5%_sample 1	0.31	0.48	0.54											2115
	1.5%_sample 2	0.2	0.24	0.3	0.35	0.52	0.53	0.58	0.52	0.55	0.5	0.49	0.44	0.44	9612
	2%_sample 1	0.68	1	1	1	1	1	1	1	1	1	1	1	1	21312
	2%_sample 2	0.42	0.43												1152
	2.5%_sample 1	0.56	1	1	1	1	1	1	1	1	1	1	1	1	21204
	2.5%_sample 2	0.44	0.58	0.7	0.82	0.93	1	1	1	1	1	1	1	1	19350
Stone chips	Control-1	0	0	0	0	0	0	0	0	0	0	0	0	0	0
	Control-2	0	0	0	0	0	0	0	0	0	0	0	0	0	0
	1%_sample 1	0.22	0.19	0.18	0.18	0.18	0.2	0.22	0.19	0.19	0.19	0.19	0.19	0.19	4149
	1%_sample 2	0.04	0.04	0.04	0.06	0.08	0.1	0.1	0.1	0.08	0.08	0.08	0.08	0.08	1620
	1.5%_sample 1	0.24	0.24	0.24	0.24	0.22	0.22								2304
	1.5%_sample 2	0.15	0.22	0.34	0.27	0.29	0.33	0.36	0.3	0.7	0.49	0.39	0.37	0.23	7650
	2%_sample 1	0.17	0.2	0.22	0.24	0.25	0.27	0.27	0.28	0.28	0.34	0.3	0.3	0.3	5733
	2%_sample 2	0.24	0.26	0.31	0.34	0.46	0.66	0.92	1	1	1	1	1	1	15426
	2.5%_sample 1	0.76	1	1	1	1	1	1	1	1	1	1	1	1	21384
	2.5%_sample 2	0.3	0.31	0.36	0.36	0.42	0.48								3744

APPENDIX C

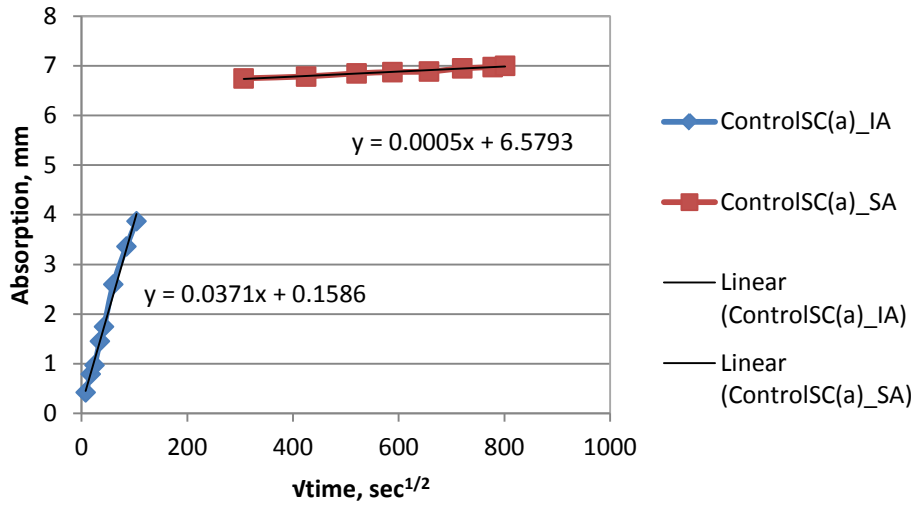

Figure C-1: Absorption curve for Control sample-1 with stone chips

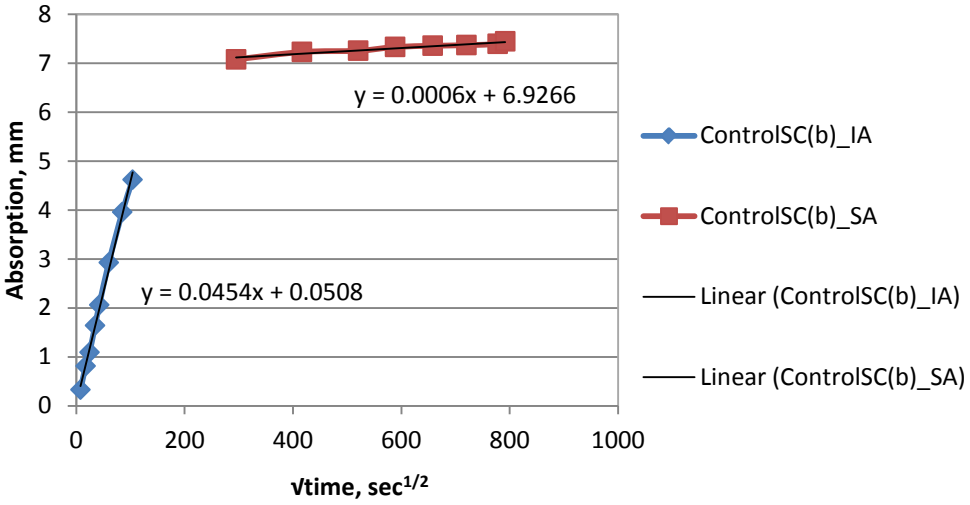

Figure C-2: Absorption curve for Control sample-2 with stone chips

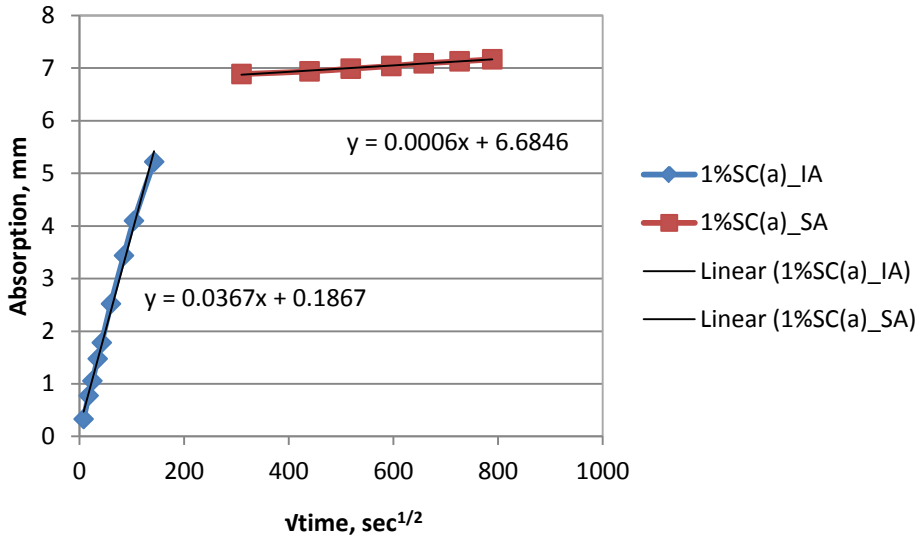

Figure C-3: Absorption curve for 1% GWRC sample-1 with stone chips

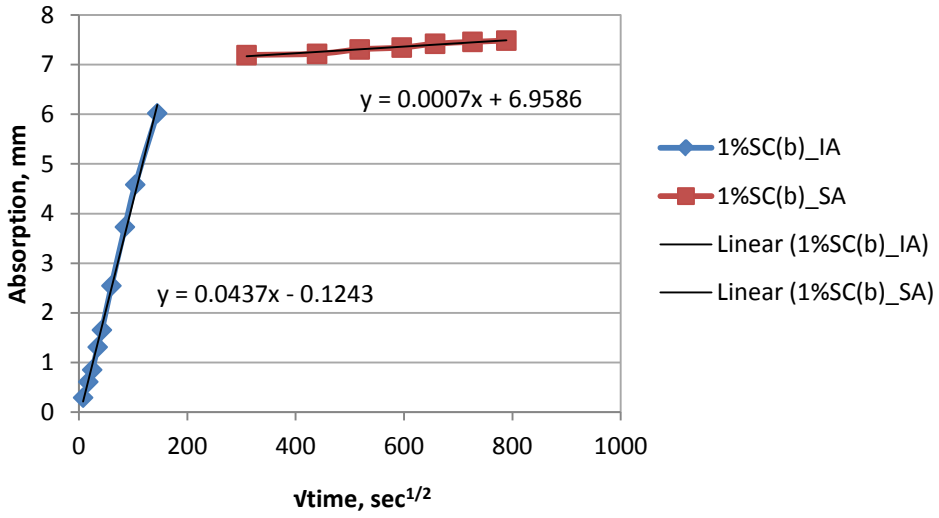

Figure C-4: Absorption curve for 1% GWRC sample-2 with stone chips

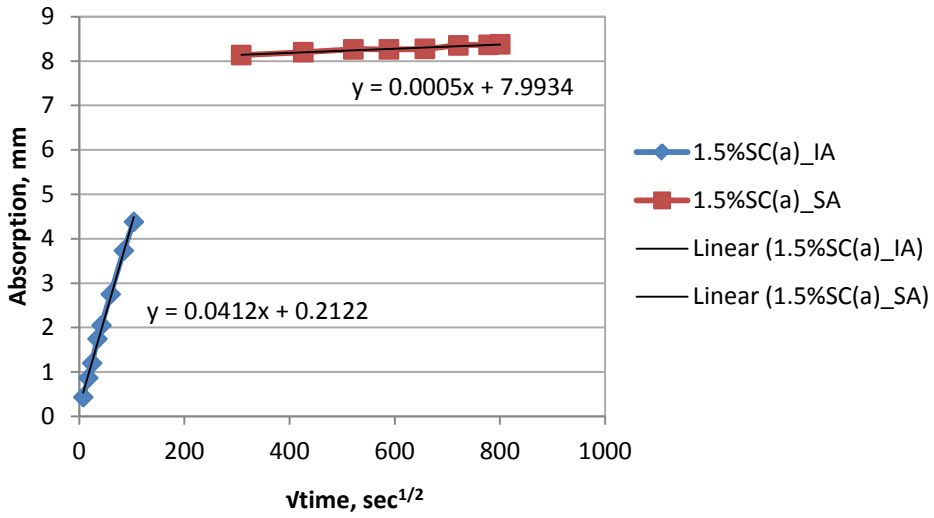

Figure C-5: Absorption curve for 1.5% GWRC sample-1 with stone chips

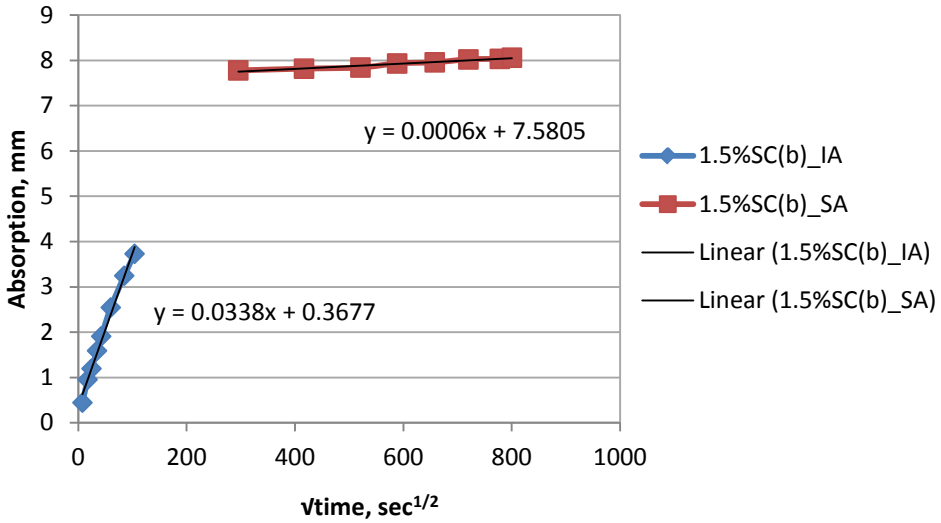

Figure C-6: Absorption curve for 1.5% GWRC sample-2 with stone chips

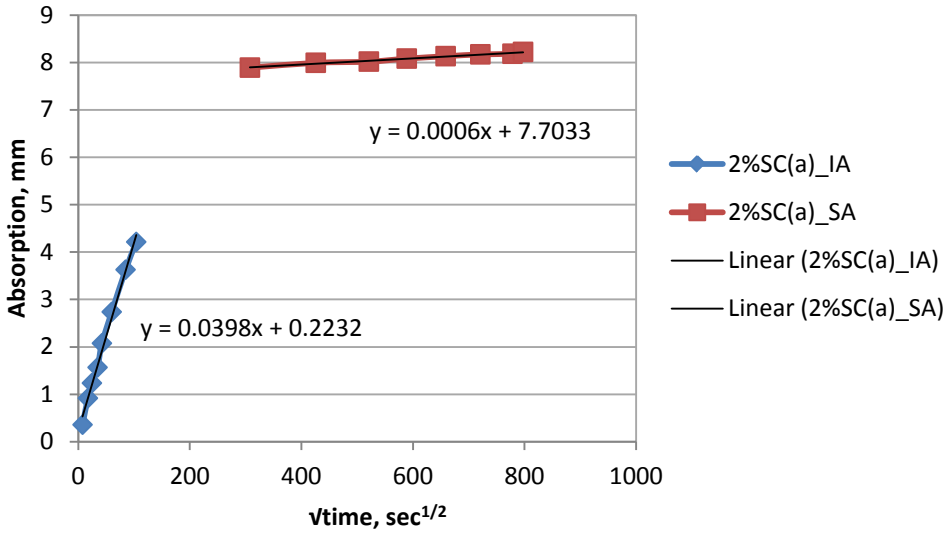

Figure C-7: Absorption curve for 2% GWRC sample-1 with stone chips

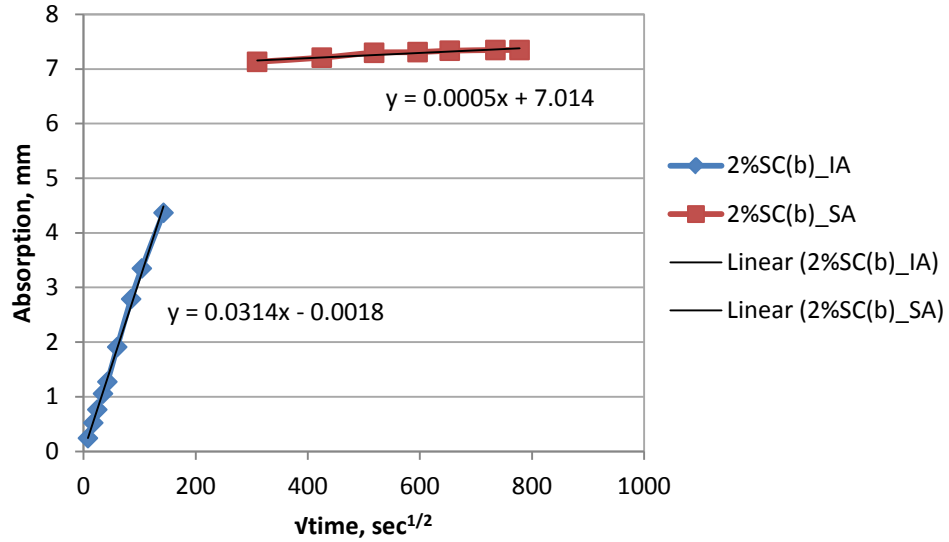

Figure C-8: Absorption curve for 2% GWRC sample-2 with stone chips

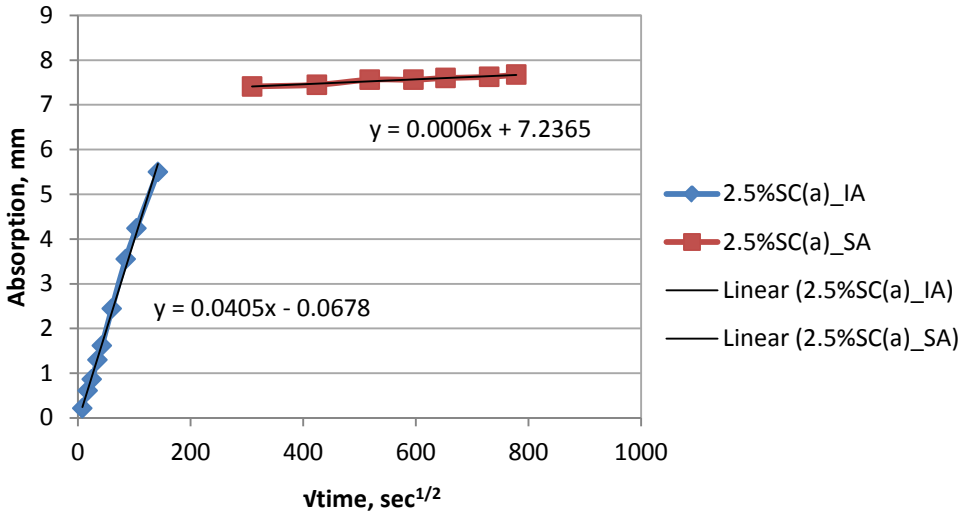

Figure C-9: Absorption curve for 2.5% GWRC sample-1 with stone chips

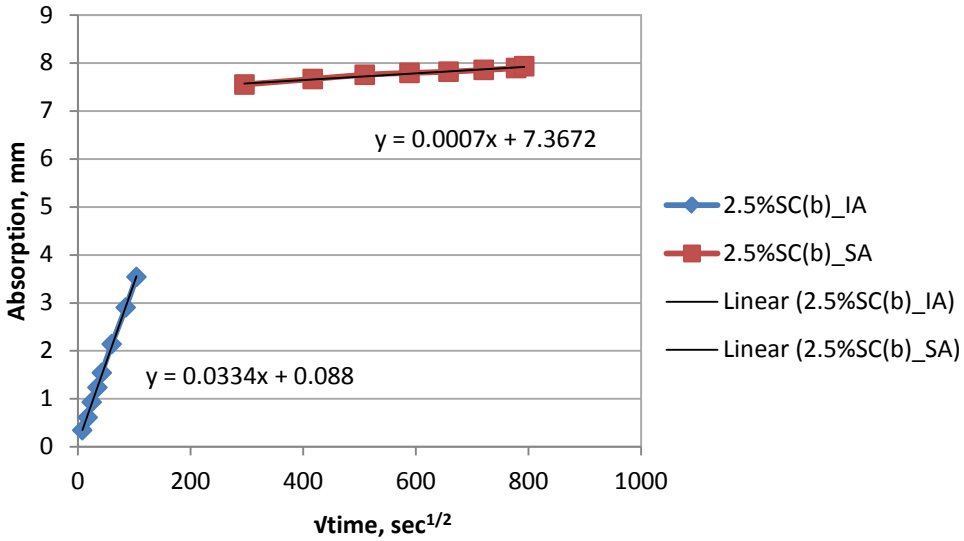

Figure C-10: Absorption curve for 2.5% GWRC sample-2 with stone chips

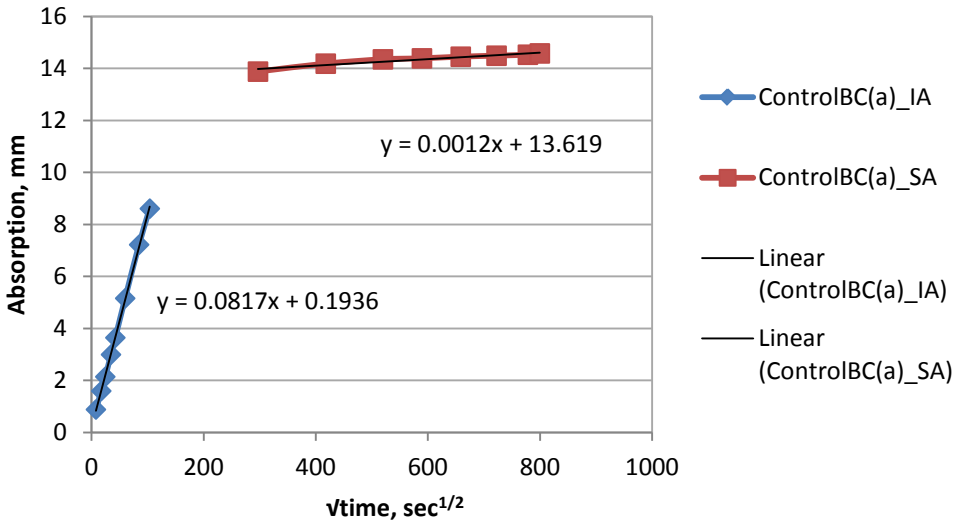

Figure C-11: Absorption curve for Control sample-1 with brick chips

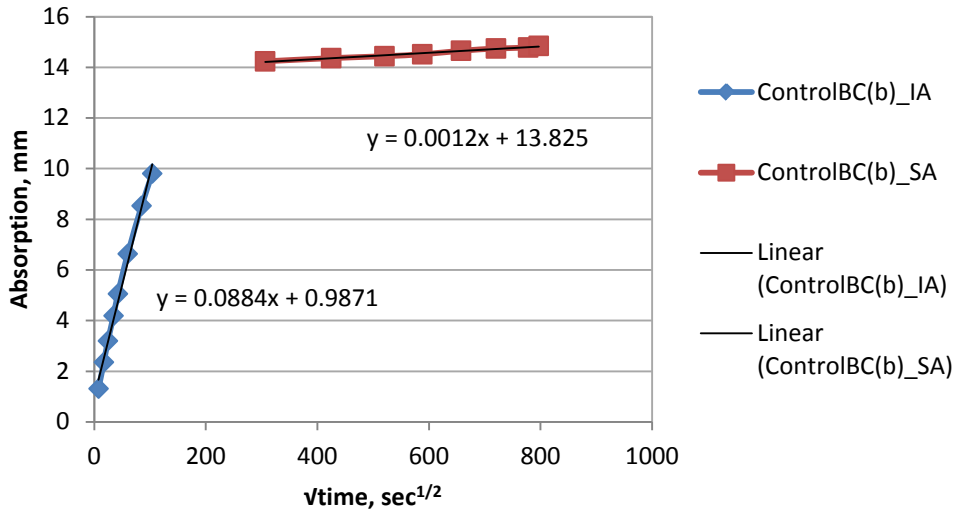

Figure C-12: Absorption curve for Control sample-2 with brick chips

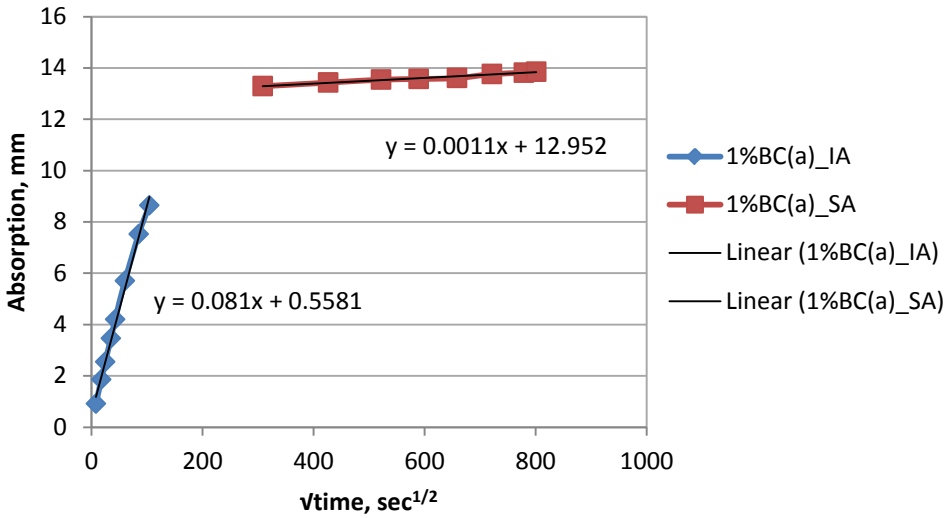

Figure C-13: Absorption curve for 1% GWRC sample-1 with brick chips

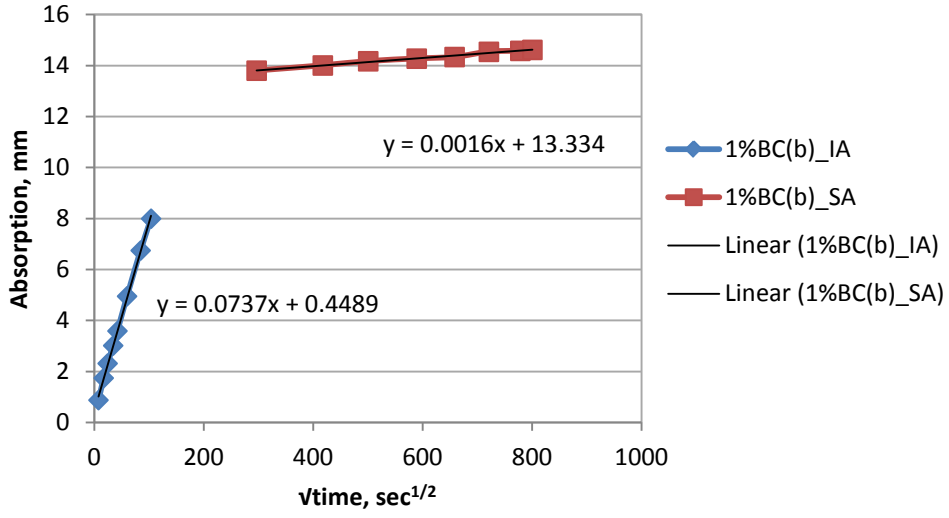

Figure C-14: Absorption curve for 1% GWRC sample-2 with brick chips

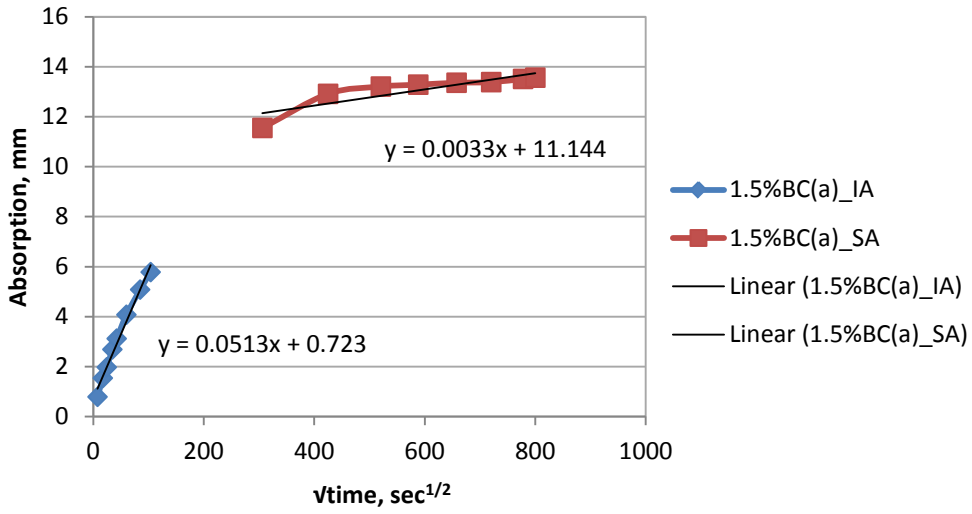

Figure C-15: Absorption curve for 1.5% GWRC sample-1 with brick chips

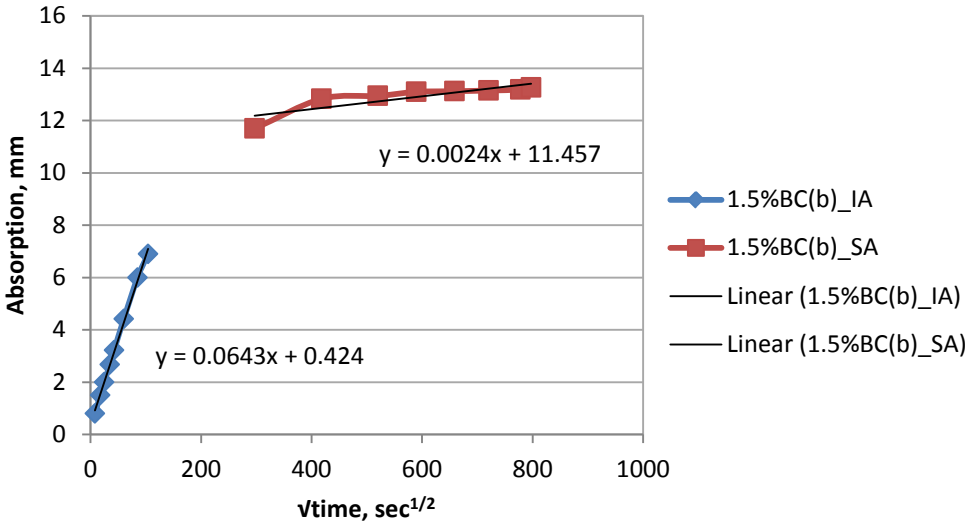

Figure C-16: Absorption curve for 1.5% GWRC sample-2 with brick chips

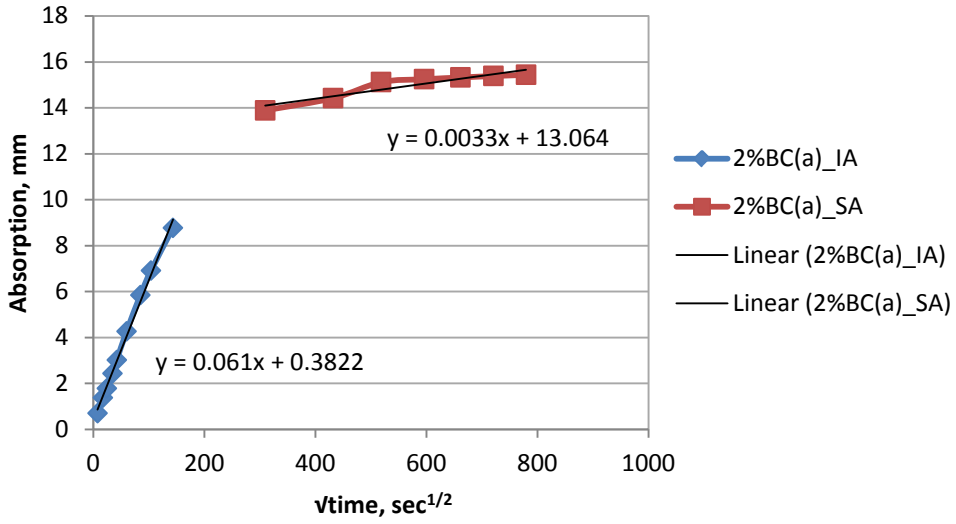

Figure C-17: Absorption curve for 2% GWRC sample-1 with brick chips

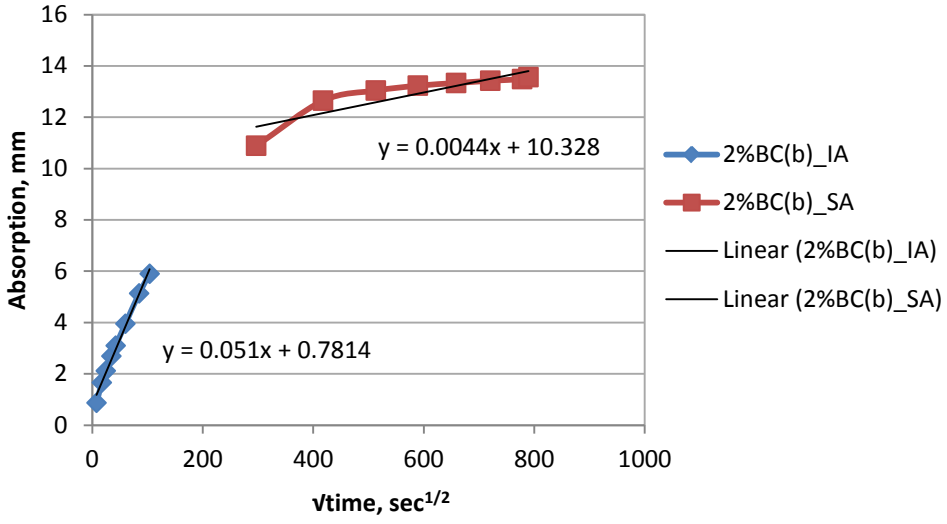

Figure C-18: Absorption curve for 2% GWRC sample-2 with brick chips

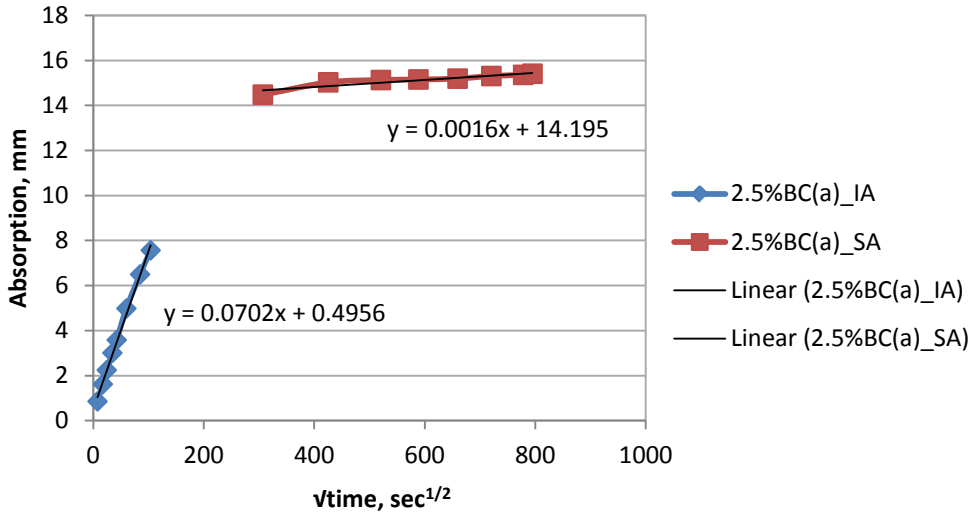

Figure C-19: Absorption curve for 2.5% GWRC sample-1 with brick chips

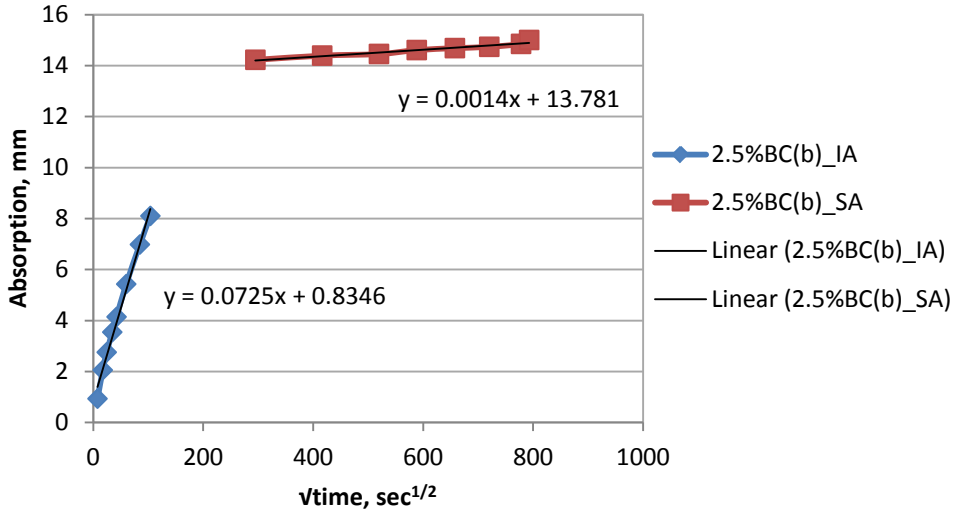

Figure C-20: Absorption curve for 2.5% GWRC sample-2 with brick chips